Transmission in Multimode Waveguide with Random Imperfections

By H. E. ROWE and W. D. WARTERS

(Manuscript received November 27, 1961)

The effects of random geometric imperfections on the transmission of the TE_{01} wave in circular waveguide are studied; the necessary theory of guides with known arbitrary imperfections is first developed. The TE_{01} transmission statistics are determined in terms of the statistics of the various types of geometric imperfections. Both discrete mode converters — i.e., localized imperfections such as tilts, offsets, or diameter changes at joints between pipes that are perfect right-circular cylinders — and continuous geometric imperfections — such as straightness deviation, diameter variation, ellipticity, etc., that vary smoothly with distance along the guide — are considered. The average, variance, power spectrum, and probability distribution of the TE_{01} loss-frequency curve are discussed.

Continuous straightness deviation (of the individual pipes of the guide) appears to be the most serious tolerance in present copper waveguide, and a significant factor in helix guide as well. The power spectrum of the straightness deviation is all-important in determining the TE_{01} loss due to mode conversion. Fourier components of straightness deviation having wavelengths between roughly 1.4 and 4.4 feet are the significant ones for the present 2-inch I.D. guide operated in a frequency band from 35 to 90 kmc.

TABLE OF CONTENTS

APPENDICES

I. INTRODUCTION

Long distance waveguide transmission via the TE_{01} mode in circular waveguide is an attractive goal because the theoretical TE_{01} heat loss decreases monotonically as the operating frequency increases. As is well known, operating frequencies far above the TE_{01} cutoff frequency are required to realize sufficiently low heat loss and delay distortion, so that the guide must operate far into the multimode region. Thus, considering a typical case, a 2-inch I.D. perfect copper circular guide operating at 55 kmc will have a theoretical TE_{01} heat loss of 1.54 db/mile; but this guide will propagate 223 additional modes, which we call spurious modes, at this frequency.[1]

The TE_{01} transmission loss will approach the theoretical TE_{01} heat loss in a copper waveguide only if the waveguide is a geometrically perfect right-circular cylinder over its entire length. Any departure from this ideal geometry will couple the TE_{01} mode to some of the spurious modes [2 to 7] the net effect of this coupling will be to increase the TE_{01} transmission loss above the theoretical heat loss, and to cause the TE_{01} transmission loss to vary with frequency.[1,8]

Two types of geometric imperfections are of interest:

(a) Intentional deformations introduced in the guide for various reasons, e.g., to go around corners,[3,6,7,9] to taper from a small guide to a larger one,[10] etc. Mode conversion effects control the design of such devices, but we will not discuss them further.

(b) Random geometric imperfections arising during the manufacturing or the laying of the guide; these imperfections will increase the TE_{01} loss and cause it to vary randomly with frequency.[8] The study of such effects is the purpose of the present paper.

The transmission characteristics of multimode waveguide with such random imperfections may be improved by adding heat loss to the spurious modes while keeping the TE_{01} heat loss low, i.e., close to its value for ideal copper guide. Examples are helix waveguide[11] and copper waveguide with a thin lossy dielectric lining.[12,13] This additional spurious mode loss will reduce the TE_{01} loss fluctuations with frequency, but will not reduce the average TE_{01} loss. (In contrast, for large intentional bends, it is desirable to alter the phase constant of one particular copper guide mode without increasing the heat loss to either TE_{01} or any of the spurious modes.[3,14])

The present paper is concerned primarily with determining the statistics of the TE_{01} transmission in terms of the statistics of the various geometric imperfections. The results of this analysis will indicate the required tolerances on the various types of geometric imperfections in different types of guide as a function of the allowable transmission degradation. Finally, the computed transmission statistics will be useful in determining the over-all degradation in various possible communication systems using imperfect waveguide as a transmission medium.

II. THEORY OF GUIDES WITH KNOWN IMPERFECTIONS

In this section we summarize the theory of circular waveguide with known geometric imperfections. These results yield, at least in principle, the TE_{01} transfer function for a circular waveguide with an arbitrary, known departure from perfect geometry. If the various geometric imperfections are assumed to be random processes, then the TE_{01} transfer function will also be a random process. In Sections III and IV these results for known imperfections are used to determine the TE_{01} transmission statistics in terms of the statistics of the various geometric imperfections.

We first require a solution to Maxwell's equations, in terms of the normal modes of the guide in question, for boundary conditions given by different types of geometric imperfections in various types of guide. Several people have studied these problems over the past ten years; we will give below a brief description of some of this work.

Transmission of TE_{01} through bends was first studied by M. Jouguet,[6] and by S. O. Rice in unpublished work. S. E. Miller made use of these results to devise several methods for transmitting TE_{01} around intentional bends.[7]

S. P. Morgan first computed via perturbation theory the first-order spurious modes scattered from a unit incident TE_{01} wave by small, abrupt tilts, offsets, and diameter changes in ideal lossless metallic guide.[15] These results were derived independently and published by S. Iiguchi.[16] Such discontinuities will often be called discrete mode converters, because the guide possesses perfect cylindrical geometry except at isolated, discrete points along its axis.

Next, Morgan determined the first-order spurious modes scattered by an arbitrary small continuous deformation of the surface of an ideal lossless metallic guide, again via perturbation theory.[5] These results may be used to determine the first-order spurious modes excited by small continuous diameter variation, straightness deviation, ellip-

ticity, and higher-order cross-sectional deformations of metallic guide. In addition, Morgan used these results to evaluate the expected value of the additional TE_{01} loss due to mode conversion caused by random distortion of the guide for a rather special mathematical model of the guide distortion.

Finally, Morgan applied the generalized telegraphist's equations of Schelkunoff[4] to the problem of lossless metallic waveguide with an arbitrary curvature of its axis;[2] if desired, the dielectric constant of the material filling the guide may be an arbitrary function of position. By this analysis, Maxwell's equations are reduced to an infinite set of coupled differential equations, the coupled line equations,[17] in which the dependent variables are the complex mode amplitudes of the normal modes of the unperturbed metallic guide. In principle, the coupled line equations provide an exact description of a lossless metallic waveguide with an arbitrary straightness deviation, and are not subject to the severe restrictions of the perturbation theory which was described in the preceding paragraph. Thus, if this infinite set of differential equations could be solved for an arbitrary straightness deviation, we would have an exact solution for Maxwell's equations for the particular deformed guide. As will appear below, solutions to these equations in the general case are not available, and useful results are obtained only by applying perturbation theory of one form or another to the coupled line equations;[18] however, the equations themselves are an exact description of the field problem.

Since the loss in real copper guide is low, we expect that the above coupling coefficients, which strictly speaking apply only to lossless metallic guide, will provide a good approximation for copper guide, and that the coupled line equations for lossless metallic guide need be modified only by changing the propagation constants for the various modes to take account of the small losses actually present in copper guide.

Equivalent results have been derived by H. G. Unger for various geometric imperfections in helix waveguide via the generalized telegraphist's equations;[4] these analyses have been carried out both in terms of metallic guide modes and helix guide modes.[11] Unger has studied straightness deviations[3] and cross-sectional deformations[19,20] in helix, as well as winding imperfections[21] in helix, and has given propagation constants and coupling coefficients for the various cases.[22] He has similarly studied continuous diameter variations (tapers),[10] which have identical behavior in both helix and metallic guide.

Thus, the study of random geometric imperfections in copper or helix waveguide has been reduced to the study of solutions to an infinite set

of differential equations with random coupling coefficients. However, this latter problem is a formidable one for which there is no really satisfactory treatment except in rather special cases. In the present paper, we use perturbation theory to approximate the solution to the coupled line equations; however, there is so far no rigorous justification for this approach. The convergence of this approximate solution is discussed elsewhere in this issue for the idealized case in which there are only two modes (rather than an infinite number of modes).[18] Even in this simple case, we do not know how good an approximation the perturbation solution provides.

It is obvious that the various results of S. P. Morgan for metallic guide must be related to each other, even though they may appear somewhat dissimilar. In this section, after first developing the necessary theory for a long guide with many discrete mode converters, we show how the coupled line equations and Morgan's results for discrete mode converters may be derived from each other, and how perturbation theory derived from either the discrete case or from the coupled line equations yields equivalent results to perturbation theory applied directly to the field equations.[5] This discussion is intended to provide a better physical understanding of the coupled line equations themselves, as well as of the approximate solution that we use, than would be obtained by merely a formal treatment based entirely on the coupled line equations. We will often simplify the problem by including only a few of the spurious modes (sometimes only a single spurious mode), in addition to the TE_{01} signal mode. While this procedure is useful in studying some of the basic problems, it of course does not provide a rigorous treatment for the real problem, which involves an infinite number of modes. However, experimental results for copper guides show that often only one or two spurious modes are present with significant magnitude,[8] and thus provide some additional justification for the study of the idealized problem.

2.1 *Scattering Matrices of Discrete Mode Converters*

While S. P. Morgan has performed a field analysis for discrete mode converters in lossless metallic guide, many of the general properties of the scattering matrices for discrete mode converters may be derived from conservation of energy, reciprocity, and the symmetry properties of the different mode converters. We give such a discussion in the present section, making use of Morgan's results[15,16] where necessary. Most of the discussion will be confined to cylindrical guides of infinite conduc-

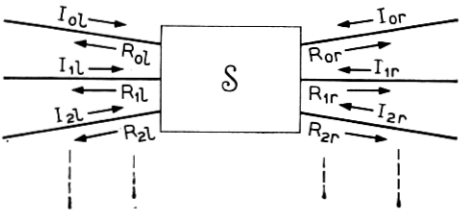

Fig. 1 — Generalized mode converter.

tivity. We choose the particular case of the discrete tilt to illustrate the general approach; briefer discussions are given for offsets and diameter changes.

2.1.1 *General Properties of Scattering Matrices*

Consider the general mode converter illustrated in Fig. 1. On the left of the obstacle we have the modes $0l,1l,2l, \cdots$, and on the right the corresponding modes $0r,1r,2r,3r, \cdots$, where the letters l and r stand for "left" and "right" respectively. The subscript zero will denote the TE_{01} mode and the other subscripts will denote the spurious modes. This convention will be used throughout this paper. We assume that there are the same number of propagating modes on each side of the obstacle, thus ruling out cases in which one of the spurious modes is below cutoff on one side of the obstacle, above cutoff on the other side. Cutoff modes are neglected throughout this analysis.

Denoting the normalized complex amplitudes of the modes incident on the obstacle from the right and left as I_{nr} and I_{nl} respectively, and of those leaving the obstacle as R_{nr} and R_{nl} respectively, the matrix equations[23] of the obstacle may be written:

$$\mathfrak{R} = \mathcal{S}\mathcal{I}$$

$$\mathfrak{R} = \begin{bmatrix} R_l \\ \hline R_r \end{bmatrix} \qquad \mathcal{I} = \begin{bmatrix} I_l \\ \hline I_r \end{bmatrix}$$

$$R_l = \begin{bmatrix} R_{0l} \\ R_{1l} \\ R_{2l} \\ \vdots \end{bmatrix} \qquad R_r = \begin{bmatrix} R_{0r} \\ R_{1r} \\ R_{2r} \\ \vdots \end{bmatrix} \tag{1}$$

$$I_l = \begin{bmatrix} I_{0l} \\ I_{1l} \\ I_{2l} \\ \vdots \end{bmatrix} \qquad I_r = \begin{bmatrix} I_{0r} \\ I_{1r} \\ I_{2r} \\ \vdots \end{bmatrix}.$$

Morgan's results show that except very close to the cutoff of a spurious mode, the power scattered from TE_{01} to the forward modes greatly exceeds the power scattered to the backward modes for "small" mode converters. Consequently, in the following treatment we shall neglect all reflected waves. Using this assumption, and the fact that $\mathbb{S}$ must be symmetric (reciprocity),

$$\mathbb{S} = \begin{bmatrix} 0 & \tilde{S} \\ S & 0 \end{bmatrix}, \qquad S = \begin{bmatrix} s_{00} & s_{01} & s_{02} & \cdots \\ s_{10} & s_{11} & s_{12} & \cdots \\ s_{20} & s_{21} & s_{22} & \cdots \\ \cdots & \cdots & \cdots & \cdots \end{bmatrix}, \tag{2}$$

and from (1),

$$\begin{bmatrix} R_l \\ R_r \end{bmatrix} = \begin{bmatrix} 0 & \tilde{S} \\ S & 0 \end{bmatrix} \begin{bmatrix} I_l \\ I_r \end{bmatrix}, \tag{3}$$

where $\tilde{S}$ denotes the transpose of the submatrix S. Thus,

$$R_l = \tilde{S} I_r , \tag{4a}$$

$$R_r = S I_l . \tag{4b}$$

If the obstacle is assumed lossless

$$\tilde{\mathbb{S}}\mathbb{S}^* = [1], \tag{5}$$

where the * denotes the complex conjugate and [1] denotes the unit matrix. From (2) we thus have

$$\tilde{S}S^* = [1] \quad \text{or equivalently} \quad S\tilde{S}^* = [1]. \tag{6}$$

2.1.2 *Scattering Matrix for a Tilt*

Consider the tilt of Fig. 2(a). Neglecting reflected waves, this mode converter may be characterized by the matrices of (3) or (4). Since the tilt is symmetric about the plane A-A' of Fig. 2(a), its input and output terminals may be interchanged without altering its behavior. From this fact and (4), we have

$$S = \tilde{S}; \tag{7}$$

the matrix S is symmetric for a tilt. If we consider a tilt in perfectly conducting guide, so that energy is conserved, we have from (6) and (7)

$$SS^* = S^*S = [1]. \tag{8}$$

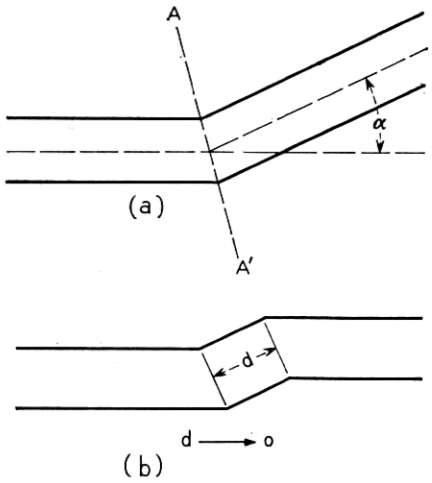

Fig. 2 — Waveguide with tilt.

Next, consider a cascade connection of the tilt of Fig. 2(a) and an identical tilt rotated 180°, as shown in Fig. 2(b); we may consider that the first tilt has an angle $+\alpha$, the second an angle $-\alpha$. Let the scattering matrix for the first tilt be S, for the second (rotated) tilt be S'. Then as the distance d between the two tilts approaches zero, the over-all scattering matrix of the two tilts becomes $S'S$ (neglecting reflected waves). But it is clear from physical considerations that this cascade connection of two opposite tilts of equal magnitude must be equivalent to a straight piece of guide (of zero length); thus we must have

$$S'S = SS' = [1]. \tag{9}$$

From (8) and (9) we have in the lossless case

$$S^* = S'. \tag{10}$$

By utilizing the symmetry properties of the various modes involved, further restrictions on the elements of S are easily found. For the sake of definiteness, consider the case where the only modes considered are the signal mode, TE_{01}, and the first-order forward spurious modes scattered by a discrete tilt from TE_{01}, i.e., one polarization of the forward TM_{11} and TE_{1m} modes, denoted by TM_{11}^+ and TE_{1m}^+, as shown by Morgan.[15,16] It is obvious by symmetry that only the (linear) polarization having an asymmetric transverse field distribution with respect to the plane of the tilt will be excited by an incident TE_{01} wave.[23] While

the backward TE_{1m} modes, denoted by TE_{1m}^{-}, are excited to first order by a tilt, their magnitudes are much smaller than the magnitudes of the corresponding forward spurious modes, as stated earlier, and consequently we neglect the backward modes for the present. We recall the convention of (1), i.e. the top elements in the R and I column vectors of (4), having the subscript 0, denote the TE_{01} signal mode; the other elements denote the various spurious modes. Let the elements of the S and S' matrices be s_{ij} and s_{ij}' respectively. Thus, for example, if a unit TE_{01} wave is incident on the tilt of Fig. 2(a) from the left, a TE_{01} wave of (complex) amplitude s_{00} will emerge on the right. We now observe that rotation of the tilt by 180° leaves the TE_{01} mode unaffected, but reverses the sign of the field components of all of the spurious modes, since their field components vary as $\cos \varphi$ or $\sin \varphi$. Consequently, the matrix components s_{ij}' for the rotated tilt are related to the matrix components s_{ij} as follows:

$$s_{ij}' = \begin{cases} -s_{ij}; & i = 0, \quad j \neq 0. \\ & i \neq 0, \quad j = 0. \\ +s_{ij}; & i = 0, \quad j = 0. \\ & i \neq 0, \quad j \neq 0. \end{cases} \tag{11}$$

From (10) we have

$$s_{ij}^{*} = s_{ij}'. \tag{12}$$

Equations (11) and (12) thus yield

$$s_{ij} = \begin{cases} \text{pure imaginary}; & i = 0, \quad j \neq 0. \\ & i \neq 0, \quad j = 0. \\ \text{pure real}; & i = 0, \quad j = 0. \\ & i \neq 0, \quad j \neq 0. \end{cases} \tag{13}$$

The coupling coefficients between TE_{01} and the spurious modes are pure imaginary, while all other matrix components are pure real.

Summarizing the above results, the scattering matrix S of a discrete tilt in lossless metallic guide must satisfy the following relations, if we include only TE_{01} and the propagating first-order forward spurious modes:

$$S = \tilde{S}, \qquad s_{ij} = s_{ji}. \tag{14}$$

$$SS^{*} = [1]. \tag{15}$$

$$s_{ij} = \begin{cases} \text{pure imaginary;} & \begin{matrix} i = 0, & j \neq 0. \\ i \neq 0, & j = 0. \end{matrix} \\ \text{pure real;} & \begin{matrix} i = 0, & j = 0. \\ i \neq 0, & j \neq 0. \end{matrix} \end{cases} \tag{16}$$

As an example, let us determine the form of S for the case where only a single spurious mode is considered, in addition to the TE_{01} signal mode. (For a guide with a large intentional bend, the most significant spurious mode might be one polarization of forward TM_{11}. For a guide with a small random straightness deviation confined to a single plane, the most significant spurious mode might be one polarization of forward TE_{12}, as discussed in Section 2.3 below.) Then (14) to (16) yield for the S-matrix

$$S = \begin{bmatrix} \sqrt{1 - c^2} & jc \\ jc & \sqrt{1 - c^2} \end{bmatrix}. \tag{17}$$

For small tilts in lossless metallic guide, Morgan[15,16] has given the coupling coefficients s_{0j} [or jc of (17)] in terms of the tilt angle α of Fig. 2(a) to first order in α, as follows;

$$s_{0j} = jC_{t(j)}{}^{+} \cdot \alpha + \cdots, \quad j \neq 0, \tag{18}$$

where the first j on the right-hand side of (18) represents $\sqrt{-1}$, the subscripts j indicate the spurious mode. $C_{t(j)}{}^{+}$ is a constant depending on the (forward) spurious mode; formulas and numerical values at a frequency of 55 kmc in 2-inch diameter guide for the $C_t{}^{+}$'s are given in Appendix A. In addition, the coupling coefficients $C_t{}^{-}$ to the corresponding backward spurious modes are also given in Appendix A; as indicated above, these are much smaller than the forward mode coupling coefficients.

Consider a tilt of angle α_1 followed by a tilt of angle α_2; as the distance between the two tilts approaches zero, it is obvious that the structure approaches simply a single tilt of angle $\alpha_1 + \alpha_2$. If $S(\alpha)$ is the matrix for a tilt of angle α, then the S-matrix must satisfy the further requirement that

$$S(\alpha_1) \cdot S(\alpha_2) = S(\alpha_1 + \alpha_2), \tag{19}$$

for every value of α_1 and α_2, where we again neglect reflected modes. Consider again the idealized case where only a single spurious mode is allowed, in addition to the TE_{01} signal mode. We show in Section 2.3.3 that the "exact" matrix for a large tilt for this idealized two-mode case

is given by

$$S(\alpha) = \begin{bmatrix} \cos C_t\alpha & j \sin C_t\alpha \\ j \sin C_t\alpha & \cos C_t\alpha \end{bmatrix}, \tag{20}$$

where C_t is Morgan's coupling coefficient for the spurious mode in question. The matrix of (20) can readily be seen to satisfy the consistency condition of (19), and to approach the results of (17) and (18) for $C_t\alpha \ll 1$. However, the reader should be warned again that (20) will *not* be valid for large tilts in the physical case, because such large tilts will excite many spurious modes with significant magnitude, and hence can *not* be described in terms of only two modes.

The above results for tilts in metallic waveguide include only one polarization of each of the forward spurious modes, i.e., $TE_{1m}{}^{+}$ and $TM_{11}{}^{+}$. We wish to extend these results to include both polarizations of each of these spurious modes so that we will be able to treat a long line containing arbitrary tilts with arbitrary angular orientation, i.e., *not* confined to a single plane.

We first write the general results of (4b) as follows, dropping as unnecessary the subscripts l and r since we will always assume that all modes travel in the forward direction, from left to right.

$$R] = [S]\cdot I]. \tag{21}$$

$$R] = \begin{bmatrix} R_0 \\ \hline R_x] \\ \hline R_y] \end{bmatrix}, \quad I] = \begin{bmatrix} I_0 \\ \hline I_x] \\ \hline I_y] \end{bmatrix}; \tag{22a}$$

$$R_x] = \begin{bmatrix} R_{1x} \\ R_{2x} \\ \vdots \end{bmatrix}, \quad R_y] = \begin{bmatrix} R_{1y} \\ R_{2y} \\ \vdots \end{bmatrix}, \quad I_x] = \begin{bmatrix} I_{1x} \\ I_{2x} \\ \vdots \end{bmatrix}, \quad I_y] = \begin{bmatrix} I_{1y} \\ I_{2y} \\ \vdots \end{bmatrix}. \tag{22b}$$

In these and following matrix relations, we adopt the convenient notation that column vectors ($n \times 1$ matrices) are denoted by the symbol], row vectors ($1 \times n$ matrices) by symbol __, and square matrices by the symbol [ ] where it is not obvious from the context that something else is intended (e.g., the column vectors on the right-hand sides of (22a) and (22b)). The top elements in (22a), R_0 and I_0, represent the transmitted and incident TE_{01} wave. $R_x]$, $I_x]$ and $R_y]$, $I_y]$ are column vectors whose elements represent the two orthogonal (linear) polarizations of each of the spurious modes.

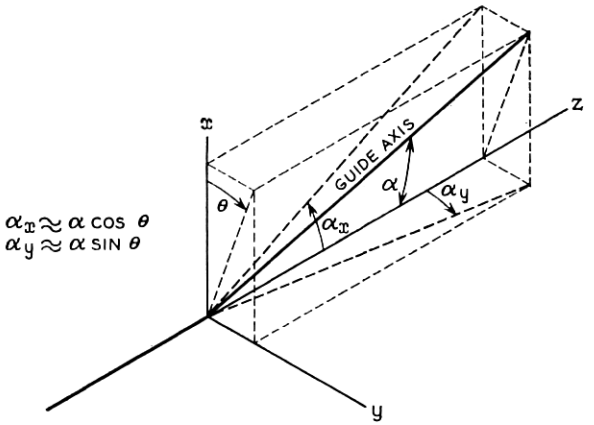

Fig. 3 — Geometry of a tilt in waveguide.

Consider the tilt of Fig. 3, in which the two polarizations of each of the TE_{1m}^{+} and TM_{11}^{+} spurious modes are defined along the x and y axes. To use the previous treatment including only a single polarization of each spurious mode, we must set $\theta = 0$ in Fig. 3, so that the plane of the tilt lies in one of the planes defining the spurious mode polarization. Then, using the notation of (22), we may write the results for the x-polarization as follows:

$$\begin{bmatrix} R_0 \\ \hline R_x \end{bmatrix} = \left[\begin{array}{c|c} s_{00} & j\underset{\sim}{\tilde{C}} \\ \hline jC] & [D] \end{array}\right] \cdot \begin{bmatrix} I_0 \\ \hline I_x \end{bmatrix}, \tag{23}$$

$$C] = \begin{bmatrix} c_1 \\ c_2 \\ \vdots \end{bmatrix}, \quad jc_j \equiv s_{0j}. \tag{24}$$

The components of the column vector of (24) are given to first order by (18). In (23), we have partitioned the S-matrix to conform to the partitioning of the R and I column vectors. The restrictions of (14) to (16) become respectively, in terms of the submatrices of (23):

$$[D] = [\tilde{D}]. \tag{25}$$

$$s_{00}^{2} + \sum_j c_j^{2} = 1,$$

$$(s_{00} - [D]) \cdot C] = 0], \tag{26}$$

$$C] \cdot \underset{\sim}{\tilde{C}} + [D]^2 = [1].$$

$$s_{00}, \quad C], \quad [D] \quad \text{pure real.} \tag{27}$$

In (26), [1] denotes the unit matrix.

Now by symmetry an incident TE_{01} wave in this particular tilt ($\theta = 0$) will not excite the y-polarization of any of the spurious modes as stated earlier, and by reciprocity the y-polarization of any of the spurious modes will not excite TE_{01}. Further, the x- and y-polarizations of all of the spurious modes are uncoupled from each other by symmetry. Therefore, we may expand the matrix relation of (23) to include the y-polarization of the spurious modes as follows:

$$\begin{bmatrix} R_0 \\ \hline R_x] \\ \hline R_y] \end{bmatrix} = \begin{bmatrix} s_{00} & j\tilde{C} & 0 \\ \hline jC] & [D] & [0] \\ \hline 0] & [0] & [1] \end{bmatrix} \cdot \begin{bmatrix} I_0 \\ \hline I_x] \\ \hline I_y] \end{bmatrix}, \tag{28}$$

where (18) and (24) to (27) still apply.

Now let us rotate the axes by an angle $-\theta$ with respect to the plane of the tilt, as shown in Fig. 3, and write the field in the guide in terms of modes referred to these new axes. The geometry of the rotated tilt may be specified precisely in the following way. Imagine that before the guide is tilted, lines φ = constant are drawn on the surface of the guide parallel to the guide axis. Then the tilt, of orientation θ, is constructed at a specified point on the axis by tilting the guide in the plane defined by the axis and the $\varphi = \theta$ line, by an angle α. If

$$\begin{aligned} \rho &= \text{distance from the (tilted) guide axis in a plane perpendicular to the guide axis,} \\ s &= \text{distance measured along the (tilted) guide axis,} \end{aligned} \tag{29}$$

the three coordinates ρ, φ, s constitute "bent cylindrical coordinates," as used by Morgan for continuous bends confined to a single plane.[2] In subsequent analysis for a guide with many tilts of arbitrary orientation, we will adopt the convention that $\alpha > 0$ while θ is unrestricted; in contrast, for a guide with tilts confined to a single plane, we will set $\theta = 0$ and allow α to be unrestricted.

Now let $R_0]$ and $I_0]$ denote the fields with respect to the old axes and $R_\theta]$ and $I_\theta]$ the fields with respect to the rotated axes. First, we note that TE_{01} is the same in both sets of coordinates. Next, we note that the field components of all of the spurious modes under consideration, i.e., TE_{1m}^{+} and TM_{11}^{+}, vary as $\cos\varphi$ or $\sin\varphi$. If we call φ_0 the "old" and φ_θ the "rotated" angular coordinates, the transformation is simply

$$\varphi_\theta = \varphi_0 + \theta. \tag{30}$$

For each spurious mode this yields in terms of wave amplitudes

$$\begin{bmatrix} R_{x_0} \\ R_{y_0} \end{bmatrix} = \begin{bmatrix} \cos\theta & \sin\theta \\ -\sin\theta & \cos\theta \end{bmatrix} \begin{bmatrix} R_{x\theta} \\ R_{y\theta} \end{bmatrix}, \tag{31}$$

with a similar result for the I's. Note that (31) applies to a single spurious mode only (two polarizations); the index denoting the particular mode has been omitted for convenience. Thus, the R's (or I's) in (31) are single (complex) numbers, and not column vectors. We may write the corresponding general rotation matrix including TE_{01} and all spurious modes in the following convenient form:

$$R_0] = [M]\cdot R_\theta], \qquad I_0] = [M]\cdot I_\theta]. \tag{32a}$$

$$[M] = \begin{bmatrix} 1 & \underbrace{0} & \underbrace{0} \\ 0] & \cos\theta\cdot[1] & \sin\theta\cdot[1] \\ 0] & -\sin\theta\cdot[1] & \cos\theta\cdot[1] \end{bmatrix}. \tag{32b}$$

$$\tilde{M} = M^{-1}. \tag{32c}$$

R and I in (32a) are as given in (22); the [1]'s in (32b) represent the unit matrix. We note from (32c) that M is an orthogonal matrix.

Now rewriting (28) as

$$R_0] = [S_0]\cdot I_0], \tag{33}$$

we substitute the relations of (32a) into (33) to obtain

$$\begin{aligned} [M]\cdot R_\theta] &= [S_0]\cdot[M]\cdot I_\theta] \\ R_\theta] &= [M]^{-1}\cdot[S_0]\cdot[M]\cdot I_\theta] \\ &= [\tilde{M}]\cdot[S_0]\cdot[M]\cdot I_\theta]. \end{aligned} \tag{34}$$

Therefore,

$$R_\theta] = [S_\theta]\cdot I_\theta], \tag{35a}$$

$$[S_\theta] = [\tilde{M}]\cdot[S_0]\cdot[M]. \tag{35b}$$

Substituting $[S_0]$ from (28) and $[M]$ from (32b), we have

$$[S_\theta] = \begin{bmatrix} s_{00} & j\cos\theta\cdot\underbrace{\tilde{C}} & j\sin\theta\cdot\underbrace{\tilde{C}} \\ j\cos\theta\cdot C] & \cos^2\theta\cdot[D] + \sin^2\theta\cdot[1] & \sin\theta\cos\theta([D] - [1]) \\ j\sin\theta\cdot C] & \sin\theta\cos\theta([D] - [1]) & \sin^2\theta\cdot[D] + \cos^2\theta\cdot[1] \end{bmatrix} \tag{36}$$

as the scattering matrix for a tilt in lossless metallic guide, having an orientation of θ radians with respect to the axes defining the polarization of the spurious modes. $C]$ remains as defined in (24), with components given to first order by (18), and the restrictions of (25) to (27) still apply.

The above transformation may readily be seen to yield the correct results in a few simple cases:

1. $\theta = \pi$. $[S_\pi]$ is readily seen to be identical to the matrix $[S']$ described in connection with (11).

2. $\theta = \pi/2$. Here we see that $R_x]_{\theta=0} = R_y]_{\theta=\pi/2}$, $R_y]_{\theta=0} = -R_x]_{\theta=\pi/2}$, and similarly for the I's, as is obvious from geometric considerations.

The coupling coefficients between TE_{01} and the x- and y-polarizations of the j^{th} spurious mode are from (36), (24) and (18)

$$s_{0j,x} = jC_{t(j)}{}^{+} \cdot (\alpha \cos \theta), \tag{37a}$$

$$s_{0j,y} = jC_{t(j)}{}^{+} \cdot (\alpha \sin \theta). \tag{37b}$$

These general results simplify so that they may be simply expressed in terms of fixed x, y, z coordinates in the following special case:

1. The angular deviation of the guide axis from the z-axis is small.

2. The unit vector perpendicular to the guide axis and lying in the plane defined by the guide axis and the $\varphi = 0$ line is almost parallel to the x-axis. These conditions insure that the $\varphi = 0$ line drawn on the guide will remain almost parallel to the x-z plane. Subject to these conditions, we have approximately

$$\alpha \cos \theta \approx \alpha_x , \tag{38a}$$

$$\alpha \sin \theta \approx \alpha_y , \tag{38b}$$

where α_x and α_y are the angles made by the projections of the guide axes, adjacent to the tilt, in the x-z and y-z planes respectively. These results are readily verified for the case shown in Fig. 3. They are derived in Appendix B. Substitution of (38) into (37) [and thence into the matrix of (36)] will greatly simplify certain later calculations.

2.1.3 *Scattering Matrix for an Offset and a Diameter Change*

The scattering matrix for an offset may be found by similar methods as used in Section 2.1.2 above for a tilt. Consider the offset of Fig. 4(a), with scattering matrix S; as above we assume the offset is small, so that backward modes may be neglected and only the propagating first-order forward spurious modes (i.e., $TE_{1m}{}^{+}$)[15,16] need be considered. In Fig.

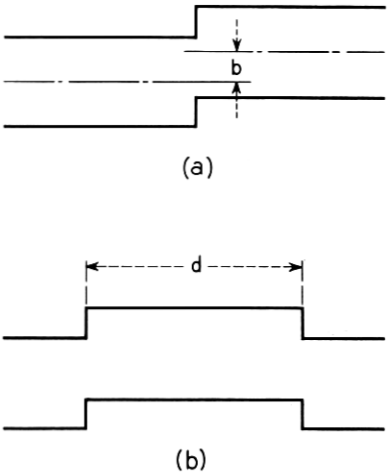

Fig. 4 — Waveguide with offset.

4(b), this offset is cascaded with an identical offset, which may be derived from the original offset in two ways:

1. Reverse input and output terminals.
2. Rotate the first offset 180°.

From 1, the matrix for the second offset is $\tilde{S}$, the transpose of S. From 2, the matrix for the second offset is S', as defined in (11) above, by an argument similar to that used for the tilt. From these facts, as the distance d separating the offsets approaches zero,

$$\tilde{S}S = S\tilde{S} = [1], \tag{39a}$$

$$S'S = SS' = [1]. \tag{39b}$$

Assuming lossless metallic guide, from (6)

$$\tilde{S}S^* = S\tilde{S}^* = [1]. \tag{40}$$

From (39) and (40) we have for an offset in lossless metallic guide:

$$\tilde{S}S = [1]. \tag{41}$$

$$s_{ij} = \text{pure real} = \begin{cases} -s_{ji}\,; & i = 0, \quad j \neq 0. \\ & i \neq 0, \quad j = 0. \\ +s_{ji}\,; & i = 0, \quad j = 0. \\ & i \neq 0, \quad j \neq 0. \end{cases} \tag{42}$$

For a single spurious mode the matrix S for an offset becomes

$$S = \begin{bmatrix} \sqrt{1 - c^2} & c \\ -c & \sqrt{1 - c^2} \end{bmatrix}, \tag{43}$$

corresponding to (17) for a tilt. For small offsets in lossless metallic guide, Morgan[15,16] has given the coupling coefficients s_{0j} [or c of (43)] in terms of the offset b of Fig. 4(a) to first order in b, as follows:

$$s_{0j} = C_{o(j)}{}^{+} \cdot b + \cdots, \quad j \neq 0. \tag{44}$$

$C_{o(j)}{}^{+}$ is a constant depending on the spurious mode; formulas and numerical values for the $C_o{}^{\pm}$'s at a frequency of 55 kmc in 2-inch diameter guide are given in Appendix A.

Analogous results to those of (19) to (38) for tilts are readily found for offsets, but will not be discussed in detail here. In particular, the scattering matrix for an offset with an arbitrary angular orientation is found in the same way as given in (21) to (37), making use of the rotation operator of (32). The geometry for offsets of arbitrary orientation is much simpler than for tilts. As before, imagine that lines φ = constant are drawn on the surface of the initially perfect guide, parallel to the guide axis. Then the offset of Fig. 5 is constructed at a specified point on the guide axis by translating the guide a distance b in the $\varphi = \theta$ plane without rotating the guide, so that corresponding φ-lines on the two sides of the offset are separated by a distance b. For a guide with many offsets of arbitrary orientation we take $b > 0$ with θ unrestricted, while for a guide with offsets confined to a single plane we set $\theta = 0$ and allow b to be unrestricted, as in the case of tilts. Then using the notation of Section 2.1.2, the scattering matrix S_θ for an offset of orientation θ is given as follows:

$$S_\theta = \left[\begin{array}{c|c|c} s_{00} & \cos\theta \cdot \underset{\sim}{\tilde{C}} & \sin\theta \cdot \underset{\sim}{\tilde{C}} \\ \hline -\cos\theta \cdot C] & \cos^2\theta \cdot [D] + \sin^2\theta \cdot [1] & \sin\theta\cos\theta([D] - [1]) \\ \hline -\sin\theta \cdot C] & \sin\theta\cos\theta([D] - [1]) & \sin^2\theta \cdot [D] + \cos^2\theta \cdot [1] \end{array}\right] \tag{45}$$

where

$$C] = \begin{bmatrix} c_1 \\ c_2 \\ \vdots \end{bmatrix}, \quad c_j \equiv s_{0j}\,. \tag{46}$$

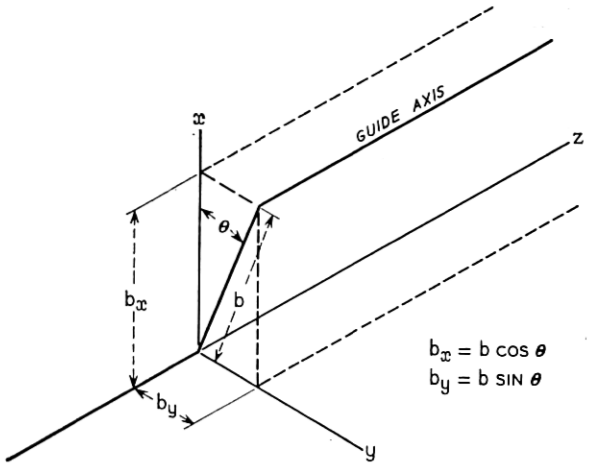

Fig. 5 — Geometry of an offset in waveguide.

The components of $C]$ are given to first order by (44). Equation (45) (for offsets) has been written in such a way that the restrictions of (41) and (42) become identical to those of (25) to (27) (for tilts).

The coupling coefficients between TE_{01} and the x- and y-polarizations of the j^{th} spurious mode are from (44) to (46)

$$s_{0j,x} = C_{o(j)}{}^{+} \cdot (b \cos \theta), \tag{47a}$$

$$s_{0j,y} = C_{o(j)}{}^{+} \cdot (b \sin \theta). \tag{47b}$$

From Fig. 5 it is readily seen that $b_x = b \cos \theta$ and $b_y = b \sin \theta$ are exactly the x- and y-components of the offset, in analogy to the approximate results of (38) for tilts.

A similar treatment may be applied to a discrete diameter change. Here the spurious modes are the higher order TE_{0m};[15] again for small offsets only the forward modes need be considered. This case differs in one fundamental respect from that of the offset. For an offset the TE_{01} signal mode and the TE_{1m} spurious modes have a different angular dependence; for a diameter change the TE_{01} signal mode and the higher order TE_{0m} spurious modes have the same (i.e., no) angular dependence. Thus, for a diameter change the signal and all spurious modes are coupled to each other to first order.

First by conservation of energy (true in helix as well as copper guide, because the TE_{0m} modes are the same in both) (6) yields

$$\tilde{S}S^* = S\tilde{S}^* = [1]. \tag{48}$$

Next, consider the cascade connection of two identical diameter changes connected back-to-back. As in the case of an offset, this yields

$$\tilde{S}S = S\tilde{S} = [1]. \tag{49}$$

From (48) and (49) we find that

$$S = S^* = \text{pure real}. \tag{50}$$

However, there is no operation corresponding to the 180° rotation, used for tilts and offsets, because the signal and spurious modes have the same symmetry in the present case. While we have obtained no further information from general considerations than contained in (49) and (50), for the case of a single spurious mode the scattering matrix for a diameter change is identical to that of (43) for an offset.

For small diameter changes, Morgan[15,16] gives the coupling coefficients s_{0j} in terms of the change in radius Δr as follows:

$$s_{0j} = C_{d(j)}{}^{+} \cdot \Delta r + \cdots, \quad j > 0. \tag{51}$$

$C_{d(j)}{}^{\pm}$ is given in Appendix A.

There is of course only a single polarization of each spurious mode in this case, and consequently, there is no analysis in the present case corresponding to those for tilts and offsets with two polarizations.

2.1.4 *Discrete Mode Converters in Helix Guide*

While the above results for diameter changes apply equally well to both helix and copper guide, those for tilts and offsets apply to only copper guide (strictly speaking, ideal lossless metallic guide). This is so because (6) no longer holds true in helix; energy is not conserved in helix, and in addition the various normal modes of helix are not even orthogonal with respect to power.[22] The coupling coefficients for discrete mode converters in helix have been obtained by Unger.[19] However, one useful result is readily obtained from general considerations without performing a detailed field analysis.

We show that at a discrete tilt or offset, the TE_{01} transfer coefficient s_{00} (the upper left-hand element in the scattering matrices for a tilt or offset given in Sections 2.1.2 and 2.1.3 above) is identical in both copper and helix guides, if we neglect backward modes and include all forward modes. This fact will permit the average TE_{01} loss in helix guide with discrete random tilts and offsets to be readily calculated in terms of similar results for copper guide.

The above statement is proven as follows. First consider an offset or tilt as a joint between a helix and a copper guide, with a unit TE_{01}

wave incident from the helix. If backward waves are neglected, the forward waves in the copper guide will be identical to those in a copper-copper joint because the incident TE_{01} is the same in helix as it would be in copper. Therefore, the TE_{01} transfer coefficient s_{00} is the same for this helix-copper joint as for a copper-copper joint. Now reverse input and output terminals, so that the TE_{01} is incident from the copper guide, and TE_{01} and spurious modes travel away from the joint in helix. The spurious modes are now quite different than before, since they must be normal modes of helix guide; however, by reciprocity s_{00} must remain the same. Finally, we may replace the copper guide containing the incident TE_{01} with helix without further altering the fields in any way. Thus if backward modes are neglected, s_{00} is identical in helix and copper guides with identical tilts or offsets.

This conclusion has been verified experimentally by the authors in 2-inch diameter helix guide at a frequency of 55 kmc. It has also been verified by a field analysis by H. G. Unger.[20]

2.2 *The Discrete Case — Single Spurious Mode*

We next apply the results of Section 2.1 to the study of long guides with many discrete mode converters separated by guide sections that are ideal, i.e., geometrically perfect right-circular cylinders. We restrict our attention to the case of a single spurious mode, in addition to the TE_{01} signal mode. (If the spurious mode is polarized, such as TE_{1m}^{+}, we consider only one of its linear polarizations.)

The over-all transmission matrix for such a guide with N discrete mode converters consists of a product of $2N$ matrices, one matrix for each mode converter (as given in the preceding section) and one diagonal matrix for each section of ideal guide. These matrix results are then used to derive a perturbation theory, valid when the mode converters are sufficiently small, that greatly simplifies further calculations.

2.2.1 *Matrix Analysis*

Consider the guide illustrated schematically in Fig. 6. This guide consists of N discrete mode converters separated by N sections of ideal copper guide, of length l_k. Since we consider only a single spurious mode, if the discrete mode converters are tilts or offsets they must lie in a single plane (taken to be the $\varphi = 0$ plane in the notation of Section 2.1). We seek the response of such a guide to a unit input TE_{01} wave.

The scattering matrix S_k for the k^{th} mode converter is given in Section 2.1 for the case of a single spurious mode, i.e., (17) and (18) for tilts,

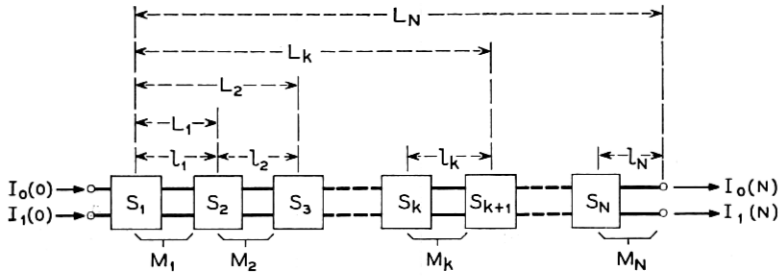

$L_k = \sum_{m=1}^{k} l_m$

S_k = SCATTERING MATRIX FOR k^{TH} MODE CONVERTER

M_k = SCATTERING MATRIX FOR k^{TH} MODE CONVERTER PLUS FOLLOWING SECTION OF GUIDE

I_0 = SIGNAL MODE (TE_{01}) NORMALIZED AMPLITUDE

I_1 = SPURIOUS MODE NORMALIZED AMPLITUDE

Fig. 6 — Waveguide line with discrete mode converters separated by ideal guide sections.

(43) and (44) for offsets, (43) and (51) for diameter changes. In the ideal guide sections connecting the discrete mode converters, the signal and spurious modes propagate independently with their respective propagation constants; the scattering matrix W_k corresponding to the k^{th} section of ideal guide, of length l_k as shown in Fig. 6, is given by

$$W_k = \begin{bmatrix} e^{-\Gamma_0 l_k} & 0 \\ 0 & e^{-\Gamma_1 l_k} \end{bmatrix}, \tag{52}$$

where Γ_0 is the propagation constant for the TE_{01} signal mode, Γ_1 the propagation constant for the spurious mode. Thus, the scattering matrix M_k for the k^{th} mode converter plus the (following) k^{th} section of guide, as shown in Fig. 6, is

$$M_k = W_k \cdot S_k \,. \tag{53}$$

For tilts M_k is given as

$$M_k = \begin{bmatrix} e^{-\Gamma_0 l_k} \cdot \sqrt{1 - c_k^2} & j e^{-\Gamma_0 l_k} \cdot c_k \\ j e^{-\Gamma_1 l_k} \cdot c_k & e^{-\Gamma_1 l_k} \cdot \sqrt{1 - c_k^2} \end{bmatrix}, \tag{54}$$

with c_k given by (18). For offsets and diameter changes

$$M_k = \begin{bmatrix} e^{-\Gamma_0 l_k} \cdot \sqrt{1 - c_k^2} & e^{-\Gamma_0 l_k} \cdot c_k \\ -e^{-\Gamma_1 l_k} \cdot c_k & e^{-\Gamma_1 l_k} \cdot \sqrt{1 - c_k^2} \end{bmatrix}, \tag{55}$$

with c_k given by (44) and (51) respectively.

The over-all transmission matrix T for the entire guide, N sections long, will be

$$T = \begin{bmatrix} T_{00} & T_{01} \\ T_{10} & T_{11} \end{bmatrix} = \prod_{k=N}^{1} M_k = M_N \cdot M_{N-1} \cdots M_2 \cdot M_1 , \qquad (56)$$

and the output mode amplitudes will be given in terms of the input mode amplitudes by

$$\begin{bmatrix} I_0(N) \\ I_1(N) \end{bmatrix} = T \begin{bmatrix} I_0(0) \\ I_1(0) \end{bmatrix}. \qquad (57)$$

We assume the guide is excited by a pure TE_{01} wave of unit amplitude and zero phase; the initial conditions on (57) become

$$I_0(0) = 1, \qquad I_1(0) = 0. \qquad (58)$$

Then,

$$I_0(N) = T_{00} I_0(0) = T_{00} , \quad TE_{01} \text{ gain.} \qquad (59)$$

$$I_1(N) = T_{10} I_0(0) = T_{10} , \quad TE_{01}\text{-spurious mode transfer coefficient.} \qquad (60)$$

It will subsequently be convenient to normalize these quantities as follows:

$$T_{00} = e^{-\Gamma_0 L_N} \cdot G_0 ; \quad G_0 = TE_{01} \text{ normalized gain.} \qquad (61)$$

$$T_{10} = e^{-\Gamma_1 L_N} \cdot G_1 ; \quad G_1 = TE_{01}\text{-spurious mode normalized transfer coefficient.} \qquad (62)$$

In each case, the propagation factor of the corresponding mode has been removed; as shown in Fig. 6, L_N is the total length of the N sections of guide being considered. Since TE_{01} has a lower heat loss (i.e., $\alpha_0 = \text{Re } \Gamma_0$) than any other mode, in a physical guide $G_0 \leqq 1$.

The exact solution above is of limited value both because of its complexity and also because, as discussed in Section 2.1, the available expressions for the coupling coefficients of discrete mode converters are valid only to first order. Consequently, we seek approximate expressions for T_{00} and T_{10}, or equivalently G_0 and G_1, valid when the coupling coefficients are sufficiently small that the guide departs only slightly from ideal. Under these conditions, it will be shown that G_1 is of first order and G_0 departs from unity only to second order.

It is convenient to write

$$G_0 = 1 - \rho, \tag{63}$$

where ρ, the (complex) departure of G_0 from unity, will be of second order. We further define the TE_{01} normalized magnitude g, complex loss Λ, loss (in nepers) A, and phase Θ as follows:

$$\begin{aligned} G_0 &= ge^{j\Theta} = e^{-\Lambda} = e^{-A}e^{j\Theta} = 1 - \rho; \\ \Lambda &= A - j\Theta. \end{aligned} \tag{64}$$

Then if the coupling coefficients are sufficiently small so that $|\rho| \ll 1$, we have to second order:

$$g \approx 1 - \text{Re } \rho. \tag{65a}$$

$$\Lambda \approx \rho. \tag{65b}$$

$$A \approx \text{Re } \rho. \tag{65c}$$

$$\Theta \approx - \text{Im } \rho. \tag{65d}$$

2.2.2 *Perturbation Theory*

Consider the transmission matrix T of (56), with the M_k given by (54) or (55). Let us expand the square root in the diagonal elements of (54) or (55) in a power series as follows;

$$\sqrt{1 - c_k^2} = 1 - \tfrac{1}{2}c_k^2 - \tfrac{1}{8}c_k^4 + \cdots. \tag{66}$$

It is apparent from the rules of matrix multiplication that the components of T may be expressed as power series in the c_k's. Since each c_k may be expressed as a power series in the appropriate geometric parameter, with the first term given by (18), (44) or (51), we can thus obtain expressions for G_1 and G_0 as power series in the geometric parameters. The first-order results of (18), (44) and (51) are sufficient to give G_1 to first order, G_0 to second order; if the mode converters are sufficiently small we may hope that these results will give a valid approximation for the TE_{01} gain and the TE_{01}-spurious mode transfer coefficient.

We first determine the first few terms of expansions for T_{10} and T_{00}. For convenience, we write for M_k in (56)

$$M_k = \begin{bmatrix} A_k & \epsilon_k \\ \delta_k & B_k \end{bmatrix}, \tag{67}$$

where A_k, ϵ_k, δ_k and B_k are determined by comparison with (54) or

(55). For small coupling, A_k and B_k will have magnitudes a little less than 1, while ϵ_k and δ_k will have magnitudes much smaller than 1. In writing out T_{10} and T_{00}, we group terms according to the number of "small" quantities (i.e., ϵ's and δ's) they contain. Thus, we have:

$$T_{10} = \sum_{i=1}^{N} A_1 \cdots A_{i-1}\delta_i B_{i+1} \cdots B_N + \sum_{i=1}^{N-2} \sum_{j=i+1}^{N-1} \sum_{k=j+1}^{N} A_1 \cdots A_{i-1}\delta_i B_{i+1} \cdots \cdots B_{j-1}\epsilon_j A_{j+1} \cdots A_{k-1}\delta_k B_{k+1} \cdots B_N + \cdots . \tag{68}$$

$$T_{00} = A_1 \cdots A_N + \sum_{i=1}^{N-1} \sum_{j=i+1}^{N} A_1 \cdots A_{i-1}\delta_i B_{i+1} \cdots B_{j-1}\epsilon_j A_{j+1} \cdots A_N + \sum_{i=1}^{N-3} \sum_{j=i+1}^{N-2} \sum_{k=j+1}^{N-1} \sum_{l=k+1}^{N} A_1 \cdots A_{i-1}\delta_i B_{i+1} \cdots B_{j-1}\epsilon_j A_{j+1} \cdots \cdots A_{k-1}\delta_k B_{k+1} \cdots B_{l-1}\epsilon_l A_{l+1} \cdots A_N + \cdots . \tag{69}$$

Consider first (68) for T_{10}. Referring to (67), (66), (54) and (55), the successive terms of (68) (of which we have written down the first two) contain components of the following orders in the c_k :

term	*order of components*
1	$c, c^3, c^5, \cdots$
2	$c^3, c^5, c^7, \cdots$
. . . . .	

Equation (18), (44) or (51) gives the c_k to first order in terms of the tilts α_k, offsets b_k, or diameter changes Δr_k. Therefore, we may obtain T_{10} to first order in the geometric parameters by retaining only the components of order c, which occur in only the first term of (68) (the single summation), and using Morgan's first-order coupling coefficients. Indeed, since we do not have the coupling coefficients to more than first order, it would be totally unjustified to retain any additional components in (68), and in particular, to seek an exact result for the matrix multiplication of (56) via numerical techniques or otherwise, without first obtaining the coupling coefficients c_k to higher order.

Similarly, the successive terms of (69) for T_{00} contain components of the following orders in the c_k :

term	*order of components*
1	$c^0, c^2, c^4, \cdots$
2	$c^2, c^4, c^6, \cdots$
. . . . .	

We obtain T_{00} to second order in the geometric parameters by retaining only the components of order c^0 and c^2 in the first term and the components of order c^2 in the second term, and using Morgan's first-order coupling coefficients. As above, any additional terms would be unjustified. We note that there are no first-order terms present in T_{00}.

We thus obtain the following approximate results for G_0 and G_1, the normalized transmission parameters defined in (61) to (64), from (66) to (69), (54), (55) and (18), (44) and (51). In these results we use the differential propagation constant $\Delta\Gamma$, defined as

$$\Delta\Gamma = \Delta\alpha + j\Delta\beta = \Gamma_0 - \Gamma_1 . \tag{70a}$$

$$\Delta\alpha = \alpha_0 - \alpha_1 , \quad \Delta\beta = \beta_0 - \beta_1 . \tag{70b}$$

The real and imaginary parts of $\Delta\Gamma$, $\Delta\alpha$ and $\Delta\beta$ respectively, are called the differential attenuation constant and the differential phase constant respectively. Since the TE_{01} signal mode has lower heat loss than any other mode, $\Delta\alpha < 0$ throughout the present paper. The geometry of the guide is shown in Fig. 6; L_{k-1} is the length of guide up to the k^{th} mode converter, l_k the distance between the k^{th} and the $(k+1)^{\text{th}}$ mode converters. x_i denotes Morgan's first-order approximation for the coupling coefficient of the i^{th} mode converter.

For tilts and offsets the diameter of the different guide sections is of course identical, so that $\Delta\Gamma$ is strictly constant. This is not true for diameter changes, so that strictly speaking we should include in the analysis the fact that $\Delta\Gamma$ changes from section to section. However, we assume that the total range of the guide diameter is very small, centered about its nominal value, and neglect the small changes in $\Delta\Gamma$ in all following analysis, both for the discrete case and for the continuous case. This approximation is not necessary; it would be possible to include the variation of $\Delta\Gamma$ in the present analysis without great difficulty. However, we choose to ignore this effect without careful study in the interests of simplicity.

i. G_0 — Tilts, Offsets and Diameter Changes

$$G_0 = 1 - \rho. \tag{71a}$$

$$\rho \approx \tfrac{1}{2}\sum_{i=1}^{N} x_i^2 + \sum_{i=1}^{N-1}\sum_{j=i+1}^{N} x_i x_j e^{\Delta\Gamma(L_{j-1}-L_{i-1})} = \tfrac{1}{2}\sum_{i=1}^{N}\sum_{j=1}^{N} x_i x_j e^{\Delta\Gamma|L_{j-1}-L_{i-1}|}. \tag{71b}$$

Special case — equally spaced mode converters

$$l_k = l_0\,, \qquad L_k = kl_0\,. \tag{71c}$$

$$\begin{aligned}\rho &\approx \tfrac{1}{2}\sum_{i=1}^{N} x_i^{\,2} + \sum_{i=1}^{N-1}\sum_{j=i+1}^{N} x_i x_j e^{\Delta\Gamma l_0(j-i)} \\ &= \tfrac{1}{2}\sum_{i=1}^{N}\sum_{j=1}^{N} x_i x_j e^{\Delta\Gamma l_0|j-i|} \qquad (71d)\\ &= \tfrac{1}{2}\sum_{i=1}^{N} x_i^{\,2} + \sum_{k=1}^{N-1} e^{\Delta\Gamma l_0 \cdot k}\sum_{i=1}^{N-k} x_i x_{i+k}\,.\end{aligned}$$

$$x_i = \begin{cases} C_t\cdot\alpha_i\,, & \text{tilts.}\\ C_o\cdot b_i\,, & \text{offsets.}\\ C_d\cdot\Delta r_i, & \text{diameter changes.}\end{cases} \tag{71e}$$

ii. G_1 — *Tilts*

$$G_1 \approx j\sum_{i=1}^{N} x_i e^{-\Delta\Gamma L_{i-1}}. \tag{72a}$$

Special case — equally spaced mode converters

$$l_k = l_0\,, \qquad L_k = kl_0\,. \tag{72b}$$

$$G_1 \approx j\sum_{i=1}^{N} x_i e^{-\Delta\Gamma l_0(i-1)}. \tag{72c}$$

$$x_i = C_t\cdot\alpha_i\,. \tag{72d}$$

iii. G_1 — *Offsets and Diameter Changes*

$$G_1 \approx -\sum_{i=1}^{N} x_i e^{-\Delta\Gamma L_{i-1}}. \tag{73a}$$

Special case — equally spaced mode converters

$$l_k = l_0\,, \qquad L_k = kl_0\,. \tag{73b}$$

$$G_1 \approx -\sum_{i=1}^{N} x_i e^{-\Delta\Gamma l_0(i-1)}. \tag{73c}$$

$$x_i = \begin{cases} C_o\cdot b_i\,, & \text{offsets.}\\ C_d\cdot\Delta r_i\,, & \text{diameter changes.}\end{cases} \tag{73d}$$

2.2.3 *Discussion*

The above results for tilts and offsets apply strictly to only lossless metallic guide, for which $\Delta\alpha = 0$. However, we expect on intuitive grounds that they provide a satisfactory approximation for real copper guide. The results for diameter changes apply equally well to both copper and helix; for tilts and offsets in helix we must use the helix guide coupling coefficients, but otherwise the analysis is the same.

The results of (71) to (73) yield the TE_{01} signal mode to second order (there are no first-order terms), the spurious mode to first order, in the appropriate geometric parameters. In each case we have determined the first correction term to the solution for a geometrically perfect guide with all $c_k = 0$, i.e., $G_0(z) = 1$, $G_1(z) = 0$ where z is distance measured along the guide axis.

A rough physical interpretation may be given for the approximate results of (71) to (73). The spurious mode at any point in the guide is regarded as a sum of waves arising at each mode converter. Each of these waves is computed by assuming an incident TE_{01} wave at each mode converter identical to the TE_{01} wave that would be present in a perfect guide, with all $c_k = 0$, and further assuming that the converted spurious mode wave is unaffected by subsequent mode converters, i.e., propagates as it would in perfect guide. The TE_{01} signal mode is regarded as the sum of three components:

1. The TE_{01} wave that would be present in a perfect guide.
2. The signal lost from TE_{01} at each mode converter, assuming an incident TE_{01} wave identical to that in perfect guide and no incident spurious mode wave.
3. A sum of waves reconverted to TE_{01} from the spurious mode at each mode converter. Each of these waves is computed by taking the approximate spurious mode as computed above, and assuming that the reconverted TE_{01} wave is unaffected by subsequent mode converters. It is easy to see that this component may be expressed as a sum over all pairs of mode converters.

The approximate solutions of (71) to (73) may be regarded as the initial terms of power series expansions in the x_i's (or equivalently the α_i's, b_i's, or Δr_i's). It is reasonable to assume that if the x_i's are sufficiently small these power series will converge sufficiently rapidly so that their first terms will provide valid approximations; under these conditions we would expect that $|\rho| \ll 1$, $|G_1| \ll 1$. However, to use these results with confidence we must have bounds on the errors introduced by these approximations that will give quantitative information on the way in which the solutions of (71) to (73) approximate the true solution. We

postpone consideration of these questions to Section 2.3 below, where we study the continuous case, since we will show there that the discrete and continuous cases are closely related to each other. It turns out that although we can give bounds on the higher terms of the series expansions that are in a sense the best possible, we still lack sufficiently precise information to make any useful statement on the way in which the perturbation solutions approximate the true solutions. Consequently, confidence in the accuracy of practical calculations using the results of (71) to (73) can at present be justified only on intuitive grounds.

In the region where we hope the perturbation solution is valid, $|\rho| \ll 1$. Under these conditions, the TE_{01} normalized magnitude g, loss A, and phase Θ are given approximately by (65), where ρ is given by (71). If $|\rho|$ is not much smaller than 1, it would seem that the approximation of (65) must be invalid. However, it will be shown in Section 2.3 on the continuous case that (65b), (65c), and (65d) together with (71) remain plausible for a wide class of interesting cases where the magnitude of the right-hand side of (71b) or (71d) becomes much greater than 1 and (65a) fails, although here again the justification is no more rigorous than that for (71) to (73) when $|\rho| \ll 1$, $|G_1| \ll 1$. This extension is important, for otherwise we should be limited to considering only cases where the total loss $|\Lambda|$, and hence, A and $|\Theta|$, are small.

2.3 *The Continuous Case — Single Spurious Mode*

In this section, we study mode conversion caused by distributed geometric imperfections, such as continuous curvature of the guide axis or continuous variation of the guide diameter. We discuss briefly the general telegraphist's equations or coupled line equations for the general case, but again restrict the detailed treatment to the case of a single spurious mode. (If the spurious mode is not TE_{0m}, we consider only one of its linear polarizations.)

It is obvious that a close relationship must exist between corresponding discrete and continuous cases. A guide with an arbitrary curved axis may be regarded as the limit of a guide with many small discrete tilts; similarly, a guide with a continuous diameter variation may be regarded as the limit of a guide with many small discrete diameter changes. We will show how the matrix equations for the discrete case and the differential equations (coupled line equations) for the continuous case may be obtained from each other by suitable limiting processes.

We next discuss the perturbation theory for the coupled line equations, and show its relationship to the discrete perturbation theory of Section

2.2. An improved perturbation theory for the TE_{01} complex loss $\Lambda = A - j\Theta$ [see (64)] is given that permits the treatment of many cases of practical interest.

For moderate lengths of copper guide the differential loss is small compared to 1, $| \Delta\alpha | L \ll 1$, where L is the guide length. We obtain an approximate treatment for this case by setting $\Delta\alpha = 0$, as in lossless metallic guide. The TE_{01} loss A for this case may be expressed in terms of the Fourier coefficients of the coupling coefficient $c(z)$; this treatment makes evident the relationship between the power spectrum of the coupling coefficient and the corresponding transmission statistics of the TE_{01} loss.

Finally, we discuss Morgan's coupling coefficients for general continuous cross-sectional deformations of copper guide, and the relationship between the various copper guide coupling coefficients.

2.3.1 *Generalized Telegraphist's Equations*

By means of the generalized telegraphist's equations,[4] Maxwell's equations for the fields in a deformed guide may be expressed in terms of the normal modes of the undeformed guide;

$$\frac{dI_m}{dz} = \sum_n \kappa_{mn} I_n . \tag{74}$$

I_m represents the normalized complex amplitude of the m^{th} mode and the summation is extended over all modes. κ_{mm} represents the propagation constant of the m^{th} mode; κ_{mn}, with $m \neq n$, represents the coupling coefficient between the n^{th} and m^{th} modes. The κ_{mn} are functions of the geometry of the guide imperfection. Of course, (74) is in rather general symbolic form; in particular problems a more specific notation is often used to denote the various modes. For example, each subscript in (74) often becomes a double subscript, to conform to the usual ways of indexing waveguide modes. Square brackets enclosing a subscript pair are often used to indicate a TE mode, round brackets a TM mode; some sort of notation, such as $\pm$ superscripts or different symbols, is used to differentiate between forward and backward modes.[2]

The κ_{mn} have been evaluated for a variety of different types of imperfections in a variety of guides, as discussed in the introduction to Section II. Morgan has given the κ_{mn} for curved metallic waveguide filled with an inhomogeneous dielectric.[2] For a homogeneous lossless dielectric, the propagation constants κ_{mm} are simply equal to the corresponding propagation constants in undeformed metallic guide;[2]

$$\kappa_{mm} = \pm j\beta_m . \tag{75}$$

Morgan finds that curvature couples the TE_{01}^{+} to only TM_{11}^{+} and $TE_{1m}^{\pm}$. (This should not be taken to mean that no other spurious modes will be excited in a curved guide with a homogeneous dielectric; such other modes will indeed arise, e.g., because of the coupling between TE_{1m} and TE_{2m}. However, in good guides these other modes will normally be negligible compared to the first-order spurious modes.) Using his results the κ's of (74) involving the TE_{01}^{+} mode may be expressed in terms of the C_t's of (18) and Appendix A as follows, for a curved circular guide with a homogeneous dielectric:

$$\kappa_{[01]^+[1m]^\pm} = \kappa_{[1m]^\pm[01]^+} = \frac{jC_{t[m]}^{\pm}}{R(z)}, \tag{76a}$$

$$\kappa_{[01]^+(11)^+} = \kappa_{(11)^+[01]^+} = \frac{jC_{t(11)}^{+}}{R(z)}. \tag{76b}$$

$R(z)$ in (76a) and (76b) is the radius of curvature of the axis of the curved guide, with z measured along the curved axis; the curvature of the axis is confined to a single plane. Similarly, Unger[10] has evaluated the κ_{mn} for a tapered metallic waveguide as follows:†

$$\kappa_{[0m]^+[0n]^\pm} = \frac{1}{r}\frac{k_{0m}k_{0n}}{k_{0n}^2 - k_{0m}^2} \cdot \frac{\beta_{0n} \pm \beta_{0m}}{\sqrt{\beta_{0m}\beta_{0n}}}\frac{dr(z)}{dz}, \tag{77}$$

$$m \neq n \text{ for the upper signs.}$$

In (77), $r(z)$ is the radius of the guide, the k's are the Bessel roots of the modes in question (see Appendix A). When the incident mode is the TE_{01}, (77) becomes

$$\kappa_{[01]^+[0m]^\pm} = C_{d[m]}^{\pm} \cdot \frac{dr(z)}{dz}, \quad m \neq 1, \tag{78}$$

in terms of C_d of (51) and Appendix A. Finally, we note from (77) that if both modes are forward modes,

$$\kappa_{[0m]^+[0n]^+} = -\kappa_{[0n]^+[0m]^+}, \tag{79}$$

which, as we shall subsequently see, must be true by (43).

Various geometric imperfections in helix guide have been similarly treated by Unger.[3,19,20,21]

The generalized telegraphist's equations of (74) contain an infinite number of modes. To simplify the problem, we wish to approximate the true situation with a finite number of modes; indeed, in much of the present study we include only two modes, the TE_{01} signal mode and the

† The sign of the second term inside the summation in (40) of Reference 10 appears to be in error.

most important spurious mode. It is obvious that this approximation must distort the results in some respects; however, we hope that if the significant spurious modes are included, any errors will be small. Thus, in (74) we will set all I's equal to zero except those corresponding to the TE_{01}^{+} signal mode and one or a few of the forward spurious modes. Other ways of approximating the true situation with a finite number of modes might of course be possible, but we choose this one as the simplest.

In (76) and (78) above we observe that the coupling coefficients for continuous bends and diameter changes may be expressed in terms of the coupling coefficients for discrete tilts and diameter changes. This, plus the obvious fact that a continuous deformation may be regarded as the limit of many small, closely spaced discrete imperfections, suggests a closer study of the relation between the discrete and continuous cases. In Sections 2.3.2 and 2.3.3 below we study the correspondence between the coupled line equations for the continuous case and the matrix equations of Section 2.2.1 above for the discrete case.

2.3.2 *Transformation from the Discrete to the Continuous Case*

Consider a lossless metallic guide containing many small discrete mode converters spaced an equal distance Δz apart. Fig. 7 illustrates three cases of interest — tilts, offsets, and diameter changes — with of course a greatly exaggerated vertical scale. c_k is in each case the conversion coefficient in the corresponding matrix, (17) or (43) for tilts or offsets and diameter changes respectively; c_k is given by (18), (44), and (51) for tilts, offsets, and diameter changes respectively. Then it is clear that by the proper limiting process, in which $\Delta z \to 0$ and the discontinuities become smaller and more closely spaced, we may approach the continuous deformations illustrated in Fig. 7 by the dotted lines.

The limiting continuous deformation of Fig. 7(a) corresponds to a guide with a continuously varying curvature of its axis. The continuous deformation of Fig. 7(b) corresponds to a waveguide made of very thin circular punchings which may slide with respect to each other like a stack of cards. Finally, the continuous deformation of Fig. 7(c) corresponds to a continuous taper. The case of Fig. 7(a) will be important in determining the effect of random straightness deviation on the TE_{01} transmission. For the continuous bend and offset of Figs. 7(a) and 7(b) the guide axis must lie in a single plane if the analysis is to be restricted to a single polarization of the most important spurious mode (TE_{12}^{+}).

For purposes of illustration we consider the transition to the continuous bend, illustrated in Fig. 7(a). A larger-scale drawing for this case

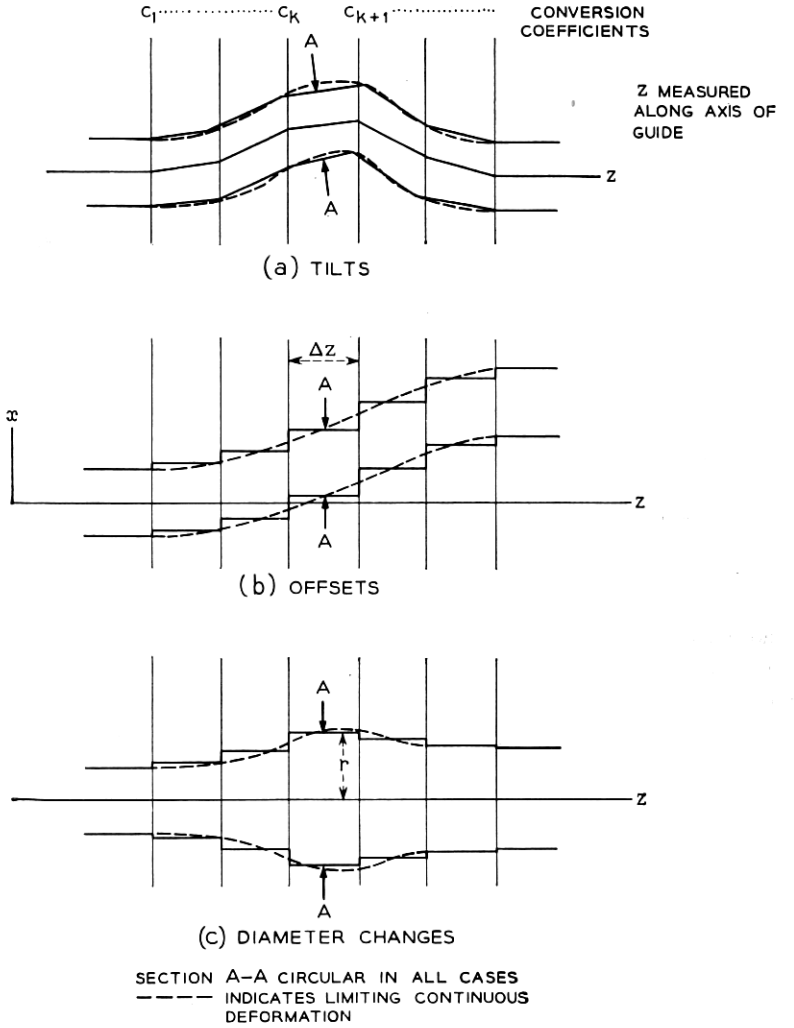

Fig. 7 — Waveguides with tilts, offsets, and diameter changes.

is shown in Fig. 8; only the center line of the continuously bent guide and of the tilt approximation to it are shown, for the two adjacent sections lying on either side of the k^{th} tilt.

Referring to Fig. 6, we set the distance between discrete tilts l_k equal to Δz. Let $I_0(z)$ and $I_1(z)$ denote the TE_{01} and spurious mode complex amplitudes just to the left of the k^{th} tilt; then $I_0(z + \Delta z)$ and $I_1(z + \Delta z)$

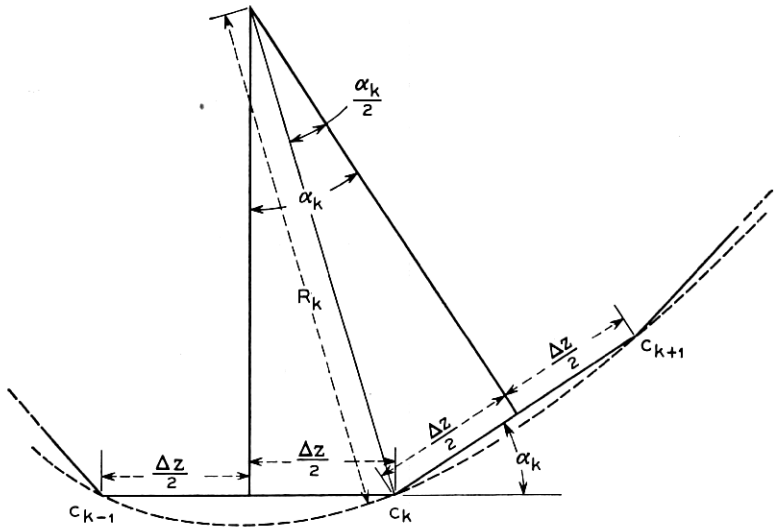

Fig. 8 — Fig. 7(a) in larger scale.

denote the corresponding complex mode amplitudes just to the left of the $(k+1)^{\text{th}}$ tilt. Then taking (17) for the scattering matrix of the tilt, and setting $l_k = \Delta z$ in (52), (53), and (54), we have

$$\begin{bmatrix} I_0(z+\Delta z) \\ I_1(z+\Delta z) \end{bmatrix} = \begin{bmatrix} e^{-\Gamma_0 \Delta z}\sqrt{1-c_k^2} & je^{-\Gamma_0 \Delta z}c_k \\ je^{-\Gamma_1 \Delta z}c_k & e^{-\Gamma_1 \Delta z}\sqrt{1-c_k^2} \end{bmatrix} \begin{bmatrix} I_0(z) \\ I_1(z) \end{bmatrix}, \tag{80}$$

where c_k is the conversion coefficient for the k^{th} tilt. From (18)

$$c_k = C_t \cdot \alpha_k + \cdots, \tag{81}$$

where C_t is Morgan's coupling coefficient for tilts for the spurious mode in question, given in Appendix A. From Fig. 8

$$\alpha_k = \frac{\Delta z}{R_k} + \cdots. \tag{82}$$

Thus,

$$c_k = \frac{C_t}{R_k}\Delta z + \cdots, \tag{83}$$

where the dots in (82) and (83) represent terms of higher than first order in Δz.

Expanding the exponentials and the square roots in the matrix of (80) in power series [see (66)], making use of (83), and writing the right-hand sides of the resulting equations as power series in Δz, we have

$$\begin{aligned} I_0(z + \Delta z) &= I_0(z) + \left[-\Gamma_0 I_0(z) + j \frac{C_t}{R_k} I_1(z) \right] \Delta z + \cdots \\ I_1(z + \Delta z) &= I_1(z) + \left[-\Gamma_1 I_1(z) + j \frac{C_t}{R_k} I_0(z) \right] \Delta z + \cdots . \end{aligned} \tag{84}$$

We transfer the terms $I_0(z)$ and $I_1(z)$ to the left-hand sides of these equations and divide by Δz. Then as $\Delta z \to 0$, $R_k \to R(z)$, where $R(z)$ is the radius of curvature of the guide axis, and (84) becomes

$$\begin{aligned} I_0'(z) &= -\Gamma_0 I_0(z) + jc(z) I_1(z) , \\ I_1'(z) &= jc(z) I_0(z) - \Gamma_1 I_1(z) , \end{aligned} \tag{85}$$

$$c(z) = \frac{C_t}{R(z)}, \quad \text{coupling coefficient}, \tag{86}$$

where the primes denote differentiation with respect to z, and $R(z)$ is the radius of curvature of the guide axis.

We now compare (85) and (86) with (74) to (76); in the case of lossless metallic guide, where $\Gamma_0 = j\beta_0$, $\Gamma_1 = j\beta_1$, the two sets of equations are identical if we retain only two modes in the results of (74) to (76). Thus by taking the proper limiting form of Morgan's results for discrete tilts we arrive at Morgan's results for continuous bends obtained via the generalized telegraphist's equations, in the two-mode case. It is easy to see that this method extends readily to additional first-order spurious modes. It should in principle be possible to include as many modes as desired in this type of discussion, but such calculations have not been actually carried out. We will be content in the present paper to take the two-mode model as suggestive of these more general results.

As in the discrete case, we assume the guide is excited by a pure TE_{01} wave of unit amplitude. Thus, the initial conditions on the differential equations (85) become

$$I_0(0) = 1, \qquad I_1(0) = 0, \tag{87}$$

corresponding to (58) for the discrete case. Then $I_0(z)$ will be the TE_{01} gain, $I_1(z)$ the TE_{01}-spurious mode transfer coefficient, corresponding to (59) and (60).

It proves convenient to follow the normalization used in the discrete case [see (61) and (62)], removing the propagation factor of each mode in ideal guide;

$$I_0(z) = e^{-\Gamma_0 z} \cdot G_0(z) \tag{88}$$

$$I_1(z) = e^{-\Gamma_1 z} \cdot G_1(z). \tag{89}$$

$G_0(z)$ and $G_1(z)$ are again the TE_{01} normalized gain and the TE_{01}-spurious mode normalized transfer coefficient. Substituting the transformation of (88) and (89) into (85), we have:

$$\begin{aligned} G_0'(z) &= jc(z)e^{\Delta\Gamma z}G_1(z) \\ G_1'(z) &= jc(z)e^{-\Delta\Gamma z}G_0(z) \end{aligned} \tag{90}$$

$\Delta\Gamma = \Gamma_0 - \Gamma_1$, differential propagation constant.

$$c(z) = \frac{C_t}{R(z)}, \quad \text{coupling coefficient.} \tag{91}$$

The initial conditions of (87) become

$$G_0(0) = 1, \qquad G_1(0) = 0. \tag{92}$$

A similar treatment may be given for the limiting case of many discrete offsets or diameter changes, illustrated in Figs. 7(b) and 7(c) respectively. For continuous offsets we find:

$$\begin{aligned} I_0'(z) &= -\Gamma_0 I_0(z) + c(z)I_1(z), \\ I_1'(z) &= -c(z)I_0(z) - \Gamma_1 I_1(z). \end{aligned} \tag{93}$$

$$c(z) = C_o \cdot x'(z), \quad \text{coupling coefficient.} \tag{94}$$

C_o is Morgan's offset coupling coefficient for the spurious mode in question, given in Appendix A. $x(z)$ is the transverse displacement of the guide axis, as illustrated in Fig. 7(b); primes of course denote differentiation with respect to z. Equations (93) and (94) must agree with the generalized telegraphist's equations for a guide with a continuous offset, when restricted to two modes. Using the transformation of (88) and (89), (93) and (94) become:

$$\begin{aligned} G_0'(z) &= c(z)e^{\Delta\Gamma z}G_1(z), \\ G_1'(z) &= -c(z)e^{-\Delta\Gamma z}G_0(z), \end{aligned} \tag{95}$$

$$\begin{aligned} \Delta\Gamma &= \Gamma_0 - \Gamma_1\ ; \quad \text{differential propagation constant.} \\ c(z) &= C_o \cdot x'(z), \quad \text{coupling coefficient.} \end{aligned} \tag{96}$$

The continuous diameter change may be similarly treated by replacing $x'(z)$ by $r'(z)$, C_o by C_d in (93) to (96), where $r(z)$ is the guide radius.

2.3.3 *Transformation from the Continuous to the Discrete Case*

We next determine the scattering matrix for a discrete mode converter by considering the limiting form of the generalized telegraphist's equations as the continuous coupling coefficient approaches a δ-function. For purposes of illustration we consider the case of a discrete tilt, regarded as the limiting form of a continuous bend. We again restrict our treatment to only two modes, the TE_{01} signal mode and a single spurious mode, for simplicity.

Fig. 9 shows a tilt of angle α obtained as the limit of a continuous bend. From (86) or (91) the continuous coupling coefficient is given by

$$c(z) = \begin{cases} 0, & z < 0; \\ \dfrac{C_t \alpha}{\Delta}, & 0 < z < \Delta; \\ 0, & \Delta < z. \end{cases} \tag{97a}$$

$$\lim_{\Delta \to 0} c(z) = C_t \alpha \cdot \delta(z). \tag{97b}$$

Thus the coupling coefficient is zero for $z < 0$ and $z > \Delta$, constant in the region $0 < z < \Delta$, z being measured along the guide axis as usual. Now exact solutions for (85) or (90) are known for only a few special $c(z)$; indeed this is why we are forced to use approximate solutions of various types in the present paper. One important case in which exact solutions are available is the present case $c(z) =$ constant;[17] this is obvious from the fact that the equations (85) then become simply two simultaneous differential equations with constant coefficients, whose solutions are well known.

The solution for (85) with $c(z) = c_0$ is given as follows:

$$\begin{bmatrix} I_0(z) \\ I_1(z) \end{bmatrix} = T(z) \begin{bmatrix} I_0(0) \\ I_1(0) \end{bmatrix} \tag{98a}$$

$$T(z) = \frac{\exp\left(-\dfrac{\Gamma_0 + \Gamma_1}{2} z\right)}{K_+ - K_-} \cdot \begin{bmatrix} -K_- e^{(\Delta\Gamma/2)z\sqrt{}} + K_+ e^{(-\Delta\Gamma/2)z\sqrt{}} & e^{(\Delta\Gamma/2)z\sqrt{}} - e^{(-\Delta\Gamma/2)z\sqrt{}} \\ e^{(\Delta\Gamma/2)z\sqrt{}} - e^{(-\Delta\Gamma/2)z\sqrt{}} & K_+ e^{(\Delta\Gamma/2)z\sqrt{}} - K_- e^{(-\Delta\Gamma/2)z\sqrt{}} \end{bmatrix} \tag{98b}$$

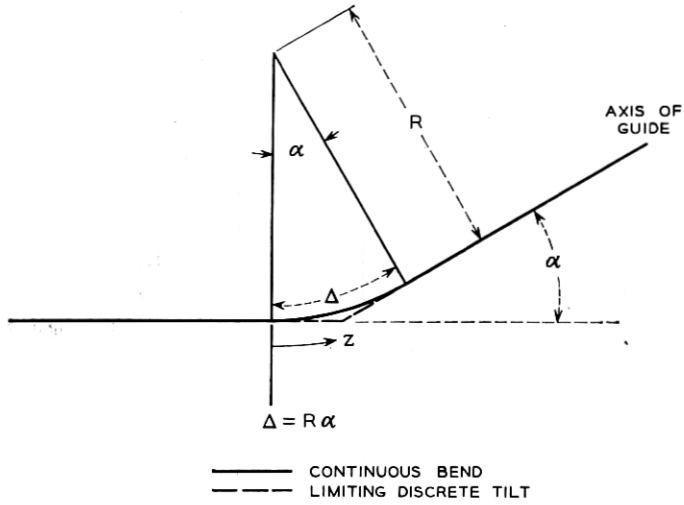

Fig. 9 — Tilt of angle α as limit of continuous bend.

$$K_{\pm} = -j\frac{1 \pm \sqrt{\ }}{2\frac{c_0}{\Delta\Gamma}}; \qquad K_+K_- = -1 \tag{98c}$$

$$\frac{1}{K_+ - K_-} = j\frac{c_0/\Delta\Gamma}{\sqrt{\ }} \tag{98d}$$

$$\sqrt{\ } = \sqrt{1 - \left(\frac{2c_0}{\Delta\Gamma}\right)^2}. \tag{98e}$$

These results are applied to the situation of Fig. 9 and (97) by setting

$$\begin{aligned} z &\to \Delta, \\ c_0 &\to \frac{C_t\alpha}{\Delta}. \end{aligned} \tag{99}$$

Thus

$$\begin{bmatrix} I_0(\Delta) \\ I_1(\Delta) \end{bmatrix} = T(\Delta)\begin{bmatrix} I_0(0) \\ I_1(0) \end{bmatrix}. \tag{100}$$

Now in (97) and Fig. 9 let us keep α fixed and let $\Delta \to 0$, $R \to 0$; then the curved guide of Fig. 9 will approach a discrete tilt of angle α, and

the matrix T should approach the scattering matrix of this discrete tilt. From (98) and (99) we have:

$$\begin{aligned}
&\lim_{\Delta\to 0} \frac{\Delta\Gamma}{2} \sqrt{1 - \left(\frac{2C_{t}\alpha}{\Delta\Gamma\cdot\Delta}\right)^{2}} \cdot\Delta = jC_{t}\alpha \\
&\lim_{\Delta\to 0} K_{\pm} = \pm 1 \\
&\lim_{\Delta\to 0} \frac{1}{K_{+} - K_{-}} = \frac{1}{2} \\
&\lim_{\Delta\to 0} \exp\left(-\frac{\Gamma_{0} + \Gamma_{1}}{2}\Delta\right) = 1
\end{aligned} \tag{101}$$

Then from (98) to (101) we have

$$\lim_{\Delta\to 0} T(\Delta) \equiv T(0) = \begin{bmatrix} \cos C_{t}\alpha & j\sin C_{t}\alpha \\ j\sin C_{t}\alpha & \cos C_{t}\alpha \end{bmatrix} \tag{102a}$$

for

$$\lim_{\Delta\to 0} c(z) = C_{t}\alpha\cdot\delta(z) \tag{102b}$$

as the scattering matrix of a discrete tilt of angle α. This is the result given in (20) as the "exact" two-mode scattering matrix for a finite tilt.

We have thus found the scattering matrix for a two-mode, finite tilt starting from the scattering matrix for an infinitesimal tilt by first passing to the limit of continuous mode conversion and then transforming back to the discrete case by allowing the continuous coupling coefficient to approach a δ-function. Alternately, we have found the scattering matrix that satisfies the following requirements (for a single forward spurious mode):

1. Conservation of energy and symmetry.
2. Agrees with Morgan's small tilt theory [see (17) and (18)].
3. Satisfies an additional requirement for finite tilts, so that the matrix for the sum of two tilts equals the product of the matrices of the individual tilts [see (19)]. In practice the above matrix for a finite tilt will of course not provide an exact description for large tilts because of the presence of additional spurious modes.

An offset and a diameter change may be similarly treated. For a finite offset of magnitude b we have corresponding to (102) as the "exact" two-mode scattering matrix

$$\lim_{\Delta \to 0} T(\Delta) \equiv T(0) = \begin{bmatrix} \cos C_o b & \sin C_o b \\ -\sin C_o b & \cos C_o b \end{bmatrix}. \tag{103}$$

Diameter changes may be similarly treated if they are small enough so that the variation of $\Delta\Gamma$ may be neglected.

The present analysis readily extends to include additional first-order spurious modes. It should in principle be possible to generalize it further to include as many modes as desired, but such calculations have not actually been carried out.

The astute reader may have noted a potential difficulty with the analysis above. This potential paradox may be stated as follows. The above discussion shows that the continuous bend and the discrete tilt of Fig. 9 are approximately equivalent to each other so long as the following conditions are satisfied:

$$\frac{2C_t \alpha}{|\Delta\Gamma| \cdot \Delta} \gg 1. \tag{104a}$$

$$\frac{|\Delta\Gamma|}{2} \cdot \Delta \ll 1. \tag{104b}$$

But if (104a) is *not* satisfied it is no longer obvious that the discrete tilt and continuous bend remain approximately equivalent. Stated physically, consider a short continuous bend, with length Δ fixed and small enough so that $\frac{|\Delta\Gamma|}{2} \cdot \Delta \ll 1$. Then we should expect on physical grounds that this continuous bend is approximately equivalent to its corresponding discrete tilt for all angles α. However the above analysis seems to guarantee this equivalence only for large α, and not in an obvious way for small α.

While it is not obvious, it is true that this equivalence remains valid for small α, or more precisely when (104a) is violated but (104b) remains true. To study this matter let us consider the case of a guide with zero differential attenuation constant, $\Delta\alpha = 0$, so that

$$\Delta\Gamma = j\Delta\beta. \tag{105}$$

For brevity we restrict our attention to the TE_{01}-spurious mode conversion coefficient, which for convenience we call T_{10} (e.g., see the labeling of matrix components in (56)). For the discrete tilt

$$T_{10\,\text{discrete}} = j \sin C_t \alpha \cdot \exp\left(-\frac{\Gamma_0 + \Gamma_1}{2} \Delta\right). \tag{106}$$

For the continuous bend the results of (98) may be written [using (105)] as follows:

$$T_{10\text{ continuous}} = j \frac{\sin\left[f\left(\frac{2C_t\alpha}{\Delta\beta\cdot\Delta}\right)\cdot C_t\alpha\right]}{f\left(\frac{2C_t\alpha}{\Delta\beta\cdot\Delta}\right)} \cdot \exp\left(-\frac{\Gamma_0+\Gamma_1}{2}\Delta\right); \qquad (107)$$

$$f(x) = \frac{\sqrt{1+x^2}}{x}.$$

Now when $x \gg 1$, $f(x) \approx 1$; thus when $\frac{2C_t\alpha}{|\Delta\beta|\cdot\Delta} \gg 1$ [see (104a)] then from (106) and (107) we have $T_{10\text{ discrete}} \approx T_{10\text{ continuous}}$, as stated above.

Next consider the case where $\frac{2C_t\alpha}{|\Delta\beta|\cdot\Delta}$ is not large compared to 1. From (106) and (107) we see that $T_{10\text{ discrete}} \approx T_{10\text{ continuous}}$ if

$$f\left(\frac{2C_t\alpha}{\Delta\beta\cdot\Delta}\right)\cdot C_t\alpha \ll 1. \qquad (108)$$

If $\frac{2C_t\alpha}{|\Delta\beta|\cdot\Delta} \ll 1$, then noting that $f(x) \approx \frac{1}{x}$ for $x \ll 1$, (108) becomes

$$\frac{|\Delta\beta|}{2}\cdot\Delta \ll 1, \qquad (109)$$

which is simply the condition of (104b). If $\frac{2C_t\alpha}{|\Delta\beta|\cdot\Delta} = 1$, noting that $f(1) = \sqrt{2}$, (108) becomes

$$\sqrt{2}C_t\alpha \ll 1, \qquad (110)$$

i.e., the conversion coefficient must be moderately small. However a more detailed calculation for this case shows that

$$0.95T_{10\text{ discrete}} \leqq T_{10\text{ continuous}} \leqq T_{10\text{ discrete}} \qquad (111a)$$

for

$$C_t\alpha \leqq 0.55 \text{ radian}, \qquad \sin C_t\alpha \leqq 0.523. \qquad (111b)$$

The condition of (111b) is far less restrictive than that of (110); (111) states that for $\frac{2C_t\alpha}{|\Delta\beta|\cdot\Delta} = 1$, the continuous bend and its corresponding discrete tilt will have conversion coefficients that differ by less than 5

per cent provided that the coupling coefficient to the spurious mode is less than 0.523, which is quite large.

These considerations render it plausible that the corresponding discrete and continuous cases approximate each other well if (104b) is satisfied, for both large and small tilts.

2.3.4 *Perturbation Theory for the Coupled Line Equations*

Exact solutions to the coupled line equations, (85) and (86) or (90) and (91) [or (93) and (94), (95) and (96)], are known in only a very few special cases, i.e., for a few special $c(z)$. In subsequent work we will require a solution for an arbitrary $c(z)$ so that we may eventually treat the case of random $c(z)$. Therefore it is necessary to consider approximate solutions to the coupled line equations, as we have done in the discrete case.

These or similar equations arise in the design of a variety of devices in which the coupling between two modes is of interest, such as directional couplers, tapers or impedance transformers, and bends. In dominant mode transmission systems the signal mode is the forward TEM wave, the spurious mode the reflected TEM wave.[24,25,26,27] Directional couplers in a variety of waveguide systems have been similarly studied.[17,28] Tapers and bends in a variety of waveguides have been studied; several recent papers deal with this type of problem when the principal wave is the TE_{01} mode in circular guide[3,9,10] as noted earlier. In much of this work an approximate solution is used which is similar or identical to the one employed here. This approximate solution has also been used to study randomly distributed nonuniformities in ordinary (dominant mode) transmission lines.[29,30]

The approximate solution that we use is most readily found via Picard's method of successive approximations.[31,32] This is discussed in detail in a companion paper,[18] where it is shown that the solution to (90) and (91) may be written as follows:

$$G_0(z) = \sum_{n=0}^{\infty} g_{0(n)}(z), \tag{112a}$$

$$G_1(z) = \sum_{n=0}^{\infty} g_{1(n)}(z). \tag{112b}$$

$$g_{0(n)}(z) = j \int_0^z c(s)\, e^{\Delta\Gamma s} g_{1(n-1)}(s)\, ds, \quad n \geqq 1. \tag{113a}$$

$$g_{1(n)}(z) = j \int_0^z c(s)\, e^{-\Delta\Gamma s} g_{0(n-1)}(s)\, ds, \quad n \geqq 1. \tag{113b}$$

$$g_{0(0)}(z) = 1, \qquad g_{1(0)}(z) = 0. \tag{113c}$$

It is readily seen that

$$g_{0(n)}(z) = 0, \quad n \text{ odd} \tag{114a}$$

$$g_{1(n)}(z) = 0, \quad n \text{ even}. \tag{114b}$$

Bounds on the terms of the series solution of (112) are given as follows:[18]

$$|\, g_{C(n)}(z)\,| \begin{cases} \leqq \dfrac{\left[\displaystyle\int_0^z |\, c(s)\,|\, ds\right]^n}{n!}, & n \text{ even} \\ = 0, & n \text{ odd} \end{cases} \tag{115a}$$

$$|\, g_{1(n)}(z)\,| \begin{cases} = 0, & n \text{ even} \\ \leqq \dfrac{\left[\displaystyle\int_0^z |\, c(s)\,|\, ds\right]^n}{n!} e^{-\Delta\alpha z}, & n \text{ odd}. \end{cases} \tag{115b}$$

These bounds are in a sense the best possible, since cases are known where the equalities in (115a) and (115b) are satisfied.[18]

Now suppose that the series solutions for $G_0(z)$ and $G_1(z)$ given in (112) and (113) converge so rapidly that only the first nonzero terms that depend on the coupling coefficient $c(z)$ need be retained. From (114) we see that the $n = 1$ term of (112a) for $G_0(z)$ is identically zero; therefore we retain in this equation only the $n = 2$ term in addition to the $n = 0$ term, which is simply 1. The first nonzero term in (112b) for $G_1(z)$ is the $n = 1$ term. We again use the notation of (63) and (64):

$$\begin{aligned} G_0 &= 1 - \rho = ge^{j\Theta} = e^{-\Lambda} = e^{-A}e^{j\Theta}; \\ \Lambda &= A - j\Theta. \end{aligned} \tag{116}$$

Then we have:

$$\rho(z) \approx \int_0^z c(s)\, e^{\Delta\Gamma s}\, ds \int_0^s c(t)\, e^{-\Delta\Gamma t}\, dt. \tag{117}$$

$$G_1(z) \approx j \int_0^z c(s)\, e^{-\Delta\Gamma s}\, ds. \tag{118}$$

Since we have assumed that $c(z)$ is sufficiently small so that $|\rho| \ll 1$, we have to second order from (65) and (117):

$$g \approx 1 - \text{Re} \int\int \tag{119a}$$

$$\Lambda \approx -\ln G_0 = \int\int \tag{119b}$$

$$A \approx -\ln |G_0| = \text{Re} \int\int \tag{119c}$$

$$\Theta \approx \angle G_0 = -\text{Im} \int\int \tag{119d}$$

where $\int\int$ is shorthand for

$$\int\int = \int_0^z c(s)\, e^{\Delta\Gamma s}\, ds \int_0^s c(t)\, e^{-\Delta\Gamma t}\, dt \tag{120a}$$

$$= \int_0^z e^{\Delta\Gamma u}\, du \int_0^{z-u} c(s)c(s+u)\, ds \tag{120b}$$

$$= \frac{1}{2} \int_0^z \int_0^z c(s)c(t)\, e^{\Delta\Gamma|t-s|}\, ds\, dt. \tag{120c}$$

These results for the continuous bend are analogous to those of (63) to (65) and (71) and (72) for the case of discrete tilts. The continuous offset and diameter change are of course readily handled in the same way, and the above relations hold with only minor modifications. In particular, for the corresponding solutions to (95) and (96) for the continuous offset and diameter change the j in (113a) is dropped, the j in (113b) replaced by -1, and the j in (118) replaced by -1 (compare (73) for the discrete case); the remainder of the equations in the present section are unaltered. (For the continuous diameter change we have neglected the variation of $\Delta\Gamma$.)

These perturbation results for the continuous case may be regarded, as in the discrete case, as the first terms of power series expansions in the geometric parameter characterizing the deformed guide. Again, it is reasonable to assume that if the deformation is sufficiently small, these power series will converge so rapidly that their first terms will provide valid approximations. Equation (115) gives bounds on the magnitudes of the higher terms; for guides short enough so that $\int_0^z |c(s)|\, ds \ll 1$, these bounds converge rapidly. But the fact that the bounds converge rapidly does not guarantee that the terms themselves converge rapidly. For example, it might be possible for the second term of (112a) to be much smaller than its bound, while at the same time the fourth term was close to its bound, so that the fourth term would be comparable to the second term, even though the bound on the fourth term was much

smaller than the bound on the second term. (On the other hand this might not be possible; we just do not know.) Consequently we have no precise information on the way in which these perturbation solutions approximate the true solutions; the accuracy of these approximate solutions, which are used throughout the following statistical analysis of random guides, must be accepted largely on faith at present.

In Section 2.3.5 we show how the discrete and continuous perturbation theories may be obtained as limiting cases of each other. Section 2.3.6 discusses a modified perturbation theory, which makes it appear plausible that the results of (119b), (119c), and (119d) for the TE_{01} complex loss Λ, loss A, and phase Θ hold true in a wide range of important cases where $|\int\int| \gg 1$, so that the other approximations of (117), (118), and (119a) fail. This extension is important in permitting the analysis of long guides.

2.3.5 *Transformation between Discrete and Continuous Perturbation Theory*

In this section we consider the relationship between the discrete and continuous perturbation theories; we select the case of discrete tilts and continuous bends for purposes of illustration.

Let us first consider the transformation from the discrete to the continuous case, as illustrated in Fig. 7(a); but instead of considering a single differential section of line with a single discrete mode converter, as in Section 2.3.2, we consider the entire line. Let the tilts be equally spaced, with spacing Δz, and further let the position of the k^{th} tilt be z_k ; thus

$$z_k = k\Delta z. \tag{121}$$

Let the angle of the k^{th} tilt be α_k . From Fig. 8 we have, as in (82),

$$\alpha_k = \frac{\Delta z}{R_k} + \cdots, \tag{122}$$

where the dots indicate terms of higher order in Δz. R_k is defined in Fig. 8; in the limit as $\Delta z \to 0$, R_k approaches the radius of curvature of the guide axis at z_k .

Consider first the spurious mode normalized transfer coefficient, G_1 . From (72) we have, setting $l_0 = \Delta z$ and neglecting terms of higher order than Δz, and substituting (122) for α_k ,

$$G_1 \approx j \sum_{i=1}^{N} \frac{C_t}{R_i} \Delta z \cdot e^{-\Delta\Gamma(i-1)\Delta z}. \tag{123}$$

Setting

$$z_i = i\Delta z = s_i\,, \qquad \Delta z = \Delta s, \qquad R_i = R(s_i), \tag{124}$$

(123) becomes

$$G_1 \approx j \sum_{i=1}^{N} \frac{C_t}{R(s_i)}\, e^{-\Delta\Gamma s_i}\, e^{\Delta\Gamma \cdot \Delta s}\, \Delta s. \tag{125}$$

We now let $\Delta s \to 0$ and $N \to \infty$ in such a way that $N\Delta s$ remains constant,

$$N\Delta s = L, \tag{126}$$

where L is the length of line under consideration. Then $R(s_i) \to R(s)$, the radius of curvature of the guide axis, $e^{\Delta\Gamma \cdot \Delta s} \to 1$, and the summation of (125) becomes the following integral.

$$G_1 \approx j \int_0^L \frac{C_t}{R(s)}\, e^{-\Delta\Gamma s}\, ds. \tag{127}$$

Finally, noting (86) or (91), (127) becomes

$$G_1 \approx j \int_0^L c(s)\, e^{-\Delta\Gamma s}\, ds, \tag{128}$$

which is identical to the Picard approximate solution for the coupled ine equations for the continuous case, given in (118).

Similarly the approximate solution for ρ given in (71) for the discrete case can be shown to approach the Picard approximation for the continuous case, given in (117). Setting $l_0 = \Delta z$ in (71) and substituting (122), we have on neglecting higher-order terms in Δz

$$\rho \approx \frac{1}{2} \sum_{i=1}^{N} \left(\frac{C_t}{R_i}\, \Delta z_i \right)^2 + \sum_{i=1}^{N-1} \sum_{j=i+1}^{N} \frac{C_t^2 \Delta z_i \Delta z_j}{R_i R_j}\, e^{\Delta\Gamma(j-i)\Delta z}. \tag{129}$$

Setting

$$\begin{aligned} z_i &= i\Delta z = s_i\,, \qquad \Delta z_i = \Delta s, \qquad R_i = R(s_i), \\ z_j &= j\Delta z = t_j\,, \qquad \Delta z_j = \Delta t, \qquad R_j = R(t_j), \end{aligned} \tag{130}$$

(129) becomes

$$\rho \approx \frac{1}{2} \sum_{i=1}^{N} \left(\frac{C_t^{\,2}}{R^2(s_i)}\, \Delta s \right) \Delta s + \sum_{i=1}^{N-1} \frac{C_t}{R(s_i)}\, e^{-\Delta\Gamma s_i} \Delta s \sum_{j=i+1}^{N} \frac{C_t}{R(t_j)}\, e^{\Delta\Gamma t_j} \Delta t. \tag{131}$$

We now let $\Delta s \to 0$ and $\Delta t \to 0$ in such a way that $N\Delta s$ and $N\Delta t$ remain constant,

$$N\Delta s = L, \qquad N\Delta t = L, \tag{132}$$

where L is again the total length of line. Then $R(s_i) \to R(s)$, $R(t_i) \to R(t)$, where $R(s)$ and $R(t)$ are the radius of curvature of the guide axis.

The first term of (131) (the single summation) approaches zero; the second, however, approaches a double integral to yield

$$\rho \approx \int_0^L \frac{C_t}{R(s)}\, e^{-\Delta\Gamma s}\, ds \int_s^L \frac{C_t}{R(t)}\, e^{\Delta\Gamma t}\, dt. \tag{133}$$

Using (86) or (91), and further interchanging the order of integration and the integration variables,

$$\rho \approx \int_0^L c(s)\, e^{\Delta\Gamma s}\, ds \int_0^s c(t)\, e^{-\Delta\Gamma t}\, dt, \tag{134}$$

which is identical to the Picard approximation for the solution to the coupled line equations, given in (117). From (120) we see that the two other forms of (71d) also have their equivalents in the continuous case.

Next let us reverse the above process, and go from the continuous approximate solutions back to the discrete ones. Consider a line of length Nl_0 with N equally spaced tilts a distance l_0 apart. The k^{th} tilt is located at z_k, where

$$z_k = (k - 1)l_0, \tag{135}$$

and has an angle α_k. (The form of (135) was chosen to be consistent with the notation of Fig. 6 and Section 2.2.) From (97b) or (102b) we may write the continuous coupling coefficient for this case as

$$c(z) = C_t \sum_{k=1}^{N} \alpha_k \cdot \delta[z - (k - 1)l_0]. \tag{136}$$

We now substitute (136) into the approximate solution for the continuous case, and derive the approximate solution for the discrete case. Substituting (136) into (118), we find

$$G_1(Nl_0) \approx j \sum_{i=1}^{N} C_t\, \alpha_i e^{-\Delta\Gamma(i-1)l_0}, \tag{137}$$

in agreement with (72c) and (72d). Substituting (136) into (117), we have

$$\begin{aligned}\rho(Nl_0) &\approx \int_0^{Nl_0} C_t \sum_{i=1}^{N} \alpha_i \cdot \delta[s - (i - 1)l_0]\, e^{\Delta\Gamma s}\, ds \\ &\quad \cdot \int_0^s C_t \sum_{j=1}^{N} \alpha_j \cdot \delta[t - (j - 1)l_0]\, e^{-\Delta\Gamma t}\, dt \\ &= \int_0^{Nl_0} C_t \sum_{i=1}^{N} \alpha_i \cdot \delta[s - (i - 1)l_0]\, e^{\Delta\Gamma s}\, ds \\ &\quad \cdot \sum_{j=1}^{N} C_t \alpha_j \cdot u[s - (j - 1)l_0]\, e^{-\Delta\Gamma(j-1)l_0},\end{aligned} \tag{138}$$

where $u(x)$ is the unit step function,

$$u(x) = \begin{cases} 1, & x > 0 \\ 0, & x < 0. \end{cases} \tag{139}$$

Continuing,

$$\rho(Nl_0) \approx \sum_{i=2}^{N} C_t \alpha_i e^{\Delta\Gamma(i-1)l_0} \sum_{j=1}^{i-1} C_t \alpha_j e^{-\Delta\Gamma(j-1)l_0} + \tfrac{1}{2}\sum_{i=1}^{N} (C_t \alpha_i)^2. \tag{140}$$

The second term of (140) (the single summation) was obtained via the relation

$$\int_a^b f(x)u(x)\delta(x)\,dx = \tfrac{1}{2}f(0), \quad a < 0 < b. \tag{141}$$

Alternately, the result of (140) may be obtained by regarding the δ-functions as the limit of some continuous functions [e.g., (97a)], taking the limit after the integrations have been performed. Finally, interchanging the order of summation and the summation indices, (140) becomes

$$\rho(Nl_0) = \tfrac{1}{2}\sum_{i=1}^{N} (C_t \alpha_i)^2 + \sum_{i=1}^{N-1} \sum_{j=i+1}^{N} (C_t \alpha_i)(C_t \alpha_j) e^{\Delta\Gamma l_0 (j-i)}, \tag{142}$$

which agrees with (71d) for the discrete case. We see that the single summation, which "disappeared" in going from the discrete to the continuous case, has satisfactorily "reappeared." The alternate forms for ρ given in (120) may similarly be transformed to their discrete equivalents in (71d) via the substitution of (136) and appropriate manipulation of δ-functions.

The corresponding analysis for offsets and diameter changes is readily performed.

One consequence of the results of the present section is that bounds derived for the approximate solution in the continuous case may be directly applied to the approximate solutions given in Section II for the discrete case.

2.3.6 *Logarithmic Form of the Coupled Line Equations, and Improved Approximate Solution*

The perturbation results of Section 2.3.4, given in (116) to (120), were expected on intuitive grounds to be valid for short lines, whose additional loss due to mode conversion is small. In particular, the results of (117) and (119) depend on having $|\rho| \ll 1$, $|\int\int| \ll 1$. These relations may

again be regarded as the first terms in power series expansions for the various quantities.

As the length of guide increases we expect the mode conversion loss to increase; for example in Sections III and IV below it is shown that for all random guides that we deal with, $< \mathrm{Re} \int\int >$ is proportional to the total length of the guide. It is clear that as the length of guide increases, eventually $| \int\int | \gg 1$. Under these conditions we no longer obtain a valid approximation from the first two terms of (112a); many terms become significant, and (117) and (118) are no longer valid. It would seem that the results of (119) are also invalid for long guides. However while (119a) is certainly invalid, we will see that it is plausible that (119b), (119c), and (119d) will remain good approximations for long guides with large mode conversion loss if the differential attenuation constant is large enough in a certain sense compared to the coupling coefficient. The detailed mathematical analysis for this problem is given in a companion paper;[18] however, it is not difficult to see on physical grounds that something of this sort is to be expected.

Consider a long guide of length L with a large enough differential loss so that the total differential loss $| \Delta\alpha | z$ in a short section of length z is large;

$$| \Delta\alpha | z \gg 1, \qquad z \ll L. \tag{143}$$

Now let this guide be divided up into M equal sections of length z by ideal mode filters, so that

$$Mz = L. \tag{144}$$

An ideal mode filter by definition transmits TE_{01} without loss or phase shift, and suppresses all other modes completely. (Practical mode filters may consist of a section of helix guide that has low loss to TE_{01}, high loss to all other spurious modes other than the higher order TE_{0m}.) In addition to the requirement of (143), further assume that each section z is short enough so that the perturbation results of (116) to (120) do apply to the individual sections; for example, we might require from (115) that

$$\int_{(k-1)z}^{kz} | c(s) | \, ds \ll 1. \tag{145}$$

It is more or less obvious on physical grounds that under these conditions the insertion of ideal mode filters will not alter the over-all TE_{01} loss significantly, because the spurious mode level is not likely to build up to a significant magnitude.

Denote quantities applying to the k^{th} section by the symbol k in the following equation; quantities applying to the over-all guide will be written without subscripts. Then the over-all TE_{01} transmission parameters for the guide with ideal mode filters are given in terms of the TE_{01} parameters for individual sections as follows:

$$\begin{aligned} G_0 &= \prod_{k=1}^{M} {}_kG_0, \\ g &= \prod_{k=1}^{M} {}_kg, \\ \Lambda &= \sum_{k=1}^{M} {}_k\Lambda, \\ A &= \sum_{k=1}^{M} {}_kA, \\ \Theta &= \sum_{k=1}^{M} {}_k\Theta. \end{aligned} \tag{146}$$

Then, for example, Λ may be written from (119), (120) and (146) as follows:

$$\Lambda \approx \sum_{k=1}^{M} \int_{(k-1)z}^{kz} ds \int_{(k-1)z}^{s} dt \cdot c(s)c(t)\, e^{\Delta\Gamma(s-t)}. \tag{147}$$

In (147) the double integral has been taken from (120a); the other two versions of this integral could of course be used equally well. Now it is more or less obvious by inspection of the integrand and the limits and from physical considerations that (147) is approximately equivalent to

$$\Lambda \approx \int_{0}^{L=Mz} ds \int_{0}^{s} dt \cdot c(s)c(t)\, e^{\Delta\Gamma(s-t)}. \tag{148}$$

In other words, the results of (119b), (119c), and (119d) should remain valid for the whole line, as stated above. Since the requirement in the above crude argument is that the mode conversion loss must be small in a section for which the total differential loss is high, we would intuitively expect that for (119b), (119c), and (119d) to hold for a long line, the ratio of the coupling coefficient $|\, c(z)\,|$ to the differential attenuation constant $|\, \Delta\alpha\,|$ must be small in some sense which we have not yet attempted to define.

While the above argument may be physically appealing, it is obviously desirable to put these statements on firmer ground; this is done elsewhere in this issue.[18] We summarize here briefly some of the results of this investigation.

Under certain conditions we may write $\Lambda(z)$ as a series expansion;

$$\Lambda(z) = \int_0^z c(s)\, e^{\Delta\Gamma s}\, ds \int_0^s c(t)\, e^{-\Delta\Gamma t}\, dt + \sum_{n=2}^{\infty} \lambda_n(z). \qquad (149)$$

In (149) we have written out only the first term explicitly; we see that this is identical to the previous approximation of (119b) and (120a). Bounds on the higher terms are given in detail in Ref. 18; we give here some slightly poorer but simpler bounds.

$$|\lambda_1(z)| = \left| \int_0^z c(s)\, e^{\Delta\Gamma s}\, ds \int_0^s c(t)\, e^{-\Delta\Gamma t}\, dt \right| \leqq K \int_0^z |c(s)|\, ds;$$

$$|\lambda_n(z)| \leqq K^3 (2.225K^2)^{n-2} \int_0^z |c(s)|\, ds; \quad n \geqq 2, \qquad (150)$$

$$0 \leqq K \leqq 0.3;$$

where K is defined by

$$\int_0^z |c(s)|\, e^{\Delta\alpha(z-s)}\, ds \leqq K \quad \text{for every} \quad z \geqq 0. \qquad (151)$$

Finally, convergence is guaranteed only for $K < 0.455$; a case is known where the series of (149) diverges for $K > 0.5$. Equation (151) requires that $|c(z)|$ be uniformly small in a certain sense, with respect to $|\Delta\alpha|$.

Once again we take as an approximate solution the first term of (149). The bounds in Ref. 18 are again almost the best possible in the same sense as in the case of Section 2.3.4; i.e., cases are known where the higher-order terms are almost as large as their bounds. In cases of interest $K \ll 1$, and the bounds converge rapidly. However, as in the case of Section 2.3.4, this is not sufficient to guarantee that the terms themselves converge rapidly; and here again we lack precise information on the way in which the first term (perturbation solution) approximates the true solution.

Because of the relationship between discrete and continuous cases, similar statements can be made regarding the results of (65) and (71) for the discrete case.

2.3.7 TE_{01} Loss in Terms of Fourier Coefficients of $c(z)$ when $\Delta\alpha = 0$

If the differential attenuation constant is equal to zero,

$$\Delta\alpha = 0, \qquad (152)$$

the above perturbation results for the loss A [see (119c) and (120)] may be further simplified. This case is of interest as an approximation

to the situation present in real copper guides. In practical copper guides mode filters, consisting of a length of helix guide, must be inserted at regular intervals, perhaps a few hundred feet apart, for reasons that will be further discussed in Sections III and IV below. If the mode filters may be assumed ideal, we consider each section separately and simply add their individual TE_{01} loss and phase, i.e., Λ, A, and Θ, as in (146). If for each copper guide section of length L the total differential loss $| \Delta\alpha | L$ is small,

$$| \Delta\alpha | L \ll 1, \tag{153}$$

on intuitive grounds we approximate the true solution by setting $\Delta\alpha = 0$ in the various approximate solutions of (116) to (120).

Thus, let us set $\Delta\alpha = 0$ in (119c) and (120c) to obtain

$$A \approx \frac{1}{2} \operatorname{Re} \int_0^L \int_0^L c(s)c(t)\, e^{j\Delta\beta|t-s|}\, ds\, dt \tag{154}$$

for a guide of length L. Recalling that $c(s)$ and $c(t)$ are real in ideal metallic guide, (154) yields

$$\begin{aligned} A &\approx \frac{1}{2} \operatorname{Re} \int_0^L \int_0^L c(s)c(t)\, e^{j\Delta\beta(t-s)}\, ds\, dt \\ &= \frac{1}{2} \int_0^L \int_0^L c(s)c(t)\, e^{j\Delta\beta(t-s)}\, ds\, dt \\ &= \frac{1}{2} \int_0^L c(s)\, e^{-j\Delta\beta s}\, ds \int_0^L c(t)\, e^{+j\Delta\beta t}\, dt \\ &= \frac{1}{2} \left| \int_0^L c(s)\, e^{-j\Delta\beta s}\, ds \right|^2 . \end{aligned} \tag{155}$$

Summarizing,

$$A \approx \frac{1}{2} \left| \int_0^L c(s)\, e^{-j\Delta\beta s}\, ds \right|^2, \quad \Delta\alpha = 0. \tag{156}$$

We note further from (119a) and (116) that

$$| G_0 | = g \approx 1 - \frac{1}{2} \left| \int_0^L c(s)\, e^{-j\Delta\beta s}\, ds \right|^2 . \tag{157}$$

From (157) we have to second order

$$| G_0 |^2 \approx 1 - \left| \int_0^L c(s)\, e^{-j\Delta\beta s}\, ds \right|^2 . \tag{158}$$

But from (118), for $\Delta\alpha = 0$

$$|G_1|^2 \approx \left| \int_0^L c(s)\, e^{-j\Delta\beta s}\, ds \right|^2. \tag{159}$$

Therefore from (158) and (159) we have to second order

$$|G_0|^2 + |G_1|^2 \approx 1, \quad \Delta\alpha = 0. \tag{160}$$

In Appendix C it is shown that (160) must hold exactly for $\Delta\alpha = 0$ [see (C-13)]. This is something like conservation of energy; in fact if $\alpha_0 = \alpha_1 = 0$, (C-13) is precisely conservation of energy.

We note in passing that a similar result to that of (156) is readily found for the discrete case of Section II. Proceeding in an analogous way from (65c) and the second form of (71d), we find for the discrete case

$$A \approx \frac{1}{2} \left| \sum_{i=1}^{N} x_i\, e^{-j\Delta\beta l_{0i}} \right|^2, \qquad \Delta\alpha = 0. \tag{161}$$

Similarly the result of (160) is readily seen to hold true to second order, and by Appendix C must also be true exactly.

Equation (156) states that the loss in nepers A is one half the square of the magnitude of the Fourier transform of the coupling coefficient, with transform variable $\Delta\beta$, the differential propagation constant. Since we deal with the case $\Delta\alpha = 0$, the logarithmic perturbation theory of Section 2.3.6 does not indicate that (156) is valid for long lines; consequently, this approximate result will remain valid only for short line sections, perhaps subject to a condition such as $\int_0^L |c(s)|\, ds \ll 1$.

It will prove convenient to rewrite (156) in a slightly modified form. Define

$$I = e^{j\pi(\Delta\beta L/2\pi)} \int_0^L c(s)\, e^{-j\Delta\beta s}\, ds. \tag{162}$$

We have

$$|I| = \left| \int_0^L c(s)\, e^{-j\Delta\beta s}\, ds \right|. \tag{163}$$

I is closely related to the approximate expression for the spurious mode transfer coefficient, given in (118). From (162) and (163), (156) may be written as

$$A \approx \tfrac{1}{2} |I|^2. \tag{164}$$

It turns out to be useful to expand the coupling coefficient $c(z)$ in a Fourier series as follows:†

$$c(z) = \sum_{n=-\infty}^{\infty} c_n \; e^{j2\pi nz/L} \; ; \; c_{-n} = c_n^* . \tag{165}$$

Substituting (165) into (162), we have after some algebraic simplification:

$$I = L \sum_{n=-\infty}^{\infty} c_n (-1)^n \frac{\sin \pi \left(\frac{\Delta\beta L}{2\pi} - n \right)}{\pi \left(\frac{\Delta\beta L}{2\pi} - n \right)} . \tag{166}$$

Now, (166) has a rather striking form. Assume for a moment that the only variation of I (and hence A) with the frequency f of the radiation in the guide occurs through $\Delta\beta$. If we take the independent variable in (166) to be proportional to $\Delta\beta$, then (166) is simply the sampling theorem representation of a complex band-limited function,[33,34] i.e., a complex function whose real and imaginary parts are each band-limited. Taking the dimensionless quantity $\frac{\Delta\beta L}{2\pi}$ as the independent variable, $I\left(\frac{\Delta\beta L}{2\pi}\right)$ will contain no frequencies $| \nu |$ greater than $\frac{1}{2}$.‡ By (164) the loss A is proportional to the square of the magnitude of I, or alternately to the sum of the squares of the magnitudes of the real and imaginary parts of I; therefore the TE_{01} loss A, regarded as a function of the normalized independent variable $\frac{\Delta\beta L}{2\pi}$, will contain no frequencies greater than 1. If for the time being we neglect any variation of the c_n's with $\Delta\beta$ in (166), then $I\left(\frac{\Delta\beta L}{2\pi}\right)$ is determined by its values at the sample points. At the n^{th} sample point

† Here c_n is the n^{th} complex Fourier coefficient of the continuous coupling coefficient $c(z)$. In contrast, in Section 2.2 above we have used c_k to represent the coupling coefficient of the k^{th} discrete mode converter. In the following work the meaning will always be clear from the context.

‡ Here, and often in the sequel, we use the word frequency to denote the independent variable ν of the Fourier transform of some quantity of interest. In the present case we consider the Fourier transform of $I\left(\frac{\Delta\beta L}{2\pi}\right)$ with respect to the independent variable $\frac{\Delta\beta L}{2\pi}$; since $\frac{\Delta\beta L}{2\pi}$ is dimensionless, the corresponding Fourier transform variable ν is also dimensionless. Thus, if $g(\nu)$ is the Fourier transform of $I\left(\frac{\Delta\beta L}{2\pi}\right)$, $g(\nu) = \int_{-\infty}^{\infty} I(\xi) \; e^{-j2\pi\nu\xi} d\xi$.

$$\frac{\Delta\beta L}{2\pi} = n, \qquad B \equiv \frac{2\pi}{\Delta\beta} = \frac{L}{n}. \tag{167}$$

The n^{th} sample point occurs at the free-space wavelength or frequency (of the radiation in the guide) where the beat wavelength B is equal to the mechanical wavelength $\frac{L}{n}$ associated with the n^{th} Fourier coefficient of the coupling coefficient. The value of I at the n^{th} sample point is

$$I(n) = Lc_n(-1)^n. \tag{168}$$

By (162) and (118) the spurious mode transfer coefficient at the n^{th} sample point for the continuous bend becomes

$$G_1(n) \approx jLc_n\,, \tag{169}$$

with an analogous result for the continuous offset and diameter change. $I(n)$ and $G_1(n)$ are determined only by the n^{th} Fourier coefficient. At intermediate values of $\frac{\Delta\beta L}{2\pi}$, $I\left(\frac{\Delta\beta L}{2\pi}\right)$ is determined by interpolating between the sample values with $\frac{\sin x}{x}$ functions, as shown in (166).

Now the object of the present calculations is to determine the loss A as a function of the frequency f, and later to determine the statistics of the loss-frequency curves for guides with random imperfections. However, $\Delta\beta$ is approximately proportional to the free-space wavelength λ of the radiation in the guide, and thus *inversely* proportional to the frequency f, if the two modes involved (the TE_{01} signal mode and the spurious mode) are both far from cutoff. Therefore for analytical purposes it is more convenient to choose an independent variable proportional to the free-space wavelength λ rather than to the frequency f, and this is what is done in the present paper. If a single spurious mode is under consideration, it is most convenient to choose the dimensionless parameter $\frac{\Delta\beta L}{2\pi}$, which is approximately proportional to λ, as the independent variable. If more than one spurious mode is being considered, we see in Section 2.4 below that the loss A is given by a sum of terms of the form given in (156), with of course different c's and $\Delta\beta$'s for each spurious mode. While the different $\Delta\beta$'s are all approximately proportional to λ, they have different constants of proportionality, and hence it is perhaps most convenient to take λ itself as the independent variable.

In practice we will consider only fairly narrow percentage bandwidths (although the absolute bandwidths will be enormous compared with conventional communication channels) at any one time. Therefore the

fact that we take λ as the independent variable instead of f should cause no serious inconvenience.

The sampling theorem interpretation of (166) requires that the c_n, defined by (165), be independent of λ (or frequency) and hence $\Delta\beta$; this may or may not be true. Since $c(z)$ is given by the product of one of Morgan's coupling coefficients and a geometric parameter [see (86) or (94)], the λ-dependence of the c_n's is identical to the λ-dependence of C_t, C_o, or C_d. From the equations for these three coefficients given in Appendix A we see that far from cutoff, C_o and C_d are approximately independent of λ, as desired, but that C_t varies approximately inversely with λ. In Section 2.3.8 below we shall introduce additional coupling coefficients of Morgan, $\Xi_{[nm]}$, which permit a similar treatment for general continuous cross-sectional deformations of copper guide; the $\Xi_{[nm]}$ vary approximately directly with λ. The geometric parameters associated with C_o and C_d are the derivatives with respect to distance z of offset x and radius a respectively; hence these geometric parameters are dimensionless. The geometric parameter associated with C_t is curvature, which has the dimension of length^{-1}. The geometric parameters associated with the $\Xi_{[nm]}$ all have the dimensions of length. As a convenient device for recalling these facts, the exponent of λ in stating the λ-dependence of the coupling coefficient is the same as the exponent of length in stating the dimensions of its associated geometric parameter.

We wish to retain the sampling theorem interpretation of (166) even in those cases where the c_n's are not independent of λ and hence of $\Delta\beta$. Now in those cases where the coupling coefficients are not approximately constant (i.e., C_t, $\Xi_{[nm]}$) the variation with λ is quite slow. Since as mentioned above we need consider only narrow percentage bandwidths, the principal variation with λ in (166) occurs through $\Delta\beta$, and not through the coupling coefficient. Consequently, over the moderate bandwidths of interest we may evaluate Morgan's coefficients at the middle of the narrow band under consideration.

There are several more elegant methods for deriving this approximation that state in effect that c_n is to be evaluated at the wavelength λ_n (or frequency) corresponding to the n^{th} sample point, given in (167), rather than at the operating wavelength, as implied in (166). This is certainly true at the sample points, by (168), and appears plausible in general. In Section 2.3.9 below we show, for example, that under certain reasonable conditions a guide with a given straightness deviation may be described equally well as either a continuous bend, for which the c_n's vary approximately inversely with λ, or as a continuous offset, for which the c_n's are approximately independent of λ. By a suitable transforma-

tion it is always possible to change the geometric parameter to dimensionless form (in general, to the derivative with respect to z of a parameter with the dimensions of length, such as radius, offset, ellipticity, etc.) so that the corresponding coupling coefficient is approximately independent of λ (and hence $\Delta\beta$) far from cutoff.

Alternately, this result may be derived by fairly simple manipulation of the sampling theorem.

The final result, however, is that over the fairly narrow percentage bands of interest we are justified in neglecting the λ-(or frequency) variation of the coupling coefficient (i.e., C_t or $\Xi_{[nm]}$).

The TE_{01} loss A in terms of the Fourier coefficients c_n is, from (164) and (166),

$$A \approx \frac{L^2}{2} \sum_{m=-\infty}^{\infty} \sum_{n=-\infty}^{\infty} c_m c_n^* (-1)^{(m-n)} \cdot \frac{\sin \pi \left(\frac{\Delta\beta L}{2\pi} - m \right) \sin \pi \left(\frac{\Delta\beta L}{2\pi} - n \right)}{\pi \left(\frac{\Delta\beta L}{2\pi} - m \right) \pi \left(\frac{\Delta\beta L}{2\pi} - n \right)} . \quad (170)$$

At the sample points of I, given in (167), the TE_{01} loss becomes simply

$$A(n) \approx \frac{L^2}{2} | c_n |^2 . \quad (171)$$

As mentioned earlier the bandwidth of A is twice the bandwidth of I; thus the Fourier transform of A with respect to the independent variable $\frac{\Delta\beta L}{2\pi}$ will contain no frequencies greater than 1.

Therefore while A is also a band-limited function, it has twice as many sample points as I. Consequently A is *not* completely determined by its values given in (171) at the sample points of I. Simple examples are readily found of two different guides in which the TE_{01} loss is the same at the sample points of I, given in (167), but differs greatly between these sample points. Thus consider the following two cases, in which all but two adjacent Fourier components of the coupling coefficient are identically zero:

$$\begin{aligned} &\text{(a)} \quad c(z) = 2 \cos 2\pi k \frac{z}{L} + 2 \cos 2\pi (k+1) \frac{z}{L} . \\ &\text{(b)} \quad c(z) = 2 \cos 2\pi k \frac{z}{L} - 2 \cos 2\pi (k+1) \frac{z}{L} . \end{aligned} \quad (172)$$

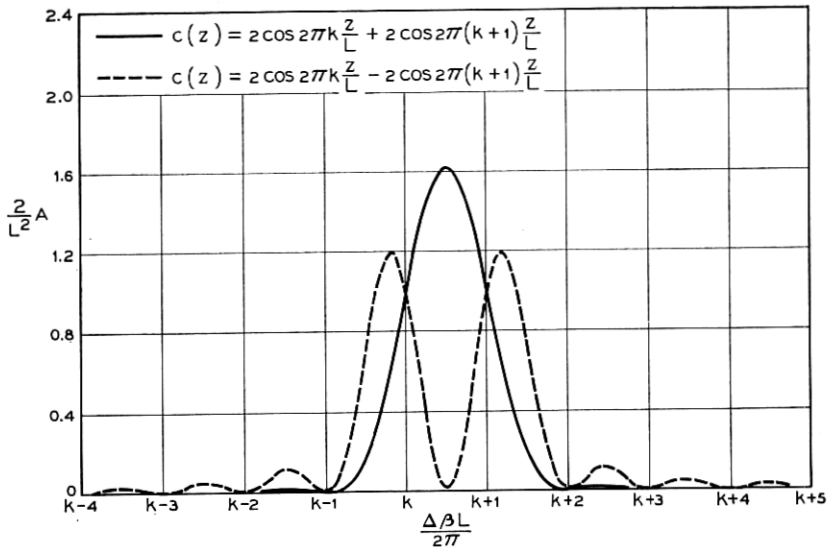

Fig. 10 — TE_{01} loss for coupling coefficient with two sinusoidal components.

The TE_{01} loss A is shown for these two cases in Fig. 10. While the losses are the same at the sample points of I, they differ markedly in between.

While A is not completely determined by its values at the sample points of I, it is clear from (170) that the principal contribution to A in the region near the k^{th} sample point arises from values of m and n close to k. This relation between the TE_{01} loss and the coupling coefficient is of great importance, as it means that the additional TE_{01} loss due to some particular spurious mode in a given frequency range is caused primarily by the components of the coupling coefficient which lie in a corresponding (mechanical) spectral region. Thus, for example, loss due to $TE_{01} - TE_{12}$ coupling in 2-inch guide between 50 and 60 kmc is caused primarily by straightness deviations with periods between 2 and 2.4 feet, the range of beat wavelength B corresponding to this frequency band.

Equation (170) is also useful in considering situations where only isolated Fourier coefficients of the coupling coefficient are nonzero; the TE_{01} loss A then becomes a series of isolated narrow peaks of shape $\left(\frac{\sin x}{x}\right)^2$. There are at least two such cases of practical interest:

i. A periodically supported copper guide that deforms elastically under its own weight (the "serpentine bend"),[35] *with support period short com-*

pared to the total length of guide between mode filters. The Fourier components occur only at the fundamental and harmonics of the support period; the amplitude of the Fourier coefficients decreases rapidly as the order of the harmonic increases. Thus the TE_{01} loss vs wavelength curve will have a series of equally spaced narrow loss peaks of rapidly decreasing magnitude.

ii. Shuttle pulse measurements in a copper waveguide without mode filters. Here, because of the absence of mode filters, the pulse traverses an iterated structure. Since the Fourier series expansion of the coupling coefficient for any number of round trips must be identical to the expansion for a single round trip, for N round trips only every N^{th} Fourier coefficient will be nonzero. Again the TE_{01} transmission will consist of equally spaced narrow loss peaks separated by wide pass bands of low loss.[8]

These two cases will not be discussed further in the present paper.

The spacing between sample points of I is an important parameter in the analysis and in the interpretation of experimental transmission data. Since $\Delta\beta$ is proportional to the free-space wavelength λ,

$$\Delta\beta = D\lambda, \tag{173}$$

where the constant D depends on the spurious mode. From (167) the wavelength corresponding to the n^{th} sample point, λ_n, is given by

$$\frac{D\lambda_n L}{2\pi} = n, \qquad \lambda_n = \frac{2\pi n}{DL}. \tag{174}$$

Therefore the sample point spacing in wavelength is

$$\Delta\lambda_n = \lambda_{n+1} - \lambda_n = \frac{2\pi}{DL}. \tag{175}$$

Thus from (173) and (175), noting the definition of beat wavelength B in (167),

$$\frac{\Delta\lambda}{\lambda} = \frac{B}{L}, \tag{176}$$

where we have dropped the subscript n since the result of (175) is independent of n. Since

$$\frac{\Delta\lambda}{\lambda} \approx \frac{\Delta f}{f}, \tag{177}$$

we have finally

$$\frac{\Delta f}{f} \approx \frac{\Delta \lambda}{\lambda} = \frac{B}{L} \tag{178}$$

for the sample point spacing, in either frequency or wavelength. We see from (175) that the sample points are equally spaced in wavelength, and consequently unequally spaced in frequency. However over a sufficiently narrow band the variation in sample point spacing in frequency will be small. The beat wavelength B between TE_{01} and all other TE modes is tabulated in Appendix D for the frequencies 50, 55, and 60 kmc in 2-inch diameter guide.

2.3.8 *Morgan's Coupling Coefficients for Small Cross-Sectional Deformations in Lossless Metallic Guide*

Morgan has determined to first order the spurious modes excited by an incident TE_{01} wave at a small arbitrary deformation of the cross section of a cylindrical metallic guide.[5] This analysis must include the continuous offset and diameter change studied above when those deformations are small; it includes in addition higher-order deformations of the cross section, such as ellipticity, tri-foil, etc.

Let the surface of the slightly deformed guide be given in cylindrical co-ordinates by

$$r = a + \rho(\varphi,z), \tag{179}$$

$$\rho(\varphi,z) = \sum_{n=0}^{\infty} [a_n(z) \cos n\varphi + b_n(z) \sin n\varphi], \qquad b_0(z) = 0, \tag{180}$$

$$\rho(\varphi,z) = 0, \qquad a_n(z) = 0, \qquad b_n(z) = 0; \qquad \begin{matrix} z \leqq 0 \\ z \geqq L \end{matrix} \tag{181}$$

where a is the radius of the perfect guide. $\rho(\varphi,z)$ must be suitably small (we have omitted Morgan's small dimensionless parameter ϵ). Then the $n = 0$ term corresponds to a continuous diameter variation, the $n = 1$ term to a continuous offset, the $n = 2$ term to ellipticity, the $n = 3$ term to what has been called tri-foil, etc. By (181) it is assumed that the guide is distorted only in the interval $0 < z < L$.

Morgan has shown that to first order a TE_{01} wave incident on the deformation of (179) to (181) excites the forward and backward TE_{nm} modes. We denote the various modes as follows:

$$\begin{aligned} &I_{[0m]}{}^{+} \text{ — forward } TE_{0m} \\ &I_{[0m]}{}^{-} \text{ — backward } TE_{0m} \\ &I_{[nm]}{}^{\parallel +},\ I_{[nm]}{}^{\perp +} \text{ — two polarizations of forward } TE_{nm} \\ &I_{[nm]}{}^{\parallel -},\ I_{[nm]}{}^{\perp -} \text{ — two polarizations of backward } TE_{nm}\,. \end{aligned} \tag{182}$$

We denote the two orthogonal polarizations of each mode (except the TE_{0m}) by the symbols $\parallel$ and $\perp$, rather than the subscripts x and y used in Section 2.1 above. The geometric imperfections of Section 2.1 — offsets and tilts — could naturally be resolved into components along the x- and y-axes; with the more general deformations of (179) to (181) this is of course not possible, and the $\parallel$ and $\perp$ notation appears more natural. In the special case $n = 1$, using the geometry of Fig. 5, we may if we wish identify $a_1(z)$ with $x(z)$, $b_1(z)$ with $y(z)$, and the $\parallel$ and $\perp$ polarizations of the resulting TE_{1m} spurious modes with the subscripts x and y respectively of Section 2.1.

We normalize the complex mode amplitudes in the usual way [see (88) and (89)]:

$$\begin{aligned} I_{[0m]}{}^{\pm}(z) &= e^{\mp\Gamma_{[0m]}z}\, G_{[0m]}{}^{\pm}(z) \\ I_{[nm]}{}^{\parallel\pm}(z) &= e^{\mp\Gamma_{[nm]}z}\, G_{[nm]}{}^{\parallel\pm}(z) \\ I_{[nm]}{}^{\perp\pm}(z) &= e^{\mp\Gamma_{[0m]}z}\, G_{[nm]}{}^{\perp\pm}(z). \end{aligned} \tag{183}$$

In lossless metallic guide the propagation constants $\Gamma_{[nm]}$ are of course pure imaginary,

$$\Gamma_{[nm]} = j\beta_{[nm]}\,. \tag{184}$$

Assuming a unit incident TE_{01} wave,

$$G_{[01]}{}^{+}(0) = 1, \tag{185}$$

the $G_{[nm]}$ become the normalized spurious mode complex transfer coefficients. They are found to first order from Morgan's analysis, and given in a slightly modified notation as follows:

$$\begin{bmatrix} G_{[nm]}{}^{\parallel\pm}(L) \\ G_{[nm]}{}^{\perp\pm}(L) \end{bmatrix} \approx -j\Xi_{[nm]} \int_0^L \begin{bmatrix} a_n(z) \\ b_n(z) \end{bmatrix} e^{-j(\beta_{01}\mp\beta_{nm})z}\, dz \tag{186}$$

where the coupling coefficient $\Xi_{[nm]}$ is given by

$$\Xi_{[nm]} = \frac{1}{\sqrt{\epsilon_n}\, a^3} \frac{k_{01}{k_{nm}}^2}{\sqrt{{k_{nm}}^2 - n^2}} \frac{1}{\sqrt{\beta_{01}\beta_{nm}}} \tag{187}$$

$$\epsilon_n = \begin{cases} 1, & n = 0 \\ 2, & n \geqq 1 \end{cases}; \qquad J_n{}'(k_{nm}) = 0. \tag{188}$$

It is worth noting that the angular index n of the spurious mode is identical to the subscript of the pertinent component of mechanical deformation, a_n or b_n; therefore, to first order the modes excited by TE_{01} at a given deformation have the same angular symmetry as the defor-

mation. $\Xi_{[nm]}$ is the same for forward and backward modes, and for both polarizations; in contrast C_o, C_t, and C_d of Appendix A are different for forward and backward modes. This contrast in behavior will be discussed in Section 2.3.9. The $\Xi_{[nm]}$ are given in Appendix D for the frequencies 50, 55, and 60 kmc, in 2-inch diameter guide. We note again that these results hold true only when there is no distortion of the guide at the ends, $z = 0$ and $z = L$, by (181).

Special comment is necessary for the $G_{[0m]}$ terms in (186), and in particular for the $G_{[01]}{}^{+}$ term. The $n = 0$ terms correspond to the TE_{0m} modes, which have only a single polarization. Since $b_0(z) = 0$ in (181), the $\|$ terms of (186) are the significant ones; and since we have only one polarization, the symbol $\|$ may be conveniently dropped. The $G_{[01]}{}^{+}$ term, corresponding to the forward TE_{01}, requires special interpretation. It is to be considered a first-order correction to be added to the unperturbed solution, i.e., $G_{[01]}{}^{+} = 1$. It is readily seen that $G_{[01]}{}^{+}$ in (186) represents a phase shift of the unperturbed TE_{01} wave, caused by a change in the average diameter of the guide.

By analogy with the previous analysis, we may use the results of (186) to (188) in any of the results of Section 2.3 above for the continuous case—e.g., (116) to (120)—by substituting $-\Xi_{[nm]}a_n(z)$ or $-\Xi_{[nm]}b_n(z)$ for the continuous coupling coefficient $c(z)$. While these coupling coefficients were derived by Morgan for lossless metallic guide, we expect as before that these results provide a satisfactory approximation for real copper guide by modifying the various propagation constants to take account of the small losses present in copper guide. The relationship of these results to previous ones for the continuous case is discussed in Section 2.3.9.

2.3.9 *Relationships between Various Metallic Guide Coupling Coefficients*

A sufficiently small straightness deviation of the guide axis may obviously be described equally well as a continuous bend, a continuous offset, or simply as a continuous displacement. For these three cases we have given above three different coupling coefficients — $C_{t[m]}$, $C_{o[m]}$, and $\Xi_{[1m]}$ — that yield, among other things, the first-order spurious mode transfer coefficient of a deformed guide. While the results of Section 2.3.4 — in particular (118) for continuous bends and its analog for continuous offsets and diameter changes — were derived for only a single forward spurious mode, the result for the first-order spurious mode transfer coefficient holds true in general, with of course the proper coupling coefficient for each of the spurious modes, as discussed in Section 2.4 below. Since a given deformation that is suitably small may be described in these three different ways, and since we must get the same

answer for the spurious mode output in each calculation, the three coupling coefficients must be related to each other. Similar statements obviously apply to the two coupling coefficients $C_{d[m]}$ and $\Xi_{[0m]}$ for diameter variations.

For a guide with a continuous bend, confined to the x-z plane, the $TE_{1m}^{\pm}$ transfer coefficient is, from (118) and (91), to first order

$$G_{[1m]}^{x\pm} \approx j \int_0^L \frac{C_{t[m]}^{\pm}}{R_x(z)} e^{-j(\beta_{01} \mp \beta_{1m})z} \, dz, \tag{189}$$

where $R_x(z)$ is the radius of curvature of the guide axis, and the superscript x indicates that the x-polarization is under consideration. If the slope of the guide axis is small compared to unity, the distance along the perturbed guide axis is approximately equal to the distance along the unperturbed guide axis, so that we may regard z in (189) as measured along a fixed rectangular co-ordinate axis. Further we may approximate the curvature as

$$\frac{1}{R_x(z)} \approx x''(z). \tag{190}$$

Then (189) may be written

$$G_{[1m]}^{x\pm} \approx jC_{t[m]}^{\pm} \int_0^L x''(z) e^{-j(\beta_{01} \mp \beta_{1m})z} \, dz. \tag{191}$$

Similarly for a guide with a continuous offset in the x-z plane the spurious mode output is, from (96) and (118) with the j replaced by -1,

$$G_{[1m]}^{x\pm} \approx -C_{o[m]}^{\pm} \int_0^L x'(z) e^{-j(\beta_{01} \mp \beta_{1m})z} \, dz. \tag{192}$$

If the ends of the guide are parallel, so that

$$x'(0) = x'(L) = 0, \tag{193}$$

and if the perturbation is small, the spurious mode output must be identical in the two cases and the right-hand sides of (191) and (192) must be equal. Integrating (191) by parts, we find subject to (193)

$$G_{[1m]}^{x\pm} \approx -(\beta_{01} \mp \beta_{1m}) C_{t[m]}^{\pm} \int_0^L x'(z) e^{-j(\beta_{01} \mp \beta_{1m})z} \, dz. \tag{194}$$

For (192) and (194) to be identical, we must have

$$\frac{C_{o[m]}^{\pm}}{C_{t[m]}^{\pm}} = \beta_{01} \mp \beta_{1m}. \tag{195}$$

Using (A-1) and (A-2) of Appendix A, (195) is easily shown to be an identity.

Similarly a line with a continuous offset, but with no net offset between its two ends, is described in terms of displacement of the guide axis by the results of (186). Thus setting

$$a_1(z) = x(z), \tag{196}$$

we have for the spurious mode output

$$G_{[1m]}^{x\pm} \approx -j\Xi_{[1m]} \int_0^L x(z) e^{-j(\beta_{01} \mp \beta_{1m})z}\, dz, \tag{197}$$

where we have replaced the superscript $\|$ in (186) by x. This result is valid only when the distortion vanishes at the ends of the guide; in this case this means that there must be no offset between the two ends of the guide,

$$x(0) = x(L) = 0. \tag{198}$$

Subject to (198), (197) must agree with the previous two results. Integrating (192) by parts, and using the condition of (198),

$$G_{[1m]}^{x\pm} \approx -j(\beta_{01} \mp \beta_{1m}) C_{o[m]}^{\pm} \int_0^L x(z) e^{-j(\beta_{01} \mp \beta_{1m})z}\, dz. \tag{199}$$

For (197) and (199) to be identical, we must have

$$\frac{\Xi_{[1m]}}{C_{o[m]}^{\pm}} = \beta_{01} \mp \beta_{1m}. \tag{200}$$

By (A-1) of Appendix A and (187), (200) is easily seen to be an identity.

An analogous study can be made for a continuous diameter change. From Sections 2.3.2 and 2.3.4

$$G_{[0m]}^{\pm} = -C_{d[m]}^{\pm} \int_0^L r'(z) e^{-j(\beta_{01} \mp \beta_{0m})z}\, dz. \tag{201}$$

From (186) we have

$$G_{[0m]}^{\pm} = -j\Xi_{[0m]} \int_0^L a_0(z) e^{-j(\beta_{01} \mp \beta_{0m})z}\, dz, \tag{202}$$

valid when

$$a_0(0) = a_0(L) = 0. \tag{203}$$

Subject to (203), (201) and (202) must be identical. From (179) we have $r'(z) = a_0'(z)$; substituting this into (201), integrating by parts, and using (203),

$$G_{[0m]}^{\pm} = -j(\beta_{01} \mp \beta_{0m}) C_{d[m]}^{\pm} \int_0^L a_0(z) e^{-j(\beta_{01} \mp \beta_{0m})z} \, dz. \quad (204)$$

For (202) and (204) to be identical, we must have

$$\frac{\Xi_{[0m]}}{C_{d[m]}^{\pm}} = \beta_{01} \mp \beta_{0m}. \quad (205)$$

Equation (A-4) of Appendix A and (187) show that (205) is an identity.

It is interesting that coupling coefficients found in such diverse ways are so simply related, and pleasing that these different calculations are all consistent with each other.

A simple physical interpretation may be given for the fact that the mode conversion caused by a given type of deformation of the guide may be described by different coupling coefficients (with of course corresponding different geometric parameters). These different descriptions correspond to using different sets of normal modes to describe the fields within the deformed guide.

For purposes of illustration we take the case of deviation from straightness of the guide axis. The coupling coefficient $\Xi_{[1m]}$ and (197) correspond to the normal modes of the original undeformed guide. The coupling coefficient $C_{o[m]}$ and (192) correspond to the normal modes of the deformed guide with cross section perpendicular to the axis of the *un*deformed guide. Finally, the coupling coefficient $C_{t[m]}$ and (191) correspond to the normal modes of the deformed guide with cross section perpendicular to the axis of the deformed guide. This process may be carried one step further, using the normal modes of a curved circular guide.[9]

A similar discussion can of course be given for the two representations of mode conversion caused by changes in diameter [$C_{d[m]}$ in (201) and $\Xi_{[0m]}$ in (202)].

2.4 *Extension to Many Spurious Modes and Two Polarizations*

Most of the above results are readily extended to include additional spurious modes, coupled to the TE_{01} signal mode to first order, and two polarizations of all such spurious modes (except TE_{0m}). First, we may proceed via the scattering matrices for discrete mode converters including many spurious modes, and thence to the continuous case via limiting processes, as above. Alternately, we may take the generalized telegraphist's equations, including all modes, and find perturbation solutions as above, and thence treat the discrete case by limiting processes. The conclusions of such a study may be summarized as follows:

1. The first-order spurious mode transfer coefficients for each of the spurious modes are given as above [e.g., (72), (73), (118) or (186)], with of course the appropriate coupling coefficient and differential propagation constant for each of the modes.

2. For the second-order TE_{01} transmission parameters (G_0 , g , Λ , A , Θ) we must replace each term involving the coupling coefficient by a summation of similar terms, each corresponding to a particular spurious mode, with of course the appropriate coupling coefficient and differential propagation constant for each mode. For this purpose we regard the two orthogonal polarizations of a spurious mode as two distinct (but degenerate) spurious modes. Thus for example we write

$$\Lambda \approx \sum_m \Lambda_m , \qquad A \approx \sum_m A_m , \qquad \Theta \approx \sum_m \Theta_m . \tag{206}$$

The quantities for the m^{th} mode are given for example by (65) and (71) or (161) for the discrete case, and (116) and (117), (119) and (120), or (156), (170) for the continuous case, with in each of these equations the subscript m attached to the coupling coefficients and differential propagation constants.

Much of this analysis is a straightforward extension of the two-mode analysis above, and will not be discussed here. The study of convergence of the approximate solutions, analogous to that discussed in Sections 2.3.4 and 2.3.6 and treated in Ref. 18, appears more difficult in the general multimode case, and little work has been done. Of course even in the simpler two-mode case we lack precise information on the validity of the approximate solutions, as discussed above; the same is certainly true here.

From the results of Section 2.3.7 and (206), the contribution to the TE_{01} loss A of each of the spurious modes arises from a different portion of the (mechanical) spectrum of the geometric imperfection. For example, consider a guide whose only imperfection is straightness deviation; the most important spurious modes are the forward TE_{1m} . Consider the frequency band from 50–60 kmc in 2-inch I.D. waveguide. The beat wavelength range, which is equal to the range of mechanical wavelengths of straightness deviation that contribute significantly to the TE_{01} loss component, is shown in Table I for each of these modes (see Appendix D).

The coupling coefficients for each polarization of each spurious mode for discrete tilts and offsets are obtained from (37), (38) and (47) respectively; for discrete diameter changes the coupling coefficients are obtained from (51). Thus in (71e) each of the C's should have a subscript denoting the spurious mode, and α_i and b_i should have subscripts

TABLE I

m	Mechanical Wavelength Range for 50–60 kmc Band in Feet
1	2.45264–2.94898
2	1.99720–2.40812
3	0.46389–0.56232
4	0.21503–0.26289
5	0.12293–0.15228
6	0.07762–0.09815
7	0.05134–0.06723
8	0.03377–0.04763

denoting the x or y components of tilt or offset, depending on the polarization of the spurious mode.

For the cross-sectional deformations of Section 2.3.8, the continuous coupling coefficients for the two polarizations of the TE_{nm} mode are

$$c_{[nm]}{}^{\parallel\pm}(z) = -\Xi_{[nm]}a_n(z), \tag{207a}$$

$$c_{[nm]}{}^{\perp\pm}(z) = -\Xi_{[nm]}b_n(z), \tag{207b}$$

in terms of the geometric parameters of (180). The corresponding differential propagation constants are for both cases

$$\Delta\Gamma_{[nm]}{}^{\pm} = \Gamma_{[01]} \mp \Gamma_{[nm]} . \tag{208}$$

For the coefficients $C_{o[m]}$ for continuous offsets, we find from (47), by taking the limiting form of the discrete case, that the coupling coefficients for the two polarizations of the TE_{1m} mode are

$$c_{[1m]}{}^{x\pm}(z) = C_{o[m]}{}^{\pm}\cdot x'(z), \tag{209a}$$

$$c_{[1m]}{}^{y\pm}(z) = C_{o[m]}{}^{\pm}\cdot y'(z), \tag{209b}$$

where as usual $x(z)$ and $y(z)$ denote the two rectangular components of the displacement of the guide axis from the z-axis (Fig. 7b) and the prime denotes differentiation with respect to z. The differential propagation constants are again given by (208).

Similarly for a continuous diameter variation

$$c_{[om]}{}^{\pm}(z) = C_{d[m]}{}^{\pm}\cdot r'(z), \tag{210}$$

where $r'(z)$ is the derivative of the guide radius, and we have again (208) for the differential propagation constants.

The geometry for general continuous bends (not confined to a single plane) is considerably more complex, as might be anticipated from the latter part of Section 2.1.2, and requires special discussion. In general the guide axis may be a quite arbitrary 3-dimensional space curve; e.g.,

it may be pretzel-shaped. In such extreme cases we require the notation of differential geometry to describe the guide axis. We will not attempt to discuss the subject of differential geometry itself,[36] but merely use some of its simpler results.

Let us treat the general continuous case as the limiting form of the discrete case, as in Section 2.3.2 where the curved axis of the guide was confined to a single plane. In the present more general case we use the bent cylindrical co-ordinates $\rho,\varphi,$s described in conjunction with (29). Note that distance along the (bent) guide axis will be called s in the present section (it has previously been called z), so that z can refer to distance along a fixed rectangular co-ordinate axis. The other co-ordinates ρ and φ are as defined in Section 2.1.2. We particularly require the definition of the φ co-ordinate. Briefly, lines φ = constant are drawn on the surface of the guide before it is bent, parallel to the (straight) axis of the guide. After bending (perhaps into a pretzel shape) these now deformed φ-lines furnish the φ-co-ordinates.

Now consider briefly the differential geometry of twisted space curves.[36] Let $\mathbf{r}$ be the vector from a fixed origin to the curve. Three unit vectors characterize the geometric properties of a general space curve:

$\mathbf{t}$ — tangent vector.

$\mathbf{p}$ — principal normal vector.

$\mathbf{b}$ — binormal vector.

Then the following relations hold true:

$$\frac{d\mathbf{r}}{ds} = \mathbf{t}. \tag{211a}$$

$$\frac{d\mathbf{t}}{ds} = \frac{1}{\rho}\mathbf{p}. \tag{211b}$$

$$\mathbf{b} = \mathbf{t} \times \mathbf{p}. \tag{211c}$$

$$\frac{d\mathbf{b}}{ds} = -\frac{1}{\tau}\mathbf{p}. \tag{211d}$$

$$\frac{d\mathbf{p}}{ds} = \frac{1}{\tau}\mathbf{b} - \frac{1}{\rho}\mathbf{t}. \tag{211e}$$

In (211) ρ is the radius of curvature, $\frac{1}{\rho}$ the curvature; similarly τ is called the radius of torsion, $\frac{1}{\tau}$ the torsion. The principal normal $\mathbf{p}$ lies

in the plane of the circle that best approximates the twisted curve in the neighborhood of a given point; the radius of this circle is of course the radius of curvature ρ.

Now let us consider the limiting process in which a guide with a continuous three-dimensional bend is considered as the limit of a guide with closely spaced discrete tilts. In the following let $\theta(s)$ represent the orientation of the elementary discrete tilt located at distance s along the (bent) guide axis, measured in the bent cylindrical co-ordinate system described above in the present section and in Section 2.1.2. Then in the limit as the discrete tilts become a continuous three-dimensional space curve, $\theta(s)$ is given by

$$\frac{d\theta(s)}{ds} = -\frac{1}{\tau}. \tag{212}$$

From (37) the continuous coupling coefficients to the two polarizations of the $TE_{1m}^{\pm}$ spurious mode are:

$$c_{[1m]}{}^{x\pm}(s) = C_{t[m]}{}^{\pm} \cdot \frac{\cos\theta(s)}{\rho(s)} \tag{213a}$$

$$c_{[1m]}{}^{y\pm}(s) = C_{t[m]}{}^{\pm} \cdot \frac{\sin\theta(s)}{\rho(s)}. \tag{213b}$$

Similarly for the TM_{11}^{+} spurious mode:

$$c_{(11)}{}^{x+}(s) = C_{t(11)}{}^{+} \cdot \frac{\cos\theta(s)}{\rho(s)} \tag{214a}$$

$$c_{(11)}{}^{y+}(s) = C_{t(11)}{}^{+} \cdot \frac{\sin\theta(s)}{\rho(s)}. \tag{214b}$$

$\rho(s)$ is the radius of curvature, determined from (211b). $\theta(s)$ is found from (212) as the negative of the integral of the torsion $\frac{1}{\tau}$, determined from (211d).

The results of (213) and (214) are sufficiently general to include such things as pretzel-shaped waveguides and other unusual deformations. However since we seldom expect such things in practice, we seek to simplify these results. We are guided by the simplification in the discrete case that is discussed following (37). We assume that the angular deviation of the guide axis from the z-axis of an x, y, z rectangular co-ordinate system remains small;

$$\begin{aligned} |\, x'(z)\,| &\ll 1, \\ |\, y'(z)\,| &\ll 1. \end{aligned} \tag{215}$$

Further we assume that the $\varphi = 0$ co-ordinate on the surface of the guide initially lies in the x-z plane, and that it remains close to this plane. Then from (38), by the usual transformation from the discrete to the continuous case, we have

$$s \approx z, \tag{216a}$$

$$\frac{\cos\theta(s)}{\rho(s)} \approx x''(z), \tag{216b}$$

$$\frac{\sin\theta(s)}{\rho(s)} \approx y''(z), \tag{216c}$$

to be substituted into (213) and (214). The superscripts x and y of (213) and (214) in this special case correspond to linear polarizations defined with respect to the x and y axes of the fixed rectangular co-ordinate system; in general the superscripts of (213) and (214) correspond to the $\varphi = 0$ and $\varphi = \pi/2$ planes in the bent cylindrical co-ordinate system. The approximations of (216) are found directly for the continuous case in Appendix E.

III. THEORY OF GUIDES WITH RANDOM DISCRETE IMPERFECTIONS

We now apply the results of Section II to the study of guides with random discrete mode converters. The following cases of practical interest will be discussed:

i. Guides made of individual pipes that are perfect right circular cylinders of identical diameter and length l_0 but that have randomly imperfect joints, with either tilts or offsets. The first-order spurious modes in this case will be the TE_{1m} family, with the most significant being the forward TE_{11} and TE_{12}, and for tilts the forward TM_{11}. Both polarizations of each spurious mode must of course be considered.

ii. Guides made of individual pipes that are perfect right circular cylinders of identical length l_0 with perfect joints (no tilts or offsets) but of slightly different random diameters. The spurious modes will be the TE_{0m} family, with forward TE_{02} the most important. Each mode now has only a single polarization.

The statistics of the TE_{01} loss will be determined in terms of the statistics of the guide imperfections. Only the case of individual pipes of identical length will be considered.

The necessary results from Section II are summarized below in Section 3.1. Section 3.2 states the statistical models adopted for guides with random tilts, offsets, and diameter changes. In Section 3.3 the expected value of the average TE_{01} loss, and the power spectrum and total

power (expected value of the mean square value) of the TE_{01} loss variation about its average value, are determined in terms of the statistics of the random offsets, tilts, or diameter variations of the guide. In Section 3.4 these results are extended to cover long guides with mode filters. Representative numerical examples are given in Section 3.5 for a 20-mile total guide length. Section 3.6 considers the application of certain of these results for tilts and offsets to helix guide.

Most of the work of Section III will be confined to copper guide. As before, we assume that the coupling coefficients for ideal metallic guide provide a good approximation to those for copper guide, but modify the (pure imaginary) propagation constants for ideal metallic guide to account for the loss present in copper guide. Of course the analysis for diameter changes applies equally well to copper or helix guide.

3.1 *TE_{01} Loss — Summary of Previous Results*

We give below the TE_{01} normalized loss (in nepers) A, written in a form suitable for the purposes of the present section. These relations are readily obtained from the results of Section II, and in particular from Section 2.4 and (37), (38), (47), (51), (61) to (65), (71d), (71e), (161), and (206). First, from (206) the total TE_{01} loss A is given as the sum of terms due to the individual first-order spurious modes;

$$A \approx \sum_m A_m . \tag{217}$$

The term A_m due to the m^{th} spurious mode is given below in (218) and (219). In these and similar relations involving only a single spurious mode we omit the subscripts denoting the spurious mode on the coupling coefficients and differential propagation constants, in order to avoid unnecessarily cluttering up the equation. Therefore for each spurious mode

$$A \approx \frac{1}{2}A_0 + \sum_{k=1}^{N-1} A_k \cos k\Delta\beta l_0 \tag{218a}$$

where

$$A_k = e^{k\Delta\alpha l_0} \sum_{i=1}^{N-k} (x_i^{\parallel} x_{i+k}^{\parallel} + x_i^{\perp} x_{i+k}^{\perp}), \quad 0 \leqq k \leqq N-1. \tag{218b}$$

Tilts:

$$\begin{aligned} x_i^{\parallel} &= C_t\, \alpha_i \cos\theta_i \approx C_t\, \alpha_i^{\parallel} \\ x_i^{\perp} &= C_t\, \alpha_i \sin\theta_i \approx C_t\, \alpha_i^{\perp}. \end{aligned} \tag{218c}$$

Offsets:

$$\begin{aligned} x_i^{\parallel} &= C_o b_i \cos\theta_i = C_o b_i^{\parallel} \\ x_i^{\perp} &= C_o b_i \sin\theta_i = C_o b_i^{\perp}. \end{aligned} \tag{218d}$$

Diameter change:

$$\begin{aligned} x_i^{\parallel} &= C_d \Delta r_i \\ x_i^{\perp} &= 0. \end{aligned} \tag{218e}$$

The distinction between A_k of (218a) and (218b), the k^{th} Fourier coefficient of the TE_{01} loss due to a single spurious mode, and A_m of (217), denoting the TE_{01} loss due to the m^{th} spurious mode, will always be clear from the context. In particular cases the subscripts indicating the spurious mode will always be enclosed in [ ] or ( ) to denote TE or TM spurious modes respectively.

For the case of zero differential attenuation constant, an alternate form is sometimes useful. From (161) for each spurious mode we have (with mode subscripts again omitted)

$$A \approx \frac{1}{2}\left|\sum_{i=1}^{N} x_i^{\parallel} e^{-j\Delta\beta l_0 i}\right|^2 + \frac{1}{2}\left|\sum_{i=1}^{N} x_i^{\perp} e^{-j\Delta\beta l_0 i}\right|^2; \quad \Delta\alpha = 0. \tag{219}$$

The x_i's are again given by (218c) to (218e).

In the above results we have chosen to group the two polarizations of each spurious mode (TE_{1m} and TM_{11}^{+}) for tilts and offsets in each term of (217). We use the symbols $\parallel$ and $\perp$ to distinguish the two polarizations, rather than x and y as in Section II. The length of the individual pipes is l_0, the total length of guide is $L_N = Nl_0$.

In these results the significant frequency dependence, at least over moderate bandwidths, occurs through the $\Delta\beta$, the differential phase constants between TE_{01} and the spurious modes. Far from cutoff (the case of greatest practical interest) the $\Delta\beta$ are approximately proportional to the free-space wavelength λ. A great simplification in the subsequent analysis is obtained by neglecting the frequency dependence of $\Delta\alpha$ and the x_i's, setting these quantities equal to their values at the middle of the band of interest. Then A_m, the contribution to the TE_{01} loss of conversion to the m^{th} spurious mode, becomes a Fourier series, periodic in λ, with random coefficients A_k, as given in (218). A, the total TE_{01} loss due to mode conversion, is given by a sum of periodic components of incommensurable periods, according to (217).

Over moderate bandwidths, the effect of the frequency dependence of $\Delta\alpha$ is small far from cutoff. For offsets and diameter changes, the fre-

quency dependence of the coupling coefficients and hence the x_i is also small far from cutoff; however, for tilts the x_i vary approximately inversely with λ. Thus, the above approximation may appear questionable for tilts, but is used even here because of the resulting simplification in the analysis. [Compare the discussion in Section 2.3.7 following (169).]

We thus regard the loss A as a function of the free-space wavelength λ, and write

$$A = \bar{A} + \delta A \tag{220}$$

where $\bar{A}$ is the average value over free-space wavelength λ of the loss over some suitable band, and δA is the deviation of the loss from its average value. The expected value of the average loss $\langle \bar{A} \rangle$, and the power spectrum of δA and its total power or the expected value of its average mean square value $\langle \overline{(\delta A)^2} \rangle$, are easily found in terms of the statistics of the random Fourier coefficients A_k ; the bar again indicates an average over the free-space wavelength λ.

A more exact treatment of the loss statistics, one that avoids the above approximations and includes the frequency dependence of all quantities, is straightforward but lengthy. A brief discussion, given in Appendix F, of the statistics of each of the two terms of (218a) as functions of λ, verifies the approximate analysis.

3.2 *Statistical Model of Guide*

3.2.1 *Tilts and Offsets*

We assume that the parallel and perpendicular components of tilt or offset ($\alpha^{\parallel}$, $\alpha^{\perp}$ or $b^{\parallel}$, $b^{\perp}$) are independent Gaussian random variables with zero mean and equal variance; tilts or offsets at different joints are assumed to be independent, and to have the same distribution. Then the magnitude of tilt or offset (α or b) will have a Rayleigh distribution and the orientation (θ) will be uniformly distributed between 0 and 2π, and these two quantities will also be independent.

From (37), (38), (47), and (218c) and (218d) we have

$$x^{\parallel} = \frac{C_t \alpha^{\parallel}}{C_o b^{\parallel}}, \qquad x^{\perp} = \frac{C_t \alpha^{\perp}}{C_o b^{\perp}}; \qquad x = \frac{C_t \alpha}{C_o b}. \tag{221}$$

Thus identical statements to those above may be made about $x^{\parallel}$, $x^{\perp}$, x and θ.

For convenience we state the following results in terms of x's; any of these equations obviously holds true if x is replaced by α or b throughout. The rms value of x is denoted by $\hat{x}$; thus

$$\hat{x}^2 \equiv \langle x^2 \rangle = \frac{C_t^2 \langle \alpha^2 \rangle}{C_o^2 \langle b^2 \rangle}, \tag{222}$$

where the symbols $\langle \ \rangle$ denote the expected value of a random variable. Then the various probability distributions at any joint may be written as follows:

$$p(x^{\parallel}) = \frac{1}{\sqrt{\pi}\hat{x}} \exp -\left(\frac{x^{\parallel}}{\hat{x}}\right)^2; \qquad p(x^{\perp}) = \frac{1}{\sqrt{\pi}\hat{x}} \exp -\left(\frac{x^{\perp}}{\hat{x}}\right)^2 \tag{223}$$

$$p(x^{\parallel}, x^{\perp}) = p(x^{\parallel})p(x^{\perp})$$

$$p(x) = \frac{2x}{\hat{x}^2} \exp -\left(\frac{x}{\hat{x}}\right)^2, \quad x > 0; \qquad p(\theta) = \frac{1}{2\pi}, \quad 0 < \theta < 2\pi \tag{224}$$

$$p(x,\theta) = p(x)p(\theta).$$

We have:

$$\langle x^{\parallel} \rangle = \langle x^{\perp} \rangle = 0, \qquad \langle x^{\parallel} x^{\perp} \rangle = 0.$$

$$\langle x^{\parallel 2} \rangle = \langle x^{\perp 2} \rangle = \frac{\hat{x}^2}{2}, \qquad \langle x^{\parallel 4} \rangle = \langle x^{\perp 4} \rangle = \frac{3\hat{x}^4}{4}. \tag{225}$$

$$\langle x \rangle = \frac{\sqrt{\pi}}{2}\hat{x}, \qquad \langle x^2 \rangle = \hat{x}^2, \qquad \langle x^4 \rangle = 2\hat{x}^4. \tag{226}$$

Subscripts indicating the joint or mode converter have been omitted in the above relations. Since different joints are independent, for two different joints i and j we have

$$\langle x_i^{\parallel} x_j^{\parallel} \rangle = \langle x_i^{\parallel} x_j^{\perp} \rangle = \langle x_i^{\perp} x_j^{\perp} \rangle = 0, \quad i \neq j. \tag{227}$$

Subscripts denoting the spurious mode have been omitted in the above equations.

3.2.2 *Diameter Changes*

The radius of the i^{th} pipe r_i is given by

$$r_i = a + \epsilon_i \tag{228}$$

where a is the average radius and ϵ_i a small random variation about the average. The ϵ_i are assumed to be independent Gaussian random variables with zero mean and variance $\hat{\epsilon}^2$.

$$p(\epsilon_i) = \frac{1}{\sqrt{2\pi}\hat{\epsilon}} \exp -\frac{\epsilon_i^2}{2\hat{\epsilon}^2} \tag{229}$$

$$\langle \epsilon_i \rangle = 0; \qquad \langle \epsilon_i^2 \rangle = \hat{\epsilon}^2; \qquad \langle \epsilon_i \epsilon_j \rangle = 0, \quad i \neq j. \tag{230}$$

Then Δr_i, the change in radius at the i^{th} joint, is given by

$$\Delta r_i = \epsilon_i - \epsilon_{i-1}, \tag{231}$$

and has a Gaussian distribution with zero mean and variance $(\hat{\Delta r})^2$

$$p(\Delta r_i) = \frac{1}{\sqrt{2\pi}\hat{\Delta r}} \exp - \frac{(\Delta r_i)^2}{2(\hat{\Delta r})^2}; \qquad \Delta r = \sqrt{2}\hat{\epsilon}. \tag{232}$$

However adjacent joints are no longer independent; from (231) Δr_i and Δr_j are independent only if $| j - i | > 1$. Therefore:

$$\begin{aligned} \langle \Delta r_i \rangle &= 0. \\ \langle (\Delta r_i)^2 \rangle &= (\Delta r)^2 = 2\hat{\epsilon}^2. \\ \langle \Delta r_i \Delta r_{i\pm 1} \rangle &= -\frac{(\hat{\Delta r})^2}{2} = -\hat{\epsilon}^2. \\ \langle \Delta r_i \Delta r_j \rangle &= 0, \quad | j - i | > 1. \end{aligned} \tag{233}$$

Equations (232) and (233) apply also to the corresponding x_i, given by (218e) for a diameter change, for any spurious mode, by making the substitution $\Delta r_i \rightarrow x_i$ and $\hat{\Delta r} \rightarrow \hat{x}$, where $\hat{x}$ is given by

$$\hat{x} = C_d \Delta r. \tag{234}$$

Subscripts denoting the spurious mode have again been omitted in the above equations.

3.3 *Statistics of the TE_{01} Loss for a Single Section of Waveguide between Mode Filters*

3.3.1 *Offsets*

For a copper waveguide section whose only defects are independent random offsets at the joints between pipes, the most important spurious modes will be the forward TE_{12} and TE_{11}, with the other forward TE_{1m} modes contributing only a small amount to the total TE_{01} loss. Neglecting the frequency dependence of all quantities except the $\Delta\beta$, we have from (218a) and (220) for each spurious mode:

$$\begin{aligned} A &= \bar{A} + \delta A, \\ \bar{A} &= \tfrac{1}{2} A_0, \\ \delta A &= \sum_{k=1}^{N-1} A_k \cos k\Delta\beta l_0, \end{aligned} \tag{235}$$

where the random Fourier coefficients A_k are given in (218b), together with (218d). The subscript indicating the spurious mode has again been omitted.

The following moments of A_k are easily determined from the results of Section 3.2.1:

$$\begin{aligned} \langle A_0 \rangle &= \hat{x}^2 N, \\ \langle A_0^2 \rangle &= \hat{x}^4 N(N+1). \end{aligned} \tag{236a}$$

$$\langle A_k \rangle = 0, \qquad \langle A_k^2 \rangle = \frac{\hat{x}^4}{2}(N-k)e^{k2\Delta\alpha l_0}; \quad 1 \leqq k \leqq N-1. \tag{236b}$$

$$\langle A_k A_l \rangle = 0, \quad k \neq l. \tag{236c}$$

From (235) and (236a) the expected value of the average TE_{01} normalized loss due to each spurious mode is

$$\langle \bar{A} \rangle = \frac{\hat{x}^2}{2} N. \tag{237}$$

From (236b) the (discrete) power spectrum of δA is

$$P_k = \tfrac{1}{2}\langle A_k^2 \rangle = \frac{\hat{x}^4}{4}(N-k)\, e^{k2\Delta\alpha l_0}, \quad 1 \leqq k \leqq N-1. \tag{238}$$

From (236c) the different Fourier components of δA are uncorrelated. The total power, or the expected value of the mean square value, of δA is found by summing over the discrete power spectrum P_k. From (238):

$$\begin{aligned} \langle \overline{(\delta A)^2} \rangle = \sum_{k=1}^{N-1} P_k &= \frac{\hat{x}^4}{4} \sum_{k=1}^{N-1} (N-k)\, e^{k2\Delta\alpha l_0} \\ &= \frac{\hat{x}^4}{4} \frac{e^{2\Delta\alpha l_0}}{1 - e^{2\Delta\alpha l_0}} \left[N - \frac{1 - e^{N2\Delta\alpha l_0}}{1 - e^{2\Delta\alpha l_0}} \right]. \end{aligned} \tag{239}$$

Strictly speaking, the average over free-space wavelength λ indicated by the bar in (237) and (239) must be taken either over a single fundamental period of δA (such that $\Delta\beta l_0$ changes by 2π) or over a band large compared to a single period. Let $\Delta\lambda$ and Δf be the interval in wavelength and frequency, respectively, corresponding to a fundamental period. From (167) and (173) we find

$$\frac{\Delta f}{f} \approx \frac{\Delta\lambda}{\lambda} = \frac{B}{l_0} \tag{240}$$

where B is the beat wavelength, tabulated in Appendix D, and l_0 is the distance between joints in the guide. (This result is similar to that of

(178) for the sample point spacing; in (178), however, the length L is the total length of guide.)

Equation (239) simplifies in two special cases of interest:

1. Small differential loss over total length $L_N = Nl_0$.

$$\langle\overline{(\delta A)^2}\rangle = \frac{\hat{x}^4}{8} N(N-1); \qquad -N2\Delta\alpha l_0 \ll 1. \tag{241}$$

2. Large differential loss over total length L_N, small differential loss over pipe length l_0.

$$\langle\overline{(\delta A)^2}\rangle = \frac{\hat{x}^4}{8} \frac{N}{-\Delta\alpha l_0}; \quad \begin{matrix} -N2\Delta\alpha l_0 \gg 1 \\ -2\Delta\alpha l_0 \ll 1. \end{matrix} \tag{242}$$

We recall again that $\Delta\alpha$ is negative throughout the present treatment, in which the TE_{01} signal mode has lower heat loss than any of the spurious modes.

Referring to Section 3.2.1, $\langle A\rangle$ and $\sqrt{\langle\overline{(\delta A)^2}\rangle}$ are both proportional to the square of the rms offset at the joints between pipes. $\langle\bar{A}\rangle$ is proportional to L_N, the length of the waveguide section. $\sqrt{\langle\overline{(\delta A)^2}\rangle}$ is initially proportional to L_N, when L_N is small enough so that the differential loss may be neglected; for large L_N it becomes proportional to $\sqrt{L_N}$.

The power spectrum P_k of (238) has its maximum value for $k = 1$, and decreases monotonically as k increases to $N - 1$. For small differential loss P_k is triangular; for large differential loss it is exponential. The "3-db bandwidth" of the power spectrum P_k, the value of k for which P_k is equal to half its maximum value, is related to the rate of variation of the TE_{01} loss component due to a particular spurious mode. We have:

$$k_{3\,db} = \frac{N}{2}; \qquad -N2\Delta\alpha l_0 \ll 1 \tag{243a}$$

$$k_{3\,db} = \frac{0.692}{-2\Delta\alpha l_0}; \quad -N2\Delta\alpha l_0 \gg 1. \tag{243b}$$

Making use of (167) and (173), we find

$$\frac{\Delta f_{3\,db}}{f} \approx \frac{\Delta\lambda_{3\,db}}{\lambda} = \frac{B}{k_{3\,db} l_0} \tag{244}$$

for the interval in free-space wavelength or frequency (of the radiation in the guide) corresponding to the 3-db bandwidth of the TE_{01} loss variation.

The statistics of the total TE_{01} loss due to mode conversion are given simply by summing over the contributions of the individual spurious modes. From (217) we have

$$\langle \bar{A} \rangle = \sum_{[m]} \langle \bar{A}_{[m]} \rangle, \tag{245}$$

$$\langle \overline{(\delta A)^2} \rangle = \sum_{[m]} \langle \overline{(\delta A_{[m]})^2} \rangle, \dagger \tag{246}$$

where $[m]$ indexes the TE_{1m}^{+} spurious modes. The individual terms in (245) and (246) for each spurious mode are given by (237) and (239) (or (241) and (242) in special cases), in which the subscript $[m]$ has been omitted for convenience. The power spectra of the $\delta A_{[m]}$ are given by (238). From (222) and (237),

$$\langle \bar{A} \rangle = \frac{\langle b^2 \rangle N}{2} \sum_{[m]} C_{o[m]}{}^2. \tag{247}$$

A practical waveguide system will contain mode filters for the TE_{1m} modes at a close enough spacing so that the differential losses for the important spurious modes are small in each section. For this special case we have from (241)

$$\langle \overline{(\delta A)^2} \rangle = \frac{\langle b^2 \rangle^2 N(N-1)}{8} \sum_{[m]} C_{o[m]}{}^4; \quad -N2\Delta\alpha_{[m]} l_0 \ll 1. \tag{248}$$

In (247) and (248) $\langle b^2 \rangle$ is the mean square magnitude of offset, $C_{o[m]}$ is Morgan's coupling coefficient between TE_{01} and TE_{1m} for offsets, given in Appendix A, and $\Delta\alpha_{[m]} = \alpha_{[01]} - \alpha_{[1m]}$, the difference in attenuation constants of the TE_{01} and TE_{1m}^{+} modes.

Formulas and numerical values for the various coupling coefficients and beat wavelengths are given in Appendix A and D. For a frequency of 55 kmc and a 1-inch guide radius, (247) and (248) become, summing over the nine propagating TE_{1m}^{+} modes:

$$\begin{aligned} \langle \bar{A} \rangle &= \frac{\langle b^2 \rangle N}{2} (1.107 + 4.581 + 0.641 + 0.271 + \cdots) \\ &= \langle b^2 \rangle N(3.519); \quad \langle b^2 \rangle \text{ in inch}^2. \end{aligned} \tag{249}$$

$$\langle \overline{(\delta A)^2} \rangle = \frac{\langle b^2 \rangle^2 N(N-1)}{8} (1.226 + 20.984 + 0.411 + 0.074 + \cdots)$$

† No cross terms appear in the summation of (246) because, subject to the approximations of the present section that neglect the frequency variation of the coupling coefficients (C_t, C_o, and C_d) and the $\Delta\alpha$'s, the Fourier components of the different $\delta A_{[m]}$ have incommensurable periods, and hence their total powers or mean square values may be simply added. The cross terms are treated exactly in Appendix F.

$$= \langle b^2\rangle^2 N(N-1)(2.842)$$

$$\sqrt{\overline{\langle(\delta A)^2\rangle}} = \langle b^2\rangle \sqrt{N(N-1)}(1.686)\,; \quad \langle b^2\rangle \text{ in inch}^2, \quad -N2\Delta\alpha_{[m]}l_0 \ll 1\,. \tag{250}$$

The most important terms are those due to TE_{11}^+ and TE_{12}^+.

3.3.2 *Tilts*

We next consider a copper guide whose only defects are random tilts at the joints between pipes. The spurious modes are the forward TE_{1m} with TE_{12}^+ and TE_{11}^+ the most important, as in the offset case above, and in addition the forward TM_{11}. The effects of the TE_{1m}^+ modes on the TE_{01} transmission are given by the results of Section 3.3.1 above [see (235) to (246)], using of course the appropriate coupling coefficients for tilts [see (218c)]. However, TM_{11}^+ requires special consideration.

Equations (235) and (236) apply to TM_{11}^+ as well as to the TE_{1m} modes. For TM_{11}^+, $\Delta\beta = \Delta\alpha$ in copper guide. Thus the beat wavelength for TM_{11}^+ is very long—3195 feet in 2-inch I.D. pipe at 55 kmc—compared to the beat wavelengths of the TE_{1m} modes, and long even compared to the length of guide sections between mode filters in a practical waveguide system.† Thus, the bandwidths we will consider (e.g., 50–60 kmc) are only a small portion of the fundamental period of $A_{(11)}^+$, the TM_{11}^+ component of the TE_{01} loss, as given in (240), and so the summation of powers of Fourier components given in (239) is no longer valid in determining the mean square loss variation. In fact $A_{(11)}^+$ will be almost independent of frequency (except for the slow variation of coupling coefficient, which is inversely proportional to free-space wavelength λ, neglected over moderate bandwidths in the present analysis).

Thus, consider a section of copper guide short compared with the TM_{11}^+ beat wavelength (3195 feet). Then both $\Delta\alpha$ and $\Delta\beta$ may be set equal to zero. From (219) the TM_{11}^+ component of the TE_{01} loss is

$$A_{(11)}^+ = \frac{1}{2}\left[\sum_{i=1}^{N} x_i^{\parallel}\right]^2 + \frac{1}{2}\left[\sum_{i=1}^{N} x_i^{\perp}\right]^2. \tag{251}$$

This is simply equal to the TE_{01} loss due to TM_{11}^+ at a single tilt equal to the net tilt between the input and output ends of the guide. This result is obvious from the fact that we have neglected both attenuation and phase shift in the relatively short sections of guide under consideration. The loss is therefore independent of the lengths of guide between

† This is true only for unmodified copper guide. A thin dielectric coating will reduce the TE_{01}-TM_{11}^+ beat wavelength to much smaller values;[12,13,14] the present treatment of TM_{11}^+ will obviously not apply in such a case.

discrete mode converters, and these lengths may thus be set equal to zero, yielding only a single tilt whose magnitude and orientation are equal to the net tilt between the ends of the guide. This result holds true for TM_{11}^{+} for any arbitrary continuous bend of the guide axis, which may be considered as the limit of a series of discrete tilts (Section 2.3).

To this approximation $A_{(11)}^{+}$ is thus independent of frequency (except for the slow variation of coupling coefficient with λ). TM_{11}^{+} thus contributes to the average loss $\bar{A}$ but not to $\overline{(\delta A)^2}$. Thus (245) contains an extra term, while (246) remains unaltered.

$$\langle \bar{A} \rangle = \langle \bar{A} \rangle_{TE} + \langle A_{(11)}^{+} \rangle \tag{252}$$

$$\langle \bar{A} \rangle_{TE} = \sum_{[m]} \langle \bar{A}_{[m]} \rangle \tag{253}$$

$$\langle \overline{(\delta A)^2} \rangle = \sum_{[m]} \langle \overline{(\delta A_{[m]})^2} \rangle \tag{254}$$

The index $[m]$ again indexes the TE_{1m}^{+} modes. $\langle \bar{A}_{[m]} \rangle$ and $\langle \overline{(\delta A_{[m]})^2} \rangle$ are again given by (237) and (239) (or (241) and (242) in special cases) and $\langle A_{(11)}^{+} \rangle$ is also given by (237), with the appropriate coupling coefficients for tilts. Equations (238), (243), and (244) remain true for the TE_{1m}^{+} components of the TE_{01} loss. The results analogous to (247) to (250) for tilts are summarized below.

$$\langle \bar{A} \rangle_{TE} = \frac{\langle \alpha^2 \rangle N}{2} \sum_{[m]} C_{t[m]}^{\ 2} \tag{255}$$

$$\langle A_{(11)}^{+} \rangle = \frac{\langle \alpha^2 \rangle N}{2} C_{t(11)}^{\ 2} \qquad (TM_{(11)}^{+}) \tag{256}$$

For small differential loss (because of mode filters),

$$\langle \overline{(\delta A)^2} \rangle = \frac{\langle \alpha^2 \rangle^2 N(N-1)}{8} \sum_{[m]} C_{t[m]}^{\ 4}; \quad -N 2\Delta\alpha_{[m]} l_0 \ll 1. \tag{257}$$

$\langle \alpha^2 \rangle$ is the mean square magnitude of tilt. Substituting numerical values for the C_t^{+}'s from Appendix A, for a frequency of 55 kmc and a 1-inch guide radius, (255)–(257) become, summing over the nine propagating TE_{1m}^{+} modes:

$$\langle \bar{A} \rangle_{TE} = \frac{\langle \alpha^2 \rangle N}{2} (29.465 + 81.085 + 0.616 + 0.057 + \cdots)$$

$$= \langle \alpha^2 \rangle N(55.619); \qquad \langle \alpha^2 \rangle \text{ in radian}^2. \tag{258}$$

$$\langle A_{(11)}^{+} \rangle = \langle \alpha^2 \rangle N(14.598); \qquad \langle \alpha^2 \rangle \text{ in radian}^2. \tag{259}$$

$$\langle\overline{(\delta A)^2}\rangle = \frac{\langle\alpha^2\rangle^2 N(N-1)}{8}(868.18 + 6574.74 + 0.38 + \cdots)$$

$$= \langle\alpha^2\rangle^2 N(N-1)(930.41)$$

$$\sqrt{\langle\overline{(\delta A)^2}\rangle} = \langle\alpha^2\rangle\sqrt{N(N-1)}\,(30.503); \qquad \langle\alpha^2\rangle \text{ in radian}^2, \quad -N2\Delta\alpha_{[m]}l_0 \ll 1. \tag{260}$$

Again the most important terms are those due to TE_{11}^+ and TE_{12}^+, and for the average loss, to TM_{11}^+ in addition.

For a given (copper) guide $A_{(11)}^+$, the TM_{11}^+ contribution to the (average) TE_{01} loss is determined simply by the net tilt between the input and output of the guide, as discussed above. The present model, which assumes that the only imperfections are tilts at the joints between perfect pipes, seems grossly unrealistic as far as the effects of TM_{11}^+ are concerned for any practical guide, for at least two reasons. First, practical pipes will have long bows or gradual curvature of the guide axis; this factor will probably be much more important in determining the net tilt between the guide input and output than tilts of the very small angles of interest here. Second, practical guides may be subject to mechanical constraints of various types which will also introduce slow variations in curvature of the guide axis.

In contrast, gradual curvature of the guide axis will have little effect on the TE_{1m} components of the TE_{01} loss for reasons indicated in Section 2.3.7 and to be discussed in detail in Section IV; this is so because only straightness deviations whose wavelengths are approximately equal to the beat wavelengths of the important spurious modes contribute to the TE_{01} loss in copper guide.

Consequently the effect of TM_{11}^+ on the average loss has been stated separately for the particular model discussed here; it is given in (256) and (259) for whatever tutorial value it may have. As stated above, TM_{11}^+ will have no significant effect on the variation of TE_{01} loss about its average value for the relatively short mode filter spacings which must be used in a practical waveguide system.

3.3.3 *Diameter Changes*

Finally, consider a copper or helix guide whose only defects are random diameters of the individual pipes, which are perfect right circular cylinders and have no tilts or offsets at their joints. Again from (218a)

and (220) for each spurious (TE_{0m}) mode we have, as in (235) for offsets or tilts:

$$\begin{aligned} A &= \bar{A} + \delta A \\ \bar{A} &= \tfrac{1}{2}A_0 \\ \delta A &= \sum_{k=1}^{N-1} A_k \cos k\Delta\beta l_0 \,. \end{aligned} \tag{261}$$

The random Fourier coefficients are again given by (218b), together with (218e).

$$A_k = e^{k\Delta\alpha l_0} \sum_{i=1}^{N-k} x_i x_{i+k} \,. \tag{262}$$

The subscript indicating the spurious mode is again omitted.

The moments of the A_k must be slightly modified from those given in (236) for independent offsets and tilts, because of the correlation between adjacent diameter changes imposed by the present mathematical model and because each spurious mode now has only one polarization rather than two. From (228) to (234):

$$\langle A_0 \rangle = \hat{x}^2 N, \qquad \langle A_0{}^2 \rangle = \hat{x}^4 (N^2 + 3N - 1) \,. \tag{263a}$$

$$\langle A_1 \rangle = -\frac{\hat{x}^2}{2} (N - 1) e^{\Delta\alpha l_0}, \qquad \langle A_1{}^2 \rangle = \frac{\hat{x}^4}{4} (N^2 + 5N - 8) e^{2\Delta\alpha l_0} \tag{263b}$$

$$\langle A_k \rangle = 0, \qquad \langle A_k{}^2 \rangle = \frac{\hat{x}^4}{2} [3(N - k) - 1] e^{k2\Delta\alpha l_0}; \quad 2 \leqq k \leqq N - 1 \,. \tag{263c}$$

$$\langle A_k A_l \rangle = \hat{x}^4 e^{(k+l)\Delta\alpha l_0} \cdot \begin{Bmatrix} -(N - l) \\ +\tfrac{1}{4}(N - l) \\ 0 \end{Bmatrix}; \begin{bmatrix} l - k = 1 \\ l - k = 2 \\ l - k \geqq 3 \end{bmatrix}, \quad 0 < k < l, \tag{263d}$$

$$\langle A_0 A_l \rangle = \hat{x}^4 e^{l\Delta\alpha l_0} \cdot \begin{Bmatrix} -\tfrac{1}{2}(N - 1)(N + 4) \\ +\tfrac{1}{2}(N - 2) \\ 0 \end{Bmatrix}; \begin{bmatrix} l = 1 \\ l = 2 \\ l \geqq 3 \end{bmatrix}. \tag{263e}$$

From (236a) and (261) the expected value of the average loss due to each spurious mode is again

$$\langle \bar{A} \rangle = \frac{\hat{x}^2}{2} N, \tag{264}$$

as in (237) for offsets or tilts. However, the statistics of the A_k's, as given in (263), differ from those of (236) for tilts and offsets. Because $\langle A_1 \rangle$ is no longer equal to zero, the expected value of the TE_{01} loss will have a fundamental periodic component, in addition to a dc component. Consequently it is convenient to rewrite the first relation of (261) as follows:

$$A = \bar{A} + \langle A_1 \rangle \cos \Delta\beta l_0 + \delta A'. \tag{265}$$

Thus,

$$\delta A' = (A_1 - \langle A_1 \rangle) \cos \Delta\beta l_0 + \sum_{k=2}^{N-1} A_k \cos k\Delta\beta l_0 . \tag{266}$$

$\langle A_1 \rangle$ is given in (263b). $\bar{A}$ is the average loss as before, $\langle A_1 \rangle \cos \Delta\beta l_0$ is a slowly varying sinusoidal component of loss whose period equals the fundamental period of the TE_{01} loss (see (240)), and $\delta A'$ includes the remaining random loss variations. The (discrete) power spectrum P_k' of $\delta A'$ is given by

$$P_k' = \begin{cases} \frac{1}{2}(\langle A_1^2 \rangle - \langle A_1 \rangle^2); & k = 1. \\ \frac{1}{2}\langle A_k^2 \rangle \quad ; & 2 \leqq k \leqq N - 1. \end{cases} \tag{267}$$

From (263d) the different Fourier components of $\delta A'$ are now uncorrelated only if their indices differ by three or more. This does not affect the calculation of the total power of $\delta A'$, which remains simply the sum of P_k'.

$$\langle \overline{(\delta A')^2} \rangle = \sum_{k=1}^{N-1} P_k' = \frac{\hat{x}^4}{4} \left\{ 3 \frac{e^{2\Delta\alpha l_0}}{1 - e^{2\Delta\alpha l_0}} \left[N - \frac{1 - e^{N2\Delta\alpha l_0}}{1 - e^{2\Delta\alpha l_0}} \right] - \frac{e^{2\Delta\alpha l_0}}{1 - e^{2\Delta\alpha l_0}} \left[1 - e^{(N-1)2\Delta\alpha l_0} \right] + \frac{(N-1)}{2} e^{2\Delta\alpha l_0} \right\}. \tag{268}$$

Again for small or large differential loss, (268) simplifies:

1. Small differential loss over total length $L_N = Nl_0$.

$$\langle \overline{(\delta A')^2} \rangle = \frac{\hat{x}^4}{8} (3N - 1)(N - 1); \qquad -N2\Delta\alpha l_0 \ll 1. \tag{269}$$

2. Large differential loss over total length L_N, small differential loss over pipe length l_0.

$$\langle\overline{(\delta A')^2}\rangle = \frac{\hat{x}^4}{8}\begin{cases} \dfrac{3N}{-\Delta\alpha l_0}; & -N2\Delta\alpha l_0 \gg 1 \\ & -2\Delta\alpha l_0 \ll 1 \end{cases}. \tag{270}$$

$\langle\bar{A}\rangle$ and $\langle\overline{(\delta A')^2}\rangle$ have the same general functional form as for tilts and offsets. The "3-db bandwidth" of P_k' is approximately the same as given in (243)–(244) for tilts and offsets.

The statistics of the total TE_{01} loss due to mode conversion are now given by summing over the TE_{0m}^{+} spurious modes.

$$\langle\bar{A}\rangle = \sum_{[m]} \langle\bar{A}_{[m]}\rangle \tag{271}$$

$$\langle\overline{(\delta A')^2}\rangle = \sum_{[m]} \langle\overline{(\delta A_{[m]}')^2}\rangle. \tag{272}$$

The individual terms in (271) and (272) are given by (264) and (268) (or (269) and (270) in special cases). In addition, each spurious mode will contribute a single sinusoidal component to the TE_{01} loss, of magnitude given by the middle term of (265). From Section 3.2.2 and (264),

$$\langle\bar{A}\rangle = \langle\epsilon^2\rangle N \sum_{[m]} C_{d[m]}{}^2 \tag{273}$$

where $\langle\epsilon^2\rangle$ is the mean square variation of pipe radius.

In discussing the effects of the TE_{1m}^{+} modes in the first two parts of this section, it was assumed that the line contained ideal mode filters at a close enough spacing so that the differential loss in each section could be neglected. However, a practical mode filter in 2-inch guide presently consists of a section of helix guide, which has a low loss for the TE_{0m} spurious modes (although it effectively suppresses all other spurious modes). In the present case it is therefore assumed that there will be no mode filters in the entire length of line between repeaters. Thus, the total differential loss will be large, and the approximate result of (270) yields

$$\langle\overline{(\delta A')^2}\rangle = \frac{3\langle\epsilon^2\rangle^2 N}{2l_0} \sum_{[m]} \frac{C_{d[m]}{}^4}{-\Delta\alpha_{[m]}}; \qquad \begin{matrix} -N2\Delta\alpha_{[m]} l_0 \gg 1, \\ -2\Delta\alpha l_0 \ll 1. \end{matrix} \tag{274}$$

Substituting numerical values for the coupling coefficients and the

$\Delta\alpha$'s, for a frequency of 55 kmc and a 1-inch guide radius, (273) and (274) become:

$$\begin{aligned}\langle\bar{A}\rangle &= \langle\epsilon^2\rangle N(2.424 + 0.771 + 0.394 + 0.244 + \cdots)\\ &= \langle\epsilon^2\rangle N(4.414)\,; \quad \langle\epsilon^2\rangle \text{ in inch}^2.\end{aligned} \tag{275}$$

$$\begin{aligned}\langle\overline{(\delta A')^2}\rangle &= \frac{3\langle\epsilon^2\rangle^2 N}{2l_0} \times 10^4(7.197 + 0.274 + 0.037 + 0.008 + \cdots)\\ &= \frac{\langle\epsilon^2\rangle^2 N}{l_0}(11.28 \times 10^4)\end{aligned}$$

$$\sqrt{\langle\overline{(\delta A')^2}\rangle} = \langle\epsilon^2\rangle\sqrt{\frac{N}{l_0}}(335.9)\,; \quad \begin{matrix}\langle\epsilon^2\rangle \text{ in inch}^2\\ l_0 \text{ in feet.}\end{matrix}$$

$$-N2\Delta\alpha_{[m]}l_0 \gg 1\,, \qquad -2\Delta\alpha_{[m]}l_0 \ll 1\,. \tag{276}$$

In these results the summation has been extended over all of the propagating $TE_{0m}{}^+$ spurious modes, $TE_{02}{}^+$-$TE_{09}{}^+$. The most important modes are the first few $TE_{0m}{}^+$; for $\langle\overline{(\delta A')^2}\rangle$ only $TE_{02}{}^+$ and $TE_{03}{}^+$ are significant.

Finally, the sinusoidal component of the TE_{01} loss contributed by the $TE_{0m}{}^+$ spurious mode is, from (265) and (263b),

$$\langle A_{1[m]}\rangle\cos\Delta\beta_{[m]}l_0 = -\langle\epsilon^2\rangle(N-1)C_{d[m]}{}^2\cos\Delta\beta_{[m]}l_0\,; \quad -\Delta\alpha_{[m]}l_0 \ll 1. \tag{277}$$

3.4 *TE_{01} Loss Statistics of a Long Guide with Ideal Mode Filters*

Consider a long guide made up of M sections of imperfect guide of equal length and the same statistical parameters, separated by ideal mode filters. We must evaluate the over-all transmission statistics of the guide in terms of the transmission statistics of each section, given in Section 3.3. The transmission parameters of such a guide with ideal mode filters are given in (146). Since for the present we are concerned with only the over-all TE_{01} loss A, we have

$$A = \sum_{k=1}^{M} {}_kA. \tag{278}$$

${}_kA$ is the total TE_{01} loss, due to all spurious modes, of the k^{th} section of guide. From (220) we write

$${}_kA = {}_k\bar{A} + \delta_kA. \tag{279}$$

Further, for the loss of the entire guide (with mode filters)

$$A = \bar{A} + \delta A \tag{280}$$

where

$$\bar{A} = \sum_{k=1}^{M} {}_k\bar{A}, \qquad \delta A = \sum_{k=1}^{M} \delta_k A. \tag{281}$$

We assume that each section of guide between mode filters is statistically independent of all other sections. Then from (281)

$$\langle \bar{A} \rangle = \sum_{k=1}^{M} \langle {}_k\bar{A} \rangle = M \langle {}_k\bar{A} \rangle, \tag{282}$$

$$\langle \overline{(\delta A)^2} \rangle = \sum_{k=1}^{M} \langle \overline{(\delta_k A)^2} \rangle = M \langle \overline{(\delta_k A)^2} \rangle, \tag{283}$$

where M is the number of sections of guide separated by ideal mode filters.

Finally, from (278) and the central limit theorem,[37] if M is large the over-all loss A, regarded as a function of free-space wavelength λ, will be a Gaussian random process; this random process in general will not be stationary, although over the relatively narrow bands of interest it may often be assumed stationary.

3.5 *Numerical Examples*

In the present section several numerical examples are presented to provide concrete illustrations of the above results. A 20-mile total guide length, made of 2-inch I.D. pipes 10 feet long, with equally spaced ideal mode filters, is considered in all cases; the operating frequency is taken to be 55 kmc. It is assumed that the mode filters have infinite loss for the TE_{1m}^{+} and TM_{11}^{+} spurious modes, zero loss for the TE_{01} signal mode and the TE_{0m}^{+} spurious modes. The results for tilts and offsets apply to copper guide; the results for diameter variations apply equally well to either copper or helix.

3.5.1 *Offsets*

Assume an rms offset such that the additional average loss due to mode conversion to the forward TE_{1m} modes is 1 db/mile (compared to the theoretical TE_{01} heat loss at 55 kmc of 1.54 db/mile). Two cases are considered (see Table II): (1) mode filter spacing such that the rms loss variation for the 20-mile line is 1 db, and (2) a 200-foot mode filter spacing. The formulas for zero differential loss are used for simplicity, since the differential loss for TE_{12}^{+}, the most important spurious mode, will remain small.

TABLE II

	Case 1	Case 2
Average loss	1 db/mile	1 db/mile
RMS total loss fluctuation for 20-mile line	1 db	0.407 db
RMS offset	7.87 mils	7.87 mils
Mode filter spacing	1160 feet	200 feet
$\Delta f_{3\,db}$ for TE_{12}^{+}	209 mc	1211 mc

3.5.2 *Tilts*

Assume an rms tilt such that the additional average loss due to mode conversion to the forward TE_{1m} modes is again 1 db/mile. The additional average loss due to conversion to TM_{11}^{+} is stated separately because the present model is unrealistic as far as TM_{11}^{+} is concerned, for reasons stated in Section 3.3.2. Two cases are again considered (see Table III): (1) mode filter spacing such that the rms loss variation for the 20-mile line is 1 db, and (2) a 200-foot mode filter spacing. The formulas for zero differential loss are again used for simplicity.

TABLE III

	Case 1	Case 2
Average loss TE_{1m}^{+} modes	1 db/mile	1 db/mile
Average loss TM_{11}^{+}	0.262 db/mile	0.262 db/mile
RMS total loss fluctuation for 20-mile line	1 db	0.465 db
RMS tilt	0.114°	0.114°
Equivalent crack on one side of joint	3.96 mils	3.96 mils
Mode filter spacing	890 feet	200 feet
$\Delta f_{3\,db}$ for TE_{12}^{+}	272 mc	1211 mc

The TE_{01} average loss due to TM_{11}^{+} conversion will depend only on the net angle between the input and output of a waveguide section between mode filters for a mode filter spacing short compared to 3195 feet, the TM_{11}^{+} beat wavelength in copper guide. As discussed in Section 3.3.2, this angle (Table IV) will depend principally on long bows in the pipes and on the way in which the guide is laid.

TABLE IV

Mode filter spacing	200 feet		1000 feet	
Average loss, TM_{11}^{+}	1 db/ mile	0.1 db/ mile	1 db/ mile	0.1 db/ mile
RMS net angle between input and output of waveguide sections	1.00°	0.316°	2.23°	0.706°

3.5.3 *Diameter Changes*

For diameter variations there are no mode filters for the spurious TE_{0m}^{+} modes. Therefore, the mechanical tolerance required to yield an rms loss fluctuation $\langle\overline{(\delta A')^2}\rangle$ of 1 db for the 20-mile line is determined (see Table V); the additional average loss will now be very small.

TABLE V

Average loss	0.214 db/mile
$\langle\overline{(\delta A')^2}\rangle$: RMS total loss fluctuation for 20-mile line	1 db
RMS diameter variation	6.50 mils
$\Delta f_{3\,db}$ for TE_{02}^{+}	11.3 mc

Sinusoidal Components of TE_{01} Loss for 20-Mile Line

Mode	Peak-to-Peak Amplitude	Period
TE_{02}^{+}	4.690 db	4791 mc
TE_{03}^{+}	1.492 db	1832 mc
TE_{04}^{+}	0.762 db	974 mc
TE_{05}^{+}	0.472 db	600 mc

3.6 *Helix Guide*

While the above results for diameter changes apply to both copper and helix guide, the results for tilts and offsets apply only to copper guide. Equivalent results for helix would require the coupling coefficients for the normal modes of the helix at tilts and offsets. However, a very simple argument shows that $\bar{A}$, the average loss, will be identical in a helix and a copper guide which have identical tilts or offsets; $\bar{A}_{(11)}$, the TM_{11}^{+} component of the TE_{01} loss, must now be included in the copper pipe average loss in the case of tilts, as shown below. In addition, the spurious modes have such a high loss in helix that the TE_{01} loss fluctuations will be very small.

From (235), (218) and Section 2.2 we see that $\bar{A}$ is simply the sum of the TE_{01} signal losses at each individual discrete mode converter (tilt or offset), where by signal loss we mean $-\ln s_{00}$, where s_{00} is the TE_{01} transfer coefficient of the discrete tilt or offset. From Section 2.1.4 s_{00} is identical in copper and helix guide with equal tilts or offsets.

Therefore the above results for the expected value of the average TE_{01} loss for tilts and offsets hold equally well for helix waveguide. The TE_{01} loss fluctuations in helix will be very small for these cases.

3.7 *Conclusions*

Experimental copper waveguides have been built whose tolerances are far better than those of the numerical examples in Section 3.5. Since the average loss and the rms loss variation are proportional to the square of the rms tolerance, it is clear that tilts and offsets at joints and uniform diameter variations of the individual pipes will not contribute significantly to the observed TE_{01} loss in these waveguides. Consequently the additional TE_{01} loss observed in present experimental waveguides must be due principally to continuous mode conversion, and in particular to continuous random deviations from straightness of the individual copper pipes themselves.[8] The continuous case will be treated in Section IV.

The added TE_{01} average loss due to TM_{11}^{+} conversion in copper waveguide (unmodified by a dielectric lining or anything else) is a function only of the net angle between the input and output of each waveguide section between mode filters, for a reasonable mode filter spacing. The tolerance on this angle must be held to a few tenths of a degree to keep this loss component down to 0.1 db/mile.

The present analysis has been restricted to equally spaced mode converters, i.e., individual pipes of the same length. If the pipe lengths are allowed to become random, instead of starting from (71d) we must start with (71a) and (71b). The TE_{01} loss due to a single spurious mode will still have a discrete power spectrum, but the discrete components will no longer be equally spaced, and consequently the TE_{01} loss will no longer be periodic. The frequencies as well as the amplitudes of the discrete components must now be treated as random variables. Aside from these minor differences, the analysis should be similar and lead to similar results.

We refer again to the treatment of Appendix F, where more exact expressions for the TE_{01} loss statistics in the discrete case are derived without neglecting the frequency (or λ) dependence of the coupling coefficients and the differential attenuation constants, as in the above treatment. It is found that these approximations are valid for our present purposes.

Finally we note that by means of the Kronecker product, it is possible to compute certain of the TE_{01} transmission statistics exactly—i.e., without using perturbation theory—for the case of statistically independent discrete mode converters.[38] This treatment requires that the individual conversion coefficients be known exactly; unfortunately only in the idealized two-mode case is the exact form of the coupling coeffi-

cients known. Such calculations may be used to check certain of the above approximate results in the two-mode case.

IV. THEORY OF GUIDES WITH RANDOM CONTINUOUS IMPERFECTIONS

This section applies the results of Section II to the study of multimode waveguides with random continuous mode conversion. Continuous mode conversion arises from gradual continuous changes in the geometric properties of the guide, such as curvature of the guide axis, variation of the guide diameter, or changes in the cross section of the guide such as ellipticity, etc., as opposed to the discrete case, studied in Section III. The statistics of the TE_{01} loss-frequency curve are determined in terms of the statistics of the different guide imperfections. In particular, the average TE_{01} loss and the rms value and the power spectrum of the TE_{01} loss variations are calculated.

The most important practical application of these results to date has been to study the effects of random straightness deviations of the guide axis. Here we consider only small unintentional straightness deviations, either arising in the manufacturing process of the individual pipes themselves or resulting from the way in which the guide is laid. We exclude from consideration the case of large intentional bends (to go around corners), which couple TE_{01} to the degenerate forward TM_{11} mode. The spurious modes of interest here are thus the TE_{1m} family, with the forward TE_{11} and TE_{12} the most important. The present analysis indicates that very small random straightness deviations in a certain spectral region (i.e., having mechanical wavelengths lying in a certain range), having an rms value of a fraction of a mil, are primarily responsible for the observed departure of the TE_{01} transmission from its theoretical value in present copper guide,[8,39] causing an increased average loss and random fluctuations about this average. In addition, the analysis indicates that random straightness deviations will be equally important in helix or dielectric coated waveguide in increasing the average TE_{01} loss; however, the high spurious mode loss in helix will effectively remove the TE_{01} loss fluctuations.[8,39]

While random straightness deviations are the most important manufacturing tolerance at present, the same methods are easily applied to study the effects of other tolerances of the guide. The present section will also consider random diameter changes, which produce the TE_{0m} modes, random ellipticity, which gives rise to the TE_{2m} modes, and higher-order deformations of the cross section, which produce TE_{nm} modes of higher angular index.

In order to specify the statistics of the guide, we assume that each

type of imperfection (e.g., deviation of the guide axis from straightness, diameter variation, ellipticity, etc.), regarded as a function of distance z along the guide axis, is a stationary Gaussian random process of known spectrum. The various continuous coupling coefficients are of course proportional to the geometric imperfections, and thus are also Gaussian random processes.

The analysis of the continuous case is greatly simplified if the differential loss between the TE_{01} signal mode and the various spurious modes may be neglected over the lengths of interest. This approximation will be made throughout the present section. As discussed above, a practical system using copper guide will contain regularly spaced mode filters that have a high loss for all spurious modes except the TE_{0m} family. The mode filter spacing will be sufficiently small so that the differential losses may be neglected for all important spurious modes except the TE_{0m} family.

For the TE_{0m} spurious modes the effective line length will be the total distance between repeaters; obviously the total differential loss is no longer negligible. However, the results for zero differential loss will be stated for this case to get at least a rough upper bound on the importance of diameter variations, for both copper and helix guide.

4.1 *TE_{01} Loss—Summary of Previous Results*

We give in the present section the normalized TE_{01} loss (in nepers) A, for the case in which the total differential loss (for each section of guide between mode filters) may be neglected, so that we may set $\Delta\alpha = 0$. From (206) the total normalized TE_{01} loss A is given by a sum of terms due to the individual first-order spurious modes;

$$A \approx \sum_m A_m . \tag{284}$$

The A_m are given by (285) to (288) below. These results are obtained from Section 2.3.7. We again omit subscripts denoting the spurious mode where no confusion will arise.

$$A \approx \tfrac{1}{2} |I|^2, \tag{285a}$$

$$I = L \sum_{n=-\infty}^{\infty} c_n (-1)^n \frac{\sin \pi \left(\dfrac{\Delta\beta L}{2\pi} - n \right)}{\pi \left(\dfrac{\Delta\beta L}{2\pi} - n \right)}. \tag{285b}$$

The c_n are the Fourier coefficients of the continuous coupling coefficient

$c(z)$, defined by

$$c(z) = \sum_{n=-\infty}^{\infty} c_n e^{j2\pi nz/L}; \quad c_{-n} = c_n^* . \tag{286}$$

At the n^{th} sample point, defined by

$$\frac{\Delta\beta L}{2\pi} = n \qquad \text{or} \qquad B \equiv \frac{2\pi}{\Delta\beta} = \frac{L}{n}, \tag{287}$$

we have

$$I(n) = Lc_n(-1)^n, \tag{288a}$$

$$A(n) \approx \frac{L^2}{2} |c_n|^2. \tag{288b}$$

The coupling coefficient $c(z)$ is given in terms of the various geometric parameters in Section 2.3.

As in the discrete case (Section 3.1), the principal frequency dependence in these results occurs through the $\Delta\beta$'s, which far from cutoff are approximately proportional to the free-space wavelength λ. Over the moderate fractional bandwidths of interest, any frequency dependence of the coupling coefficients will be slow and may be neglected. From the discussion of Section 2.3.7, any frequency dependence of the coupling coefficient may be taken into account in (285) by calculating c_n at the frequency corresponding to the n^{th} sample point, rather than at the operating frequency.

We regard the loss A as a function of the free-space wavelength λ, and write A as follows;

$$A = \langle A \rangle + \delta A. \tag{289}$$

We determine the expected value of the loss $\langle A \rangle$, and the power spectrum of δA and its total power or mean square value $\langle (\delta A)^2 \rangle$, in terms of the power spectrum of the random coupling coefficient $c(z)$ (and consequently of the random geometric imperfection of the guide).

4.2 *Statistics of Fourier Coefficients of* $c(z)$[37,40]

We assume that the geometric imperfection of the guide (e.g., deviation of the guide axis from straightness) is a stationary Gaussian random process with a known power spectrum. The continuous coupling coefficient $c(z)$ to the particular polarization of one of the spurious modes will be a similar random process, since the coupling coefficients are

simply proportional to the corresponding geometric imperfection. Therefore $c(z)$ is a stationary Gaussian random process with a power spectrum $S(\zeta)$. Thus, if $R(\tau)$ is the covariance of $c(z)$,

$$R(\tau) = \langle c(z)c(z + \tau)\rangle, \tag{290}$$

then

$$S(\zeta) = \int_{-\infty}^{\infty} R(\tau)\, e^{-j2\pi\zeta\tau}\, d\tau. \tag{291}$$

Consider the Fourier series expansion of $c(z)$ over the interval $0 < z < L$, given in (165) and (286).

$$\begin{aligned} c(z) &= \sum_{n=-\infty}^{\infty} c_n\, e^{j2\pi nz/L}; \qquad c_{-n} = c_n^*. \\ c_n &= a_n + jb_n = |\, c_n \,|\, e^{j\varphi_n} \end{aligned} \tag{292}$$

The c_n's will be complex Gaussian random variables; i.e., a_n and b_n, the real and imaginary parts of c_n, will be Gaussian random variables with zero mean. If L is sufficiently long, the a_n's and b_n's become almost independent, and hence the c_n's become almost independent complex Gaussian random variables. Thus, the magnitude and phase of each c_n are independent and have a Rayleigh and a uniform distribution respectively. The mean square value of the n^{th} Fourier coefficient $\langle |\, c_n \,|^2\rangle$ is then simply related to the power spectrum $S(\zeta)$ of $c(z)$. We have *approximately* for large L:

$$\langle |\, c_n \,|^2\rangle \equiv \hat{c}_n^{\,2} = \frac{1}{L} \cdot S\left(\frac{n}{L}\right). \tag{293}$$

$$\langle c_n c_m^*\rangle = 0, \quad n \neq m. \tag{294}$$

The quantity $\hat{c}_n$ defined in (293) is the rms magnitude of the n^{th} Fourier coefficient. The various probability distributions for the real and imaginary parts or for the magnitude and phase of the Fourier coefficients may be written approximately as follows:

$$p(a_n) = \frac{1}{\sqrt{\pi}\,\hat{c}_n} \exp -\left(\frac{a_n}{\hat{c}_n}\right)^2; \qquad p(b_n) = \frac{1}{\sqrt{\pi}\,\hat{c}_n} \exp -\left(\frac{b_n}{\hat{c}_n}\right)^2. \tag{295a}$$

$$p(a_n,b_n) = p(a_n)p(b_n). \tag{295b}$$

$$p(|c_n|) = \frac{2|c_n|}{\hat{c}_n^2} \exp -\left(\frac{|c_n|}{\hat{c}_n}\right)^2.$$
$$p(\varphi_n) = \frac{1}{2\pi}, \quad 0 < \varphi < 2\pi. \tag{296a}$$

$$p(|c_n|, \varphi_n) = p(|c_n|)p(\varphi_n). \tag{296b}$$

Since the different Fourier coefficients are approximately independent,

$$p(c_n, c_m) = p(c_n)p(c_m), \quad |n| \neq |m|. \tag{297}$$

Finally, the first few moments of the $|c_n|$ are of interest.

$$\langle |c_n| \rangle = \frac{\sqrt{\pi}}{2} \hat{c}_n; \qquad \langle |c_n|^2 \rangle = \hat{c}_n^2; \qquad \langle |c_n|^4 \rangle = 2\hat{c}_n^4. \tag{298}$$

The results of this section provide a good approximation for the practical cases of interest in which L, the line length, is of the order of a few hundred feet and the power spectrum $S(\zeta)$ varies slowly in the range of interest, which includes mechanical wavelengths from a few feet to a few inches, depending on the spurious mode. These results become exact if the coupling coefficient $c(z)$ has a white power spectrum ($S(\zeta)$ = constant, or equivalently $R(\tau) \propto \delta(\tau)$, the unit impulse).

4.3 *TE_{01} Loss Statistics for a Single Section of Waveguide between Mode Filters*

4.3.1 *Single Spurious Mode, Single Polarization*

From the relations of Section 4.2, $I\left(\frac{\Delta\beta L}{2\pi}\right)$, given in (285b), will be a complex band-limited Gaussian random process; the real and imaginary parts of I are independent Gaussian random processes with flat power spectra over the range $|\nu| < \frac{1}{2}$.† [33,34] Since by (285a) A is proportional to the square of the magnitude of I and is thus proportional to the sum of the squares of the real and imaginary parts of I, the power spectrum of A may be determined from the well-known analysis for the response of a square law device to Gaussian noise.[37,40] The square of a Gaussian random process has, in addition to a dc component, a random component whose power spectrum is twice the convolution of the input power spectrum with itself. Since the real and imaginary parts of I have flat band-limited power spectra over the range $|\nu| < \frac{1}{2}$, the random com-

† ν again indicates the independent variable of the Fourier transform of I, or some other quantity of interest, with respect to the normalized independent variable $\frac{\Delta\beta L}{2\pi}$. See the footnote on p. 1084.

ponent of $A\left(\frac{\Delta\beta L}{2\pi}\right)$ will therefore have a triangular power spectrum over the range $|\nu| < 1$.

We first separate the TE_{01} loss A as before [see (289)].

$$A = \langle A \rangle + \delta A, \tag{299}$$

where as usual we omit subscripts denoting the spurious mode. Then from the results of Section 4.1 and 4.2, the expected value of the TE_{01} loss is given by

$$\langle A(\lambda_n) \rangle = \frac{L^2}{2} \langle |c_n|^2 \rangle = \frac{L}{2} \cdot S\left(\frac{n}{L}\right), \tag{300}$$

where from (174)

$$\lambda_n = \frac{2\pi}{D} \frac{n}{L} \tag{301}$$

is the free-space wavelength corresponding to the n^{th} sample point and D is the constant relating the differential propagation constant $\Delta\beta$ to the free-space wavelength λ [see (173)]. Substituting (287) and (301) into (300), and using the result to interpolate between the sample points,

$$\langle A(\lambda) \rangle = \frac{L}{2} \cdot S\left(\frac{D}{2\pi} \lambda\right) = \frac{L}{2} \cdot S\left(\frac{1}{B}\right), \tag{302}$$

relating the expected value of the TE_{01} loss due to a single spurious mode (single polarization) to the power spectrum of the coupling coefficient between TE_{01} and the spurious mode. B is the beat wavelength between TE_{01} and the spurious mode.

The (continuous) power spectrum of δA in the region close to λ is given by

$$\begin{aligned} P(\nu) &= \frac{L^2}{4} \cdot S^2\left(\frac{D}{2\pi} \lambda\right) (1 - |\nu|) \\ &= \frac{L^2}{4} \cdot S^2\left(\frac{1}{B}\right) (1 - |\nu|), \quad |\nu| < 1. \end{aligned} \tag{303}$$

In deriving (303) we have tacitly assumed that $S(\zeta)$, the power spectrum of the coupling coefficient $c(z)$, varies only slowly in the region of interest, so that I and A are approximately stationary over moderate bandwidths; however, this is not a serious restriction. Equation (303) may be obtained either from the known results on the square of a Gaussian noise[37,40] or directly from Sections 4.1 and 4.2. The total power, or the expected value of the mean square value, of δA may be found by

integrating the power spectrum $P(\nu)$. From (303)

$$\langle(\delta A)^2\rangle = \frac{L^2}{4}\cdot S^2\left(\frac{D}{2\pi}\lambda\right) = \frac{L^2}{4}\cdot S^2\left(\frac{1}{B}\right), \tag{304a}$$

$$\sqrt{\langle(\delta A)^2\rangle} = \frac{L}{2}\cdot S\left(\frac{D}{2\pi}\lambda\right) = \frac{L}{2}\cdot S\left(\frac{1}{B}\right) = \langle A\rangle, \tag{304b}$$

for a single polarization of a single spurious mode. Alternately, the results of (304) may be obtained directly (at the sample points) from (288b), (293) and (298); it is apparent that (302) and (304) hold for quite general power spectra $S(\zeta)$.

The power spectrum $P(\nu)$ of δA is triangular; from (303) the 3-db bandwidth is

$$\nu_{3\text{db}} = \tfrac{1}{2}. \tag{305}$$

The interval in free-space wavelength or frequency corresponding to the 3-db bandwidth of δA is thus

$$\frac{\Delta f_{3\text{db}}}{f} \approx \frac{\Delta\lambda_{3\text{ db}}}{\lambda} = \frac{2B}{L}, \tag{306}$$

and is thus simply twice the sample point spacing (for I), given in (178). [Compare (306) with (244) and (243a).]

Finally, we consider the probability distribution for A, considering for the present only a single polarization of a single spurious mode. As discussed at the beginning of the present section, A is the sum of the squares of two independent Gaussian random variables. Alternately, A may be regarded as the square of a Rayleigh-distributed random variable. Consequently, for a single polarization of a single spurious mode, A has an exponential probability density.

$$p(A) = \frac{1}{\langle A\rangle}\exp -\frac{A}{\langle A\rangle}, \tag{307}$$

where the average loss $\langle A\rangle$ is given in (302). We recall that this result (and all others of the present section) is based on the assumption of zero differential loss, $\Delta\alpha = 0$. Equation (307) holds equally well for the corresponding discrete case of Section III.

4.3.2 *Single Spurious Mode, Two Polarizations*

The above results are easily extended to two polarizations of the spurious mode. We assume that the two orthogonal components of the geometric imperfection giving rise to mode conversion are independent

Gaussian random processes with the same statistics. For example, consider random straightness deviations, which couple TE_{01} to the TE_{1m} family but principally to the forward TE_{12} and TE_{11}. The position of the guide axis is specified by $x(z)$ and $y(z)$, the coordinates of the guide axis in the transverse plane as functions of distance along the axis z. We will assume that $x(z)$ and $y(z)$ are independent Gaussian random processes with identical power spectra.

The coupling coefficients $c_{[m]}{}^{\parallel}(z)$ and $c_{[m]}{}^{\perp}(z)$ between TE_{01} and the two polarizations of the m^{th} spurious mode will also be independent Gaussian random processes, since the coupling coefficients are proportional to the corresponding geometric imperfections. Thus, for straightness deviations we have from Section 2.4 for small deviations

$$c_{[m]}{}^{\parallel}(z) = C_{t[m]} \cdot x''(z), \qquad c_{[m]}{}^{\perp}(z) = C_{t[m]} \cdot y''(z), \tag{308}$$

where the symbols $\parallel$ and $\perp$ distinguish the two polarizations of the spurious mode, rather than x and y as in Section II. Since $x(z)$ and $y(z)$ are independent Gaussian random processes, $x''(z)$ and $y''(z)$ and consequently $c_{[m]}{}^{\parallel}(z)$ and $c_{[m]}{}^{\perp}(z)$ will also be independent Gaussian random processes.

The TE_{01} loss $A_{[m]}$ for both polarizations of the m^{th} spurious mode is given by

$$A_{[m]} = A_{[m]}{}^{\parallel} + A_{[m]}{}^{\perp}, \tag{309}$$

where $A_{[m]}{}^{\parallel}$ and $A_{[m]}{}^{\perp}$ are independent random processes with statistics given by the results of Section 4.3.1. Writing

$$A_{[m]} = \langle A_{[m]} \rangle + \delta A_{[m]}, \tag{310}$$

we have for the expected value of the TE_{01} loss

$$\langle A_{[m]} \rangle = \langle A_{[m]}{}^{\parallel} \rangle + \langle A_{[m]}{}^{\perp} \rangle. \tag{311}$$

Since $\delta A_{[m]}{}^{\parallel}$ and $\delta A_{[m]}{}^{\perp}$, the two ac loss components, are independent, their power spectra and total powers add. Denoting the (continuous) power spectra of $\delta A_{[m]}$, $\delta A_{[m]}{}^{\parallel}$ and $\delta A_{[m]}{}^{\perp}$ by $P_{[m]}(\nu)$, $P_{[m]}{}^{\parallel}(\nu)$, and $P_{[m]}{}^{\perp}(\nu)$ respectively, we have

$$P_{[m]}(\nu) = P_{[m]}{}^{\parallel}(\nu) + P_{[m]}{}^{\perp}(\nu), \tag{312}$$

$$\langle (\delta A_{[m]})^2 \rangle = \langle (\delta A_{[m]}{}^{\parallel})^2 \rangle + \langle (\delta A_{[m]}{}^{\perp})^2 \rangle. \tag{313}$$

Since both polarizations are assumed to have identical statistics, we have from Section 4.3.1:

$$\langle A_{[m]}(\lambda) \rangle = L \cdot S_{[m]}\left(\frac{D_{[m]}}{2\pi}\lambda\right) = L \cdot S_{[m]}\left(\frac{1}{B_{[m]}}\right). \tag{314}$$

$$P_{[m]}(\nu) = \frac{L^2}{2} \cdot S_{[m]}{}^2\left(\frac{D_{[m]}}{2\pi}\lambda\right) \cdot (1 - |\nu|)$$
$$= \frac{L^2}{2} \cdot S_{[m]}{}^2\left(\frac{1}{B_{[m]}}\right) \cdot (1 - |\nu|), \quad |\nu| < 1. \tag{315}$$

$$\langle(\delta A_{[m]})^2\rangle = \frac{L^2}{2} \cdot S_{[m]}{}^2\left(\frac{D_{[m]}}{2\pi}\lambda\right) = \frac{L^2}{2} \cdot S_{[m]}{}^2\left(\frac{1}{B_{[m]}}\right). \tag{316a}$$

$$\sqrt{\langle(\delta A_{[m]})^2\rangle} = \frac{L}{\sqrt{2}} \cdot S_{[m]}\left(\frac{D_{[m]}}{2\pi}\lambda\right) = \frac{L}{\sqrt{2}} \cdot S_{[m]}\left(\frac{1}{B_{[m]}}\right) = \frac{\langle A_{[m]}\rangle}{\sqrt{2}}. \tag{316b}$$

In these and all subsequent results $S_{[m]}(\zeta)$ is the power spectrum of *each* of the orthogonal components of the coupling coefficient.

The power spectrum $P_{[m]}(\nu)$ of course remains triangular, and the 3-db bandwidth and the corresponding interval in free-space wavelength or frequency remains as given in (305) and (306) for a single polarization of the spurious mode. These latter quantities are the same as those for the corresponding discrete case, given in (243a) and (244).

Finally, since $A_{[m]}{}^{\parallel}$ and $A_{[m]}{}^{\perp}$ are independent random variables with the same probability distribution [see (307)], the probability distribution for $A_{[m]}$ is simply the convolution of (307) with itself.

$$p(A_{[m]}) = \frac{4A_{[m]}}{\langle A_{[m]}\rangle^2} \exp -\frac{2A_{[m]}}{\langle A_{[m]}\rangle}. \tag{317}$$

This result holds true for discrete tilts and offsets for zero differential loss.

4.3.3 *Many Spurious Modes*

For many spurious modes, the total TE_{01} loss A is given as a sum over loss components $A_{[m]}$ due to the different spurious modes. From (284)

$$A = \sum_{[m]} A_{[m]}. \tag{318}$$

Writing the total TE_{01} loss as before,

$$A = \langle A\rangle + \delta A. \tag{319}$$

Then we have

$$\langle A\rangle = \sum_{[m]} \langle A_{[m]}\rangle, \tag{320a}$$

$$\delta A = \sum_{[m]} \delta A_{[m]}. \tag{320b}$$

The average TE_{01} loss is simply the sum of the contributions of each of the spurious modes.

From (320b) we have for the variance of the total TE_{01} loss

$$\langle(\delta A)^2\rangle = \sum_{[m]}\sum_{[n]} \langle\delta A_{[m]}\delta A_{[n]}\rangle. \tag{321}$$

The terms $\langle(\delta A_{[m]})^2\rangle$ are given by (316a) or (304a). It would be most convenient if the different ac components $\delta A_{[m]}$ were independent, so that the cross terms $\langle\delta A_{[m]}\delta A_{[n]}\rangle$ could be neglected.

For the spurious modes produced by a geometric imperfection of a given angular symmetry (e.g., the TE_{1m}, produced by straightness deviations) the different $\delta A_{[m]}$ are not independent. The TE_{01} loss component due to the m^{th} spurious mode at one frequency is proportional to the TE_{01} loss component due to the n^{th} spurious mode at a widely separated frequency, as in the discrete case (Appendix F). Thus, knowledge of one of the $\delta A_{[m]}$ over a sufficiently wide frequency band is sufficient to determine all of the others. However, at the same frequency $\delta A_{[m]}$ and $\delta A_{[n]}$ are almost uncorrelated, so that the cross terms in (321) may be neglected.

$\delta A_{[m]}$ and $\delta A_{[n]}$ are easily seen to be almost independent in a simple way. Consider a frequency which corresponds to a sample point of the m^{th} spurious mode. Under special conditions this frequency may also correspond to a different sample point of the n^{th} spurious mode (in general, this will not be so). From (288b), $A_{[m]}$ will depend on only a single Fourier coefficient (say the k^{th}) of the geometric imperfection. Similarly, $A_{[n]}$ will depend on only a single Fourier coefficient, but on a different one (say the l^{th}), since different spurious modes have different beat wavelengths. Since the different Fourier coefficients of the geometric imperfection are almost independent, $\delta A_{[m]}$ and $\delta A_{[n]}$ will thus also be almost independent at this frequency. Since in general the sample points corresponding to different spurious modes do not precisely coincide, the correlation coefficient between $\delta A_{[m]}$ and $\delta A_{[n]}$ at a single frequency will not be identically zero, but should be small.

The correlation coefficient between the ac components of the TE_{01} loss due to two different spurious modes generated by the same type of geometric imperfection is derived in Appendix G for the special case in which the geometric imperfection and hence the coupling coefficients have white power spectra. Numerical results are given for the important practical case of TE_{12}^{+} and TE_{11}^{+} generated by random straightness deviations, in which the second derivatives of the rectangular co-ordinates of the guide axis are independent Gaussian random processes with white spectra. The normalized correlation coefficient for reasonable guide lengths is very small indeed.

The cross terms in (321) will consequently make only a negligible contribution to the variance of the total TE_{01} loss. Therefore, $\langle(\delta A)^2\rangle$ is

given simply by the sum of the contributions of the individual spurious modes;

$$\langle(\delta A)^2\rangle = \sum_{[m]} \langle(\delta A_{[m]})^2\rangle, \tag{322}$$

where the $\langle(\delta A_{[m]})^2\rangle$ are given by (316a) (or by (304a) for a spurious mode with a single polarization, e.g., TE_{0m}).

4.3.4 *Discussion*

The TE_{01} loss in a given frequency band, resulting from a given spurious mode, depends only on the Fourier components of the corresponding geometric imperfection for a narrow range of mechanical wavelengths. This band of mechanical wavelengths corresponds to the range of beat wavelengths between TE_{01} and the spurious mode over the frequency band of interest. The statistics of the TE_{01} loss are strongly dependent on the power spectrum of the geometric imperfection.

The present results are strictly valid only for zero differential loss, $\Delta\alpha = 0$, although they will remain approximately true so long as the differential loss over the length of guide remains small, $|\Delta\alpha| L \ll 1$. However, further study shows that moderate values of differential loss $\Delta\alpha$ will change the average TE_{01} loss very little, but will smooth out the fluctuations of the TE_{01} loss, for the present case in which the coupling coefficient power spectrum is essentially flat in the range of interest.[41]

The following sections will present specific numerical examples for the various types of geometric imperfections.

4.4 *TE_{01} Loss Statistics for Random Straightness Deviations*

4.4.1 *Introduction*

In the present section we apply the results of Section 4.3 to the case of random deviations from straightness of the guide axis. In Section 4.5 other types of continuous geometric imperfections are similarly treated. There are two reasons for treating straightness deviations separately:

1. Straightness deviations introduced by the manufacturing process are almost entirely responsible for the additional TE_{01} loss of present 2-inch I.D. copper guide.

2. Experimental TE_{01} transmission measurements have provided a fair idea of the shape of the power spectrum of straightness deviations for different types of guide, at least over a limited range. This power spectrum differs in some respects from the power spectra that might be assumed for other types of geometric imperfections, in that under certain

conditions it contains an infinite low-frequency (i.e., long mechanical wavelength) content; some additional discussion of this particular case seems appropriate.

We must first specify the statistical properties of the coupling coefficient; since the coupling coefficient $c(z)$ is assumed to be a stationary Gaussian random process, its statistics are completely determined by its power spectrum $S(\zeta)$. The continuous case is inherently more complicated to discuss than the discrete case of Section III. For the discrete case only the rms offset, tilt, or diameter change must be specified. In the continuous case, however, the TE_{01} loss statistics are no longer determined only by the mean square value of straightness deviation or other geometric imperfection; the shape of the power spectrum of the mechanical imperfection strongly influences the resulting TE_{01} loss. We must therefore know the power spectrum of the imperfection before we can predict the TE_{01} loss statistics of a guide. Conversely, knowledge of the TE_{01} loss statistics enables us to estimate the power spectrum of the imperfections. Up to now there have been no existing mechanical methods for measuring the straightness deviation to the required accuracy so that its covariance and power spectrum can be determined;† TE_{01} transmission measurements have provided the only means of determining the significant Fourier components of the straightness deviation.

Present experimental measurements of the TE_{01} loss over a band extending from 33 kmc to 90 kmc, made by A. P. King and G. D. Mandeville, indicate that for one type of 2-inch I.D. copper guide, the radius of curvature of the straightness deviation has an approximately flat power spectrum over the range of interest.[39] Thus, if $x(z)$ and $y(z)$ are the rectangular components of straightness deviation with power spectra $X(\zeta)$ and $Y(\zeta)$, we have‡

$$X(\zeta) = Y(\zeta) \propto \frac{1}{\zeta^4} \tag{323}$$

for mechanical wavelengths lying in the beat wavelength range for TE_{11} and TE_{12} (the most important spurious modes), 1.4 to 4.4 feet for the 35–90 kmc band.

The power spectrum of (323) for $x(z)$ and $y(z)$, which corresponds to a white power spectrum for the radius of curvature of the guide axis or

† Methods of making these mechanical measurements are currently under development by K. J. Dahms, W. G. Nutt, and R. B. Ramsey and their associates at Bell Telephone Laboratories.

‡ ζ is the "mechanical frequency," having the dimension $\frac{1}{\text{length}}$; the corresponding mechanical wavelength is $\frac{1}{\zeta}$. [See for example (291).]

equivalently for the second derivatives $x''(z)$ and $y''(z)$, appears plausible under certain conditions, considering one way in which the guide has been made. If we imagine a guide made by drawing a copper pipe with more or less random hardness or wall thickness variations through a die, it is not hard to see that the radius of curvature of the guide axis might be a random process with a very short correlation distance, or equivalently with a very wide power spectrum. The power spectrum for $x''(z)$ and $y''(z)$ must, of course, fall off for sufficiently high mechanical frequencies (or sufficiently short mechanical wavelengths).

The coupling coefficients and hence $x''(z)$ and $y''(z)$, the second derivatives of the displacement of the guide axis, have been assumed to be stationary random processes. The displacements themselves, $x(z)$ and $y(z)$, will *not* in general be stationary random processes, unless the power spectrum of $x''(z)$ and $y''(z)$ (and the corresponding coupling coefficients) has special properties. However, this situation seems to be in accord with the physical facts. As a simple example we may consider a guide made of pipes with random uniform bows, screwed together at random; we might further assume that the first pipe of the guide starts out with zero displacement and zero slope, $x(0) = y(0) = x'(0) = y'(0) = 0$. Then it is obvious that while the second derivatives $x''(z)$ and $y''(z)$ and hence the coupling coefficients are stationary random processes, the displacements $x(z)$ and $y(z)$ are not. The variances of the displacements, $\langle x^2(z)\rangle$ and $\langle y^2(z)\rangle$, grow with distance z; the guide tends to wander more and more from the axis as z increases, unless additional mechanical constraints are imposed in laying the guide.

Since our knowledge of the power spectrum $X(\zeta)$ is limited, any example chosen to illustrate the order of magnitude of straightness tolerance that will have a significant effect on the TE_{01} transmission must be arbitrary to a considerable extent. For the present numerical example we assume that $X(\zeta)$ and $Y(\zeta)$ are as given by (323). For this power spectrum the displacement of the guide axis $x(z)$ or $y(z)$ is not a stationary random process, and the integral of (323) or the "total power" is infinite. However, the principal spurious modes are TE_{12}^{+} and TE_{11}^{+}, with beat wavelengths of about 2.2 and 2.7 feet at a frequency of 55 kmc. In order to get a rough measure of the short-wavelength straightness deviations that are responsible for the additional TE_{01} loss, we shall quite arbitrarily calculate a "total" mean square straightness deviation $\langle x^2(z)\rangle + \langle y^2(z)\rangle$ by including only those components having mechanical wavelengths less than 5 feet, $\zeta > \frac{1}{5}$. While this is a rather arbitrary choice, it makes some physical sense. The significant components for TE_{11}^{+} and TE_{12}^{+} lie between 1.4 and 4.4 feet for a band from 35–90 kmc. The

long-wavelength components (greater than 5 feet) do not affect the TE_{01} transmission in this band; in any case, these long-wavelength components will depend strongly on the random errors made in laying the guide, and perhaps very little on the straightness deviations introduced by the manufacturing process. The mean square value of the components of wavelength less than 5 feet will give us a rough idea of the order of magnitude of the tolerance on the short-wavelength "manufacturing" straightness deviations.

For the numerical example presented below we assume a 20-mile total guide length of 2-inch I.D. copper guide with equally spaced mode filters, spaced either 200 or 1000 feet apart. These mode filters are assumed to have zero loss to the TE_{01} signal mode, infinite loss to the spurious TE_{1m}^{+} modes. TM_{11}^{+} is neglected, since it has been adequately treated in Section III. The differential loss is neglected even though it is not small in the distance between mode filters for all spurious modes, particularly for the 1000-foot mode filter spacing. The differential loss will not greatly affect the average TE_{01} loss, but will reduce the TE_{01} loss fluctuations below the values computed for zero differential loss. The treatment of a long line with ideal mode filters is given in Section 3.4.

The x and y components of the straightness deviation of the guide axis are assumed to have power spectra given in (323), discussed above. The magnitude of these power spectra is chosen to yield an additional average TE_{01} loss (due to all the propagating TE_{1m}^{+} spurious modes) of 1 db per mile, at a frequency of 55 kmc. The total rms straightness deviation for components having wavelengths less than 5 feet is stated, for reasons discussed above. In addition, the rms straightness deviation for components having wavelengths between 2 and 3 feet, corresponding to the TE_{12}^{+} and TE_{11}^{+} beat wavelengths for the 50–60 kmc band, is also given. The contributions of each of the spurious modes to the average TE_{01} loss and to the TE_{01} loss fluctuations are stated separately.

4.4.2 *Analysis*

Let $X(\zeta)$ and $Y(\zeta)$ be the power spectra of the rectangular components of the straightness deviation of the guide axis, $x(z)$ and $y(z)$. Then

$$\begin{aligned} X(\zeta) &= \int_{-\infty}^{\infty} \langle x(z)x(z+\tau)\rangle\, e^{-j2\pi\zeta\tau}\, d\tau \\ Y(\zeta) &= \int_{-\infty}^{\infty} \langle y(z)y(z+\tau)\rangle\, e^{-j2\pi\zeta\tau}\, d\tau . \end{aligned} \tag{324}$$

We will always assume identical spectra for $x(z)$ and $y(z)$, i.e.,

$$X(\zeta) = Y(\zeta). \tag{325}$$

Then the power spectra of $x''(z)$ and $y''(z)$, the second derivatives of the x and y components of the displacement of the guide axis, are given by

$$\begin{aligned}(2\pi\zeta)^4 X(\zeta) &= \int_{-\infty}^{\infty} \langle x''(z)x''(z+\tau)\rangle\, e^{-j2\pi\zeta\tau}\, d\tau \\ (2\pi\zeta)^4 Y(\zeta) &= \int_{-\infty}^{\infty} \langle y''(z)y''(z+\tau)\rangle\, e^{-j2\pi\zeta\tau}\, d\tau .\end{aligned} \tag{326}$$

Noting (308), the power spectra $S_{[m]}(\zeta)$ of the coupling coefficients $c_{[m]}(z)$ [see (290) and (291)] are given by

$$\begin{aligned}S_{[m]}^{\parallel}(\zeta) &= C_{t[m]}^{\ 2}\cdot(2\pi\zeta)^4 X(\zeta), \\ S_{[m]}^{\perp}(\zeta) &= C_{t[m]}^{\ 2}\cdot(2\pi\zeta)^4 Y(\zeta),\end{aligned} \tag{327}$$

for the parallel and perpendicular polarizations of the TE_{1m} spurious mode respectively.

Far from cutoff $C_{t[m]}$ is approximately inversely proportional to the free-space wavelength λ. It is thus sometimes convenient to write $C_{t[m]}$ as

$$C_{t[m]} = \frac{\mathcal{C}_{t[m]}}{\lambda}, \tag{328}$$

where $\mathcal{C}_{t[m]}$ is now approximately independent of λ.

From (314) the average TE_{01} loss due to the TE_{1m} spurious mode (with two polarizations) is

$$\langle A_{[m]}(\lambda)\rangle = L\mathcal{C}_{t[m]}^{\ 2} D_{[m]}^{\ 4}\lambda^2\cdot X\left(\frac{D_{[m]}}{2\pi}\lambda\right). \tag{329}$$

The constant $D_{[m]}$, defined in (173), is related to the beat wavelength $B_{[m]}$ by

$$\frac{D_{[m]}}{2\pi}\lambda = \frac{1}{B_{[m]}} = \frac{\beta_0 - \beta_{[m]}}{2\pi}. \tag{330}$$

In (329), $X(\zeta)$ is the power spectrum of *each* of the rectangular components of straightness deviation [see (325)]; the only frequency- (or wavelength-) dependent terms are the factors λ^2 and the mechanical power spectrum $X\left(\frac{D_{[m]}}{2\pi}\lambda\right)$. The rms fluctuation of the TE_{01} loss component due to TE_{1m} about its average is given by (316b);

$$\sqrt{\langle(\delta A_{[m]})^2\rangle} = \frac{\langle A_{[m]}\rangle}{\sqrt{2}}. \tag{331}$$

As discussed above, for the present example we assume that over the range of interest (mechanical wavelengths less than 5 feet) $X(\zeta)$, the power spectrum for each component of the straightness deviation, has the shape given by (323). Therefore we take

$$X(\zeta) = Y(\zeta) = \frac{X_0}{(2\pi\zeta)^4}, \tag{332}$$

where X_0 is a scaling parameter determining the magnitude of the straightness deviation. Then the average loss of (329) becomes

$$\langle A_{[m]}(\lambda)\rangle = \frac{L\mathcal{C}_{t[m]}^2 X_0}{\lambda^2} = LC_{t[m]}^2 X_0. \tag{333}$$

The loss fluctuation of course remains as given by (331).

The total TE_{01} average loss $\langle A\rangle$ and mean square loss fluctuations $\langle(\delta A)^2\rangle$ are given by (320a) and (322) respectively, summing over the contributions of all the propagating TE_{1m}^+ spurious modes. We have

$$\langle A\rangle = LX_0 \sum_{[m]} C_{t[m]}^2. \tag{334}$$

$$\langle(\delta A)^2\rangle = \tfrac{1}{2}L^2X_0^2 \sum_{[m]} C_{t[m]}^4. \tag{335}$$

Substituting numerical values from Appendix A and summing over the 9 propagating TE_{1m}^+ modes, for a frequency of 55 kmc and a 1-inch guide radius (334) and (335) become

$$\langle A\rangle = 111.24\, LX_0 \tag{336}$$

$$\langle(\delta A)^2\rangle = 3721.64\, L^2X_0^2. \tag{337}$$

From (333) and (334) the average TE_{01} loss $\langle A\rangle$ is inversely proportional to λ^2, or directly proportional to f^2. This is approximately in agreement with the experimental results of A. P. King and G. D. Mandeville for one type of copper guide[39] and provides the reason for the particular choice of power spectrum for the straightness deviation that has been made here.

Finally, the rms straightness deviation in a given range is obtained by integrating the straightness deviation power spectrum over the appropriate range. For the x-component alone, we have for the mean square straightness deviation for mechanical frequencies lying between ζ_a and ζ_b, or equivalently mechanical wavelengths $\frac{1}{\zeta}$ lying between $\frac{1}{\zeta_a}$ and $\frac{1}{\zeta_b}$

$$\langle x^2\rangle = \left[\int_{-\zeta_b}^{-\zeta_a} + \int_{\zeta_a}^{\zeta_b}\right] X(\zeta)\, d\zeta, \tag{338}$$

where we recall that the straightness deviation power spectrum $X(\zeta)$ has been defined for both positive and negative mechanical frequencies. Substituting the particular power spectrum given in (332),

$$\langle x^2 \rangle = \frac{2X_0}{3(2\pi)^4}\left(\frac{1}{\zeta_a{}^3} - \frac{1}{\zeta_b{}^3}\right). \tag{339}$$

From (325) and the fact that x and y are independent, we have for the total mean square straightness deviation in this range

$$\langle x^2 \rangle + \langle y^2 \rangle = \frac{X_0}{12\pi^4}\left(\frac{1}{\zeta_a{}^3} - \frac{1}{\zeta_b{}^3}\right). \tag{340}$$

4.4.3 *Numerical Example*

We assume an added average TE_{01} loss in 2-inch I.D. guide due to mode conversion of 1 db per mile at 55 kmc. From Section 3.4 and (336), we determine X_0.

$$X_0 = \frac{1}{111.24 \times 8.6859 \times 5280} = 1.960 \times 10^{-7}\ \text{ft}^{-1}. \tag{341}$$

We will specify the rms straightness deviation (including both the x and y components of the displacement of the guide axis) for components having wavelengths less than five feet, as discussed above. From (340),

$$\sqrt{\langle x^2 \rangle + \langle y^2 \rangle} = 1.737 \text{ mils}; \quad \frac{1}{\zeta} < 5 \text{ feet}. \tag{342}$$

For purposes of illustration we shall emphasize the 50–60 kmc band. In this band the beat wavelength range for $TE_{12}{}^+$ and $TE_{11}{}^+$, the most important spurious modes, is 2–3 feet. Since these components of straightness deviation are the principal contributors to the TE_{01} loss in the 50–60 kmc band, it is of interest to give the rms straightness deviation lying in the 2–3 foot region. Again from (340),

$$\sqrt{\langle x^2 \rangle + \langle y^2 \rangle} = 0.677 \text{ mils}; \quad 2 \text{ feet} < \frac{1}{\zeta} < 3 \text{ feet}. \tag{343}$$

Table VI presents the transmission behavior of a 20-mile, 2-inch I.D. guide for two mode filter spacings, 200 feet and about 1000 feet, calculated from the present results and those of Section 3.4. In addition to the total average loss and rms loss fluctuation, the contributions of the individual spurious modes are given. The average loss is of course the same for both cases; the rms total loss fluctuation is reduced for the shorter mode filter spacing.

TABLE VI — TE_{01} LOSS STATISTICS FOR STRAIGHTNESS DEVIATION WITH A FLAT CURVATURE POWER SPECTRUM

L_{total} = 20 miles, total guide length.
$8.6859 \frac{\langle A_{total} \rangle}{L_{total}}$ = 1 db/mile, additional average loss at 55 kmc.
f = 55 kmc, midband frequency.
a = 1 inch, guide radius.

Case 1: L = 200 feet, mode filter spacing.
M = 528, number of mode filters.
$8.6859\sqrt{\langle (\delta A_{total})^2 \rangle}$ = 0.4773 db, rms total loss fluctuation for 20-mile line.

Case 2: L = 996.23 feet, mode filter spacing.
M = 106, number of mode filters.
$8.6859\sqrt{\langle (\delta A_{total})^2 \rangle}$ = 1.0652 db, rms total loss fluctuation for 20-mile line.

				Case 1		Case 2	
Spurious Mode	Beat Wavelength Range for 50–60 Kmc Band	RMS Straightness Deviation in Beat Wavelength Range	Added Average Loss	RMS Total Loss Fluctuation for 20 Mile Line	$\Delta f_{3\,db}$: 3-db Bandwidth of Power Spectrum of Loss Fluctuation	RMS Total Loss Fluctuation for 20 Mile Line	$\Delta f_{3\,db}$: 3-db Bandwidth of Power Spectrum of Loss Fluctuation
	feet	mils	db/mile	db	mc	db	mc
TE_{11}^+	2.453–2.949	0.513	0.2649	0.1630	1486	0.3638	298
TE_{12}^+	1.997–2.408	0.381	0.7290	0.4486	1212	1.0012	243
TE_{13}^+	0.464–0.562	0.043	0.0055	0.0034	282	0.0076	57
TE_{14}^+	0.215–0.263	0.014	0.0005	0.0003	131	0.0007	26
TE_{15}^+	0.123–0.152	0.006	0.0001	0.0001	76	0.0001	15

4.4.4 *Discussion*

The above results show that for the assumed mechanical power spectrum, the principal contributors to both the additional average loss and to the loss fluctuations arise from the TE_{12}^+ and the TE_{11}^+ spurious modes, as has been observed experimentally. As discussed above, the average loss measured over a very wide frequency band by A. P. King and G. D. Mandeville[39] provides the primary experimental data on the power spectrum of the straightness deviations.

For some guides both the experimental transmission data and consideration of the manufacturing process indicate that the power spectrum of the second derivative of the straightness deviation should be more or less flat up to some high mechanical frequency (short wavelength). As discussed above, this leads to a power spectrum for the straightness deviation itself with infinite power, so that the displacement of the guide

axis from a perfect straight line will not be a stationary random process However, in practice additional forces are imposed in laying the guide, so that the straightness deviation must become stationary. In order for this to be so, the power spectrum for $x''(z)$ and $y''(z)$ and for the corresponding coupling coefficients must now fall to zero as ζ approaches 0, at least as fast as ζ^4. However, it seems reasonable to assume that the modification in the coupling coefficient power spectrum will take place only for very small values of ζ (long wavelengths). In the important spectral region corresponding to the TE_{11}^{+} and TE_{12}^{+} beat wavelengths, for $\frac{1}{\zeta}$ less than a few feet, the power spectrum should be modified very little; therefore, very little change will take place in the TE_{01} transmission statistics.

Since only components of the straightness deviation having wavelengths between about 1.4 and 4.4 feet will significantly affect the TE_{01} loss (in a band from about 35–90 kmc), it is clear that random straightness deviations arising in the laying of the guide, or manufacturing imperfections such as long bows, will have very little effect on the TE_{01} transmission, because such straightness deviations will have their principal components at much longer wavelengths (e.g., perhaps greater than ten feet). One model that is readily analyzed is the "random bow line," made of pipes of identical length with uniform bows, screwed together at random. The x and y components of the coupling coefficient are simply random square waves, whose power spectrum is well known. The allowable tolerance is several orders of magnitude more lenient than the tolerance on short wavelength straightness deviations.

Finally, it is possible that quite different types of power spectra than those discussed here could arise for different manufacturing processes. For example, a process that resulted in a periodic straightness deviation in the beat wavelength range would result in a rather broadly peaked band-pass power spectrum for the coupling coefficient. Such things are of course to be avoided. In practice, different manufacturing processes have produced quite different straightness deviation power spectra.

4.5 *TE_{01} Loss Statistics for Random Diameter Variations, Ellipticity, and Higher-Order Deformations*

4.5.1 *Introduction*

In the present section we apply the results of Section 4.3 to random diameter variations, ellipticity, and higher-order deformations of the cross-section of the guide, using Morgan's coupling coefficients $\Xi_{[nm]}$.

Random straightness deviations may of course also be treated in this way, but are omitted since they have been discussed in Section 4.4.

We take the same model for the guide as in Section 4.4, i.e., a 20-mile total guide length of 2-inch I.D. copper with equally spaced mode filters, spaced either 200 feet or about 1000 feet apart. The mode filters are assumed to have zero loss for the TE_{01} signal mode, zero loss for the TE_{0m} spurious modes, and infinite loss for all other TE_{nm} spurious modes. The differential loss is assumed small in the distance between mode filters for all spurious modes; in addition, for the TE_{0m} spurious modes the present analysis forces us to assume that the differential loss is negligible for the total guide length, 20 miles in the present example.

The present analysis should provide a reasonable approximation for ellipticity and for higher-order deformations. The differential loss in these cases will not affect significantly the average TE_{01} loss, but will reduce the TE_{01} loss fluctuations somewhat below the values computed for zero differential loss in those cases where the differential loss is not completely negligible in the distance between mode filters.

However, for diameter variations the TE_{0m} differential loss is certainly not negligible in 20 miles, as required by the analysis. While this approximation will not lead to an appreciable error for the average TE_{01} loss, it will certainly lead to serious error for the mean square TE_{01} loss fluctuation, which is the really significant quantity, and for Δf_{3db}. The actual TE_{01} loss fluctuations will be much smaller than those computed here.

The power spectrum for straightness deviations is known, at least approximately, over a moderately wide range from TE_{01} transmission measurements, as discussed in Section 4.4. A very elementary consideration of the manufacturing process suggests the same shape for this power spectrum as is actually observed in certain cases. Unfortunately, for other types of deformation neither of these approaches has suggested the proper form for the power spectrum. Spurious modes, other than TE_{12}^{+} and TE_{11}^{+}, have not been observed at high enough levels to permit an estimate of the power spectrum of the corresponding mechanical imperfection to be made. As yet, no simple picture of the manufacturing processes has yielded a guess as to the shape of the power spectra. About all that can be said is that the power spectra must eventually fall off in some manner for high enough mechanical frequencies ζ (short enough mechanical wavelengths), since the mean square values of the various cross-sectional tolerances are certainly bounded.

Since the power spectra of the various deformations are not known, the numerical examples presented below are less specific than the example

for straightness deviation in Section 4.4. For example, ellipticity generates the TE_{2m}^{+} spurious modes. For *each* of these spurious modes the rms ellipticity in the mechanical wavelength range corresponding to the beat wavelength for the 50–60 kmc band is chosen to yield an additional average TE_{01} loss of 1 db per mile, assuming a flat power spectrum in this range. The same is done for trifoil and higher-order deformations.

Diameter variations are treated separately, partly because these results cannot be taken too seriously, as discussed above, and partly because the equations are somewhat different for this case. Here for *each* of the spurious TE_{0m}^{+} modes we choose the rms diameter variation in the mechanical wavelength range corresponding to the beat wavelength for the 50–60 kmc band to yield a 1-db rms loss fluctuation for the TE_{01} loss component due to the spurious mode, for the entire 20-mile line.

4.5.2 *Random Diameter Variations*

From (179) to (181) the radius of the guide is given by

$$r = a + a_0(z). \tag{344}$$

From (207) the coupling coefficient is given by

$$c_{[0m]}(z) = -\Xi_{[0m]}a_0(z). \tag{345}$$

Let $K_0(\zeta)$ be the power spectrum of $a_0(z)$, i.e.,

$$K_0(\zeta) = \int_{-\infty}^{\infty} \langle a_0(z)a_0(z+\tau)\rangle\, e^{-j2\pi\zeta\tau}\, d\tau. \tag{346}$$

Then the power spectrum $S_{[0m]}(\zeta)$ of the coupling coefficient $c_{[0m]}(z)$ is

$$S_{[0m]}(\zeta) = \Xi_{[0m]}^{2} \cdot K_0(\zeta). \tag{347}$$

Remembering that the spurious mode now has only a single polarization, we have from (302) and (304b)

$$\langle A_{[0m]}\rangle = \sqrt{\langle(\delta A_{[0m]})^2\rangle} = \frac{L}{2}\,\Xi_{[0m]}^{2} \cdot K_0\left(\frac{D_{[0m]}}{2\pi}\,\lambda\right), \tag{348}$$

where the constant $D_{[0m]}$ is related to the beat wavelength $B_{[0m]}$ by

$$\frac{D_{[0m]}}{2\pi}\,\lambda = \frac{1}{B_{[0m]}} = \frac{\beta_{01} - \beta_{0m}}{2\pi}. \tag{349}$$

The coupling coefficient $\Xi_{[0m]}$ is approximately proportional to the free-space wavelength λ.

Finally, the mean square radius variation in the range of mechanical frequencies ζ_a to ζ_b (or the range of mechanical wavelengths $\frac{1}{\zeta}$ from $\frac{1}{\zeta_a}$

to $\frac{1}{\zeta_b}$) is given by

$$\langle a_0^2(z)\rangle = \left[\int_{-\zeta_b}^{-\zeta_a} + \int_{\zeta_a}^{\zeta_b}\right] K_0(\zeta)\, d\zeta, \tag{350}$$

again integrating over positive and negative frequencies. Assuming that the power spectrum is flat over the range of integration,

$$K_0(\zeta) = K_0, \quad \zeta_a < |\zeta| < \zeta_b, \tag{351}$$

(350) becomes

$$\langle a_0^2(z)\rangle = 2K_0 \cdot (\zeta_b - \zeta_a). \tag{352}$$

These formulas are used to calculate the results in Table VII.

The present analysis could alternately have been carried out in terms of the coupling coefficients $C_{d[m]}$, as discussed in Section 2.3.9.

TABLE VII — RADIUS VARIATION YIELDING 1 DB RMS TE_{01} LOSS FLUCTUATION AND 1 DB AVERAGE TE_{01} LOSS FOR THE LOSS COMPONENT $A_{[0m]}$ DUE TO EACH OF THE TE_{0m}^+ SPURIOUS MODES, AT 55 KMC

L_{total} = 20 miles, total guide length.
$8.6859\sqrt{\langle(\delta A_{[0m]})^2\rangle}$ = 1 db, rms loss fluctuation for each component, for 20-mile line.
$8.6859\langle A_{[0m]}\rangle$ = 1 db, additional average loss for each component, for 20-mile line.
f = 55 kmc, midband frequency.
a = 1 inch, guide radius.
Differential loss assumed small over total guide length of 20 miles.

Spurious Mode	Beat Wavelength Range for 50–60 Kmc Band	RMS Radius Variation in Beat Wavelength Range	K_0 : Spectral Density of Radius Variation	$\Delta f_{3\,db}$: 3-db Bandwidth of Power Spectrum of Loss Fluctuation
	feet	mils	mils^2/foot^{-1}	mc
TE_{02}^+	0.7886–0.9532	0.087	1.7291×10^{-2}	0.907
TE_{03}^+	0.3003–0.3654	0.097	0.7942×10^{-2}	0.347
TE_{04}^+	0.1588–0.1953	0.102	0.4397×10^{-2}	0.185
TE_{05}^+	0.0964–0.1206	0.105	0.2671×10^{-2}	0.113
TE_{06}^+	0.0627–0.0805	0.109	0.1691×10^{-2}	0.075
TE_{07}^+	0.0418–0.0563	0.115	0.1064×10^{-2}	0.051
TE_{08}^+	0.0259–0.0402	0.129	0.0609×10^{-2}	0.035

4.5.3 *Random n-foils*

We now consider random cross-sectional deformations of higher order. For an "n-foil" the radius of the guide is given by (179) to (181) as

$$r = a + a_n(z) \cos n\varphi + b_n(z) \sin n\varphi. \tag{353}$$

The $n = 0$ case corresponds to diameter variations, studied in Section 4.5.2. The $n = 1$ case corresponds to straightness deviations, studied in Section 4.4; the quantities $a_1(z)$ and $b_1(z)$ are equal to $x(z)$ and $y(z)$, the rectangular components of straightness deviation. The $n = 2$ case corresponds to ellipticity, the $n = 3$ case has been designated as "trifoil," etc. All formulas in the present section hold *only* for $n \geqq 1$; the $n = 0$ case has been treated in the preceding section.

The magnitude of the n-foil distortion at a given position z along the axis is specified by the maximum departure from a perfect guide, $r = a$. From (353) we have for an n-foil

$$| r - a |_{\max} = \sqrt{a_n^2(z) + b_n^2(z)}. \tag{354}$$

For diameter variations this definition yields the change in guide radius; for straightness deviations it yields the total displacement (in the x-y plane) of the guide axis. For ellipticity and higher-order deformations, (354) yields the maximum deviation from a perfect circle $r = a$. Note that for $n = 2$ this is only one-quarter as large as a commonly accepted definition of ellipticity, the maximum diameter minus the minimum diameter.

The coupling coefficients for the two polarizations of each of the spurious modes are given from (207) by

$$c_{[nm]}^{\parallel}(z) = -\Xi_{[nm]} a_n(z), \tag{355}$$

$$c_{[nm]}^{\perp}(z) = -\Xi_{[nm]} b_n(z). \tag{356}$$

Let $K_n(\zeta)$ be the power spectrum of each of the two components $a_n(z)$ and $b_n(z)$, i.e.,

$$K_n(\zeta) = \int_{-\infty}^{\infty} \begin{bmatrix} \langle a_n(z) a_n(z+\tau) \rangle \\ \langle b_n(z) b_n(z+\tau) \rangle \end{bmatrix} e^{-j2\pi\zeta\tau}\, d\tau. \tag{357}$$

Then $S_{[nm]}(\zeta)$, the power spectrum of each of the two components of the coupling coefficient, is given by

$$S_{[nm]}(\zeta) = \Xi_{[nm]}^2 \cdot K_n(\zeta). \tag{358}$$

Using the results of (314) and (316b) for two polarizations, we have

$$\langle A_{[nm]} \rangle = \sqrt{2\langle (\delta A_{[nm]})^2 \rangle} = L \cdot S_{[nm]}\left(\frac{D_{[nm]}}{2\pi}\lambda\right), \tag{359}$$

where

$$\frac{D_{[nm]}}{2\pi}\lambda = \frac{1}{B_{[nm]}} = \frac{\beta_{01} - \beta_{nm}}{2\pi}. \tag{360}$$

The coupling coefficients $\Xi_{[nm]}$ are approximately proportional to the free-space wavelength λ.

Finally, the mean square n-foil magnitude (defined as the maximum departure from perfect circularity at a given cross section) in the range of mechanical frequencies ζ_a to ζ_b (or the range of mechanical wavelengths $\frac{1}{\zeta}$ from $\frac{1}{\zeta_a}$ to $\frac{1}{\zeta_b}$) is given from (354) by

$$\langle | r - a |^2_{\max} \rangle = \langle a_n^2(z) \rangle + \langle b_n^2(z) \rangle = 2 \left[\int_{-\zeta_b}^{-\zeta_a} + \int_{\zeta_a}^{\zeta_b} \right] K_n(\zeta)\, d\zeta . \tag{361}$$

Assuming that the power spectrum is flat in the range of integration, $K_n(\zeta) = K_n$,

$$\langle | r - a |^2_{\max} \rangle = 4K_n \cdot (\zeta_b - \zeta_a). \tag{362}$$

These formulas are used to calculate the results in Tables VIII through XII for values of n ranging from 2 to 6. The case of straightness deviations, $n = 1$, is omitted; the same results as those of Section 4.4 would of course be obtained.

4.5.4 *Discussion*

Neither TE_{01} transmission measurements nor mechanical measurements have thus far yielded information on the shape of the power spectra for diameter variations, ellipticity, and higher-order cross-sectional deformations. This is true principally because these effects are very small in present guides. We are thus unable to predict what the relative contributions of the various spurious modes to the average TE_{01} loss and to the TE_{01} loss fluctuation might be.

In the numerical examples presented in this section, the spectral density of the geometric imperfection has been chosen in such a way that for each type of imperfection the contributions of each of the spurious modes are equal. Plots of the logarithm of the spectral density K_n vs the logarithm of the mechanical frequency ζ show that in each case $K_n(\zeta)$ falls off approximately as $\frac{1}{\zeta}$. Thus, if the spectral density of the imperfection is flat, the higher modes will become progressively more important as the second mode index increases. This is quite different from the observed behavior for straightness deviations, discussed in Section 4.4, where only TE_{12}^+ and TE_{11}^+ have an appreciable effect on

TABLE VIII ($n = 2$) — ELLIPTICITY YIELDING 1 DB/MILE ADDITIONAL AVERAGE TE_{01} LOSS FOR THE LOSS COMPONENT $A_{[2m]}$ DUE TO EACH OF THE TE_{2m}^{+} SPURIOUS MODES, AT 55 KMC

L_{total} = 20 miles, total guide length.

$8.6859\frac{\langle A_{[2m]total}\rangle}{L_{total}}$ = 1 db/mile, additional average loss for each component.

f = 55 kmc, midband frequency.

a = 1 inch, guide radius.

Case 1

L = 200 feet, mode filter spacing.

M = 528, number of mode filters.

$8.6859\sqrt{\langle(\delta A_{[2m]total})^2\rangle}$ = 0.6155 db, rms total loss fluctuation for each component, for 20-mile line.

Case 2

L = 996.23 feet, mode filter spacing.

M = 106, number of mode filters.

$8.6859\sqrt{\langle(\delta A_{[2m]total})^2\rangle}$ = 1.3736 db, rms total loss fluctuation for each component, for 20-mile line.

Spurious Mode	Beat Wavelength Range for 50–60 Kmc Band	RMS Ellipticity in Beat Wavelength Range	K_2 Spectral Density of Ellipticity	Case 1	Case 2
				Δf_{3db}: 3-db Bandwidth of Power Spectrum of Loss Fluctuation	Δf_{3db}: 3-db Bandwidth of Power Spectrum of Loss Fluctuation
	feet	mils	mils²/foot⁻¹	mc	mc
TE_{21}^{+}	5.1623–6.2110	0.3737	1.0676	3128	628
TE_{22}^{+}	0.9006–1.0880	0.5142	0.3457	547	110
TE_{23}^{+}	0.3154–0.3836	0.5992	0.1592	192	39
TE_{24}^{+}	0.1631–0.2005	0.6349	0.0882	100	20
TE_{25}^{+}	0.0982–0.1226	0.6603	0.0536	61	12
TE_{26}^{+}	0.0636–0.0815	0.6861	0.0340	40	8
TE_{27}^{+}	0.0423–0.0569	0.7216	0.0214	27	5.5
TE_{28}^{+}	0.0263–0.0405	0.8103	0.0123	19	3.8

the TE_{01} loss; there, however, the straightness deviation power spectrum falls off very rapidly, as $\frac{1}{\zeta^4}$.

In any practical case the power spectrum $K_n(\zeta)$ of the geometric deformation must eventually fall off as ζ increases (for $n \neq 1$). If the derivative of the imperfection exists (which seems a reasonable requirement), $K_n(\zeta)$ must eventually fall off faster than $\frac{1}{\zeta^2}$ as ζ becomes large; of course the real question is how large ζ must be for this behavior to dominate. The higher spurious modes have very short beat wavelengths — in the range of an inch or less; if the power spectrum $K_n(\zeta)$ has begun to fall off appreciably at such wavelengths, the contribution of the higher-order spurious modes will be small.

TABLE IX ($n = 3$) — TRI-FOIL YIELDING 1 DB/MILE ADDITIONAL AVERAGE TE_{01} LOSS FOR THE LOSS COMPONENT $A_{[3m]}$ DUE TO EACH OF THE TE_{3m}^{+} SPURIOUS MODES, AT 55 KMC

$L_{\text{total}} = 20$ miles, total guide length.
$8.6859\dfrac{\langle A_{[3m]\text{total}}\rangle}{L_{\text{total}}} = 1$ db/mile, additional average loss for each component.
$f = 55$ kmc, midband frequency.
$a = 1$ inch, guide radius.

Case 1	$L = 200$ feet, mode filter spacing. $M = 528$, number of mode filters. $8.6859\sqrt{\langle(\delta A_{[3m]\text{total}})^2\rangle} = 0.6155$ db, rms total loss fluctuation for each component, for 20-mile line.
Case 2	$L = 996.23$ feet, mode filter spacing. $M = 106$, number of mode filters. $8.6859\sqrt{\langle(\delta A_{[3m]\text{total}})^2\rangle} = 1.3736$ db, rms total loss fluctuation for each component, for 20-mile line.

Spurious Mode	Beat Wavelength Range for 50–60 Kmc Band	RMS Tri-Foil in Beat Wavelength Range	K_3 Spectral Density of Tri-Foil	Case 1	Case 2
				$\Delta f_{3\text{db}}$: 3-db Bandwidth of Power Spectrum of Loss Fluctuation	$\Delta f_{3\text{db}}$: 3-db Bandwidth of Power Spectrum of Loss Fluctuation
	feet	mils	mils^2/foot^{-1}	mc	mc
TE_{31}^{+}	9.2836–11.1800	0.1876	0.4817	5628	1130
TE_{32}^{+}	0.5464–0.6617	0.5364	0.2257	332	67
TE_{33}^{+}	0.2315–0.2827	0.6045	0.1168	141	28
TE_{34}^{+}	0.1285–0.1590	0.6389	0.0684	79	16
TE_{35}^{+}	0.0801–0.1011	0.6661	0.0428	50	10
TE_{36}^{+}	0.0526–0.0687	0.6964	0.0272	34	6.7
TE_{37}^{+}	0.0346–0.0485	0.7449	0.0167	23	4.6

For ellipticity and higher-order deformations, the additional average loss in db per mile and the total loss fluctuation for a 20-mile guide are roughly comparable, for reasonable mode filter spacings. Thus if the additional average loss is small, as it is in present guides, the loss fluctuation will also be small.

For diameter variations, the total additional average loss for a 20-mile guide is roughly comparable with the total loss fluctuation. Here the total loss fluctuation can remain serious even though the additional average loss in db per mile remains small, as it does in present guides.

The results for diameter variations given here are pessimistic, since the differential loss to the TE_{0m}^{+} spurious modes is neglected over the total guide length of 20 miles in the present analysis. The loss fluctuations in practice will be much smaller than those given here. The results

TABLE X ($n = 4$) — 4-FOIL YIELDING 1 DB/MILE ADDITIONAL AVERAGE TE_{01} LOSS FOR THE LOSS COMPONENT $A_{[4m]}$ DUE TO EACH OF THE TE_{4m}^{+} SPURIOUS MODES, AT 55 KMC

$L_{\text{total}} = 20$ miles, total guide length.

$8.6859 \dfrac{\langle A_{[4m]\text{total}} \rangle}{L_{\text{total}}} = 1$ db/mile, additional average loss for each component.

$f = 55$ kmc, midband frequency.

$a = 1$ inch, guide radius.

Case 1:

$L = 200$ feet, mode filter spacing.

$M = 528$, number of mode filters.

$8.6859\sqrt{\langle (\delta A_{[4m]\text{total}})^2 \rangle} = 0.6155$ db, rms total loss fluctuation for each component, for 20-mile line.

Case 2:

$L = 996.23$ feet, mode filter spacing.

$M = 106$, number of mode filters.

$8.6859\sqrt{\langle (\delta A_{[4m]\text{total}})^2 \rangle} = 1.3736$ db, rms total loss fluctuation for each component, for 20-mile line.

Spurious Mode	Beat Wavelength Range for 50–60 kmc Band	RMS 4-Foil in Beat Wavelength Range	K_4 Spectral Density of 4-Foil	Case 1	Case 2
				$\Delta f_{3\text{db}}$: 3-db Bandwidth of Power Spectrum of Loss Fluctuation	$\Delta f_{3\text{db}}$: 3-db Bandwidth of Power Spectrum of Loss Fluctuation
	feet	mils	mils^2/foot^{-1}	mc	mc
TE_{41}^{+}	2.0190–2.4344	0.2991	0.2647	1225	246
TE_{42}^{+}	0.3757–0.4562	0.5433	0.1571	229	46
TE_{43}^{+}	0.1782–0.2186	0.6059	0.0885	109	22
TE_{44}^{+}	0.1039–0.1295	0.6414	0.0540	64	13
TE_{45}^{+}	0.0663–0.0847	0.6719	0.0344	42	8.4
TE_{46}^{+}	0.0438–0.0586	0.7091	0.0218	28	5.7
TE_{47}^{+}	0.0275–0.0416	0.7890	0.0127	19	3.9

for other cross-sectional deformations are of course valid, since the differential loss will be small in the short distance between mode filters.

4.6 *Conclusions*

The TE_{01} loss of a long waveguide has been treated as a random process, and its statistics determined in terms of the statistics of the geometric imperfections. A statistical analysis is necessary because it would be impractical to make mechanical measurements of the complete geometry of any great length of guide, even if this were possible.

The numerical results show that rms tolerances of the order of 1 mil are required, for any of the various types of imperfections, to yield an additional average TE_{01} loss of the order of 1 db per mile. The rms di-

TABLE XI ($n = 5$) — 5-FOIL YIELDING 1 DB/MILE ADDITIONAL AVERAGE TE_{01} LOSS FOR THE LOSS COMPONENT $A_{[5m]}$ DUE TO EACH OF THE TE_{5m}^{+} SPURIOUS MODES, AT 55 KMC

$L_{\text{total}} = 20$ miles, total guide length.

$8.6859 \dfrac{\langle A_{[5m]\text{total}} \rangle}{L_{\text{total}}} = 1$ db/mile, additional average loss for each component.

$f = 55$ kmc, midband frequency.

$a = 1$ inch, guide radius.

Case 1

$L = 200$ feet, mode filter spacing.

$M = 528$, number of mode filters.

$8.6859 \sqrt{\langle (\delta A_{[5m]\text{total}})^2 \rangle} = 0.6155$ db, rms total loss fluctuation for each component, for 20-mile line.

Case 2

$L = 996.23$ feet, mode filter spacing.

$M = 106$, number of mode filters.

$8.6859 \sqrt{\langle (\delta A_{[5m]\text{total}})^2 \rangle} = 1.3736$ db, rms total loss fluctuation for each component, for 20-mile line.

Spurious Mode	Beat Wavelength Range for 50–60 kmc Band	RMS 5-Foil in Beat Wavelength Range	K_5 Spectral Density of 5-Foil	Case 1	Case 2
				$\Delta f_{3\,\text{db}}$: 3-db Bandwidth of Power Spectrum of Loss Fluctuation	$\Delta f_{3\,\text{db}}$: 3-db Bandwidth of Power Spectrum of Loss Fluctuation
	feet	mils	mils^2/foot^{-1}	mc	mc
TE_{51}^{+}	1.0317–1.2458	0.3297	0.1632	626	126
TE_{52}^{+}	0.2771–0.3375	0.5439	0.1144	169	34
TE_{53}^{+}	0.1417–0.1748	0.6057	0.0687	87	17
TE_{54}^{+}	0.0855–0.1076	0.6436	0.0432	53	11
TE_{55}^{+}	0.0554–0.0719	0.6787	0.0277	35	7.1
TE_{56}^{+}	0.0363–0.0503	0.7269	0.0172	24	4.8

ameter variation of present copper waveguide is of the order of 0.1 mil. Consequently the diameter, ellipticity, tri-foil, and higher-order deformations must have comparable or smaller tolerances, so that they should have a negligible effect on present TE_{01} transmission measurements. Experimental observations support this conclusion. The only spurious modes ever observed in measurements on relatively short (i.e., a few hundred feet in length) waveguides are TE_{12}^{+} and TE_{11}^{+}, arising from straightness deviations. TE_{0m}^{+}, TE_{2m}^{+}, TE_{3m}^{+}, and higher TE_{nm}^{+} modes have never been observed with significant magnitudes.[8]

Straightness deviation is the one tolerance about which in the past we have had no information at all, via mechanical measurements; it is the only significant tolerance in present measurements. Random straightness deviations are believed to account for substantially all of the addi-

TABLE XII ($n = 6$) — 6-FOIL YIELDING 1 DB/MILE ADDITIONAL AVERAGE TE_{01} LOSS FOR THE LOSS COMPONENT $A_{[6m]}$ DUE TO EACH OF THE TE_{6m}^{+} SPURIOUS MODES, AT 55 KMC

$L_{total} = 20$ miles, total guide length.

$8.6859 \dfrac{\langle A_{[6m]total} \rangle}{L_{total}} = 1$ db/mile, additional average loss for each component.

$f = 55$ kmc, midband frequency.

$a = 1$ inch, guide radius.

Case 1

$L = 200$ feet, mode filter spacing.

$M = 528$, number of mode filters.

$8.6859\sqrt{\langle (\delta A_{[6m]total})^2 \rangle} = 0.6155$ db, rms total loss fluctuation for each component, for 20-mile line.

Case 2

$L = 996.23$ feet, mode filter spacing.

$M = 106$, number of mode filters.

$8.6859\sqrt{\langle (\delta A_{[6m]total})^2 \rangle} = 1.3736$ db, rms total loss fluctuation for each component, for 20-mile line.

Spurious Mode	Beat Wavelength Range for 50–60 kmc Band	RMS 6-Foil in Beat Wavelength Range	K_6 Spectral Density of 6-Foil	Case 1	Case 2
				Δf_{3db}: 3-db Bandwidth of Power Spectrum of Loss Fluctuation	Δf_{3db}: 3-db Bandwidth of Power Spectrum of Loss Fluctuation
	feet	mils	mils²/foot⁻¹	mc	mc
TE_{61}^{+}	0.6532–0.7902	0.3394	0.1085	397	80
TE_{62}^{+}	0.2138–0.2614	0.5418	0.0861	131	26
TE_{63}^{+}	0.1154–0.1433	0.6047	0.0543	71	14
TE_{64}^{+}	0.0714–0.0907	0.6461	0.0349	45	9
TE_{65}^{+}	0.0465–0.0617	0.6873	0.0223	30	6
TE_{66}^{+}	0.0295–0.0434	0.7582	0.0133	20	4.1

tional loss observed in present copper waveguides, and to account for a substantial part of the additional loss in helix as well.

Diameter variations in both copper and helix guide give rise to the TE_{0m} spurious modes, which cannot be satisfactorily attenuated by existing structures. It may not be sufficient to have a good enough diameter tolerance to yield a small additional average TE_{01} loss, since the TE_{01} loss fluctuations may still remain objectionable. The diameter tolerance must thus be substantially better than the tolerance for ellipticity, tri-foil, etc., in copper guide. However, the present results for diameter variations are too pessimistic, since the differential loss over the entire length of guide was neglected.

Tolerances on diameter, ellipticity, tri-foil, etc. for drawn copper guide are tolerances at a single cross section, and are controlled primarily by the accuracy of the die through which the guide is drawn. A

good straightness tolerance requires accurate alignment between different cross sections separated by substantial distances (equal to the beat wavelength of TE_{12}^{+}, TE_{11}^{+}). This depends on many factors other than the dimensional accuracy of the dies; for example, random variations in hardness or wall thickness may cause the axis of the guide to curve as it is being drawn. Consequently, a good straightness tolerance is more difficult to attain than any of the other cross-sectional tolerances, in drawing copper guide. Numerous other manufacturing processes for copper guide are currently under study.[42]

The variation of the TE_{01} loss statistics with mode filter spacing is illustrated in the examples given above. The average loss is unaffected by the mode filter spacing, but the rms loss fluctuation is inversely proportional to the square root of the number of mode filters. As discussed in Section 3.4, the total TE_{01} loss will be approximately a Gaussian random process.

While the present analysis applies only to copper waveguide with the differential loss neglected, further study[41] shows that adding loss to the spurious mode has an effect similar to that of increasing the number of mode filters; for moderate values, as $\Delta\alpha$ increases the average loss changes very little, while the loss fluctuation will be progressively reduced. Thus, accurate tolerances will be important in helix (or in copper guide with a lossy dielectric lining) as well as copper guide, although in helix the principal effect of poor tolerances will be an increased average loss, the loss fluctuations remaining small (diameter variations excluded).

Finally, the shape of the power spectra of the different mechanical imperfections is all-important in determining the resulting TE_{01} loss due to mode conversion. Only components of the mechanical imperfection in the beat wavelength range of the important spurious modes have any effect on the TE_{01} transmission. The short-wavelength straightness deviations "built in" to the guide in the manufacturing process will be principally responsible for additional loss due to mode conversion to modes such as TE_{12}^{+} and TE_{11}^{+} in copper guide; long bows or random straightness deviations due to imperfect laying of the guide will have only a very small effect.

REFERENCES

1. Miller, S. E., Waveguide as a Communication Medium, B.S.T.J., **33**, Nov. 1954, pp. 1209–1266.
2. Morgan, S. P., Theory of Curved Circular Waveguide Containing an Inhomogeneous Dielectric, B.S.T.J., **36**, Sept. 1957, pp. 1209–1251.
3. Unger, H. G., Helix Waveguide Theory and Application, B.S.T.J., **37**, Nov. 1958, pp. 1599–1647.

4. Schelkunoff, S. A., Conversion of Maxwell's Equations into Generalized Telegraphist's Equations, B.S.T.J., **34,** Sept. 1955, pp. 995–1043.
5. Morgan, S. P., Mode Conversion Losses in Transmission of Circular Electric Waves Through Slightly Noncylindrical Guides, J. Appl. Phys., **21,** April 1950, pp. 329–338.
6. Jouguet, M., Effects of the Curvature on the Propagation of Electromagnetic Waves in Guides of Circular Cross-Section, Cables and Trans., **1,** No. 2, July 1947, pp. 133–153.
7. Miller, S. E., Notes on Methods of Transmitting the Circular Electric Wave around Bends, Proc. I.R.E., **40,** Sept. 1952, pp. 1104–1113.
8. Rowe, H. E., and Warters, W. D., Transmission Deviations in Waveguide Due to Mode Conversion: Theory and Experiment, Proc. I.E.E., **106,** Part B, Supplement No. 13, Sept. 1959, pp. 30–36; Warters, W. D., and Rowe, H. E., The Effects of Mode Conversion in Long Circular Waveguide, I.R.E. Wescon Convention Record, 1958, Part 1, pp. 13–20.
9. Unger, H. G., Normal Mode Bends for Circular Electric Waves, B.S.T.J., **36,** Sept. 1957, pp. 1292–1307.
10. Unger, H. G., Circular Waveguide Taper of Improved Design, B.S.T.J., **37,** July 1958, pp. 899–912.
11. Morgan, S. P., and Young, J. A., Helix Waveguide, B.S.T.J., **35,** Nov. 1956, pp. 1347–1384.
12. Unger, H. G., Round Waveguide with Lossy Lining, Proc. of the Symposium on Millimeter Waves, Polytechnic Inst. of Brooklyn, 1959, pp. 535–541.
13. Unger, H. G., Round Waveguide with Double Lining, B.S.T.J., **39,** Jan. 1960, pp. 161–168.
14. Unger, H. G., Circular Electric Wave Transmission in a Dielectric-Coated Waveguide, B.S.T.J., **36,** Sept. 1957, pp. 1253–1278.
15. Morgan, S. P., unpublished memoranda, 1951.
16. Iiguchi, S., Mode Conversion in the Transmission of TE_{01} Waves Through a Slight Tilt and a Slight Offset of Waveguide, J. Inst. Elec. Comm. Engrs., Japan, **40,** 1957, pp. 870–876, 1095–1102.
17. Miller, S. E., Coupled Wave Theory and Waveguide Applications, B.S.T.J., **33,** May 1954, pp. 661–720.
18. Rowe, H. E., Approximate Solutions for the Coupled Line Equations, B.S.T.J. this issue, pp. 1011.
19. Unger, H. G., Noncylindrical Helix Waveguide, B.S.T.J., **40,** Jan. 1961, pp. 233–254.
20. Unger, H. G., Mode Conversion in Metallic and Helix Waveguide, B.S.T.J., **40,** March 1961, pp. 613–626.
21. Unger, H. G., Winding Tolerances in Helix Waveguide, B.S.T.J., **40,** March 1961, pp. 627–643.
22. Unger, H. G., Normal Modes and Mode Conversion in Helix Waveguide, B.S.T.J., **40,** Jan. 1961, pp. 255–280.
23. Montgomery, C. G., Dicke, R. H., and Purcell, E. M., *Principles of Microwave Circuits*, McGraw-Hill Book Co., Inc., New York, N. Y.; 1948.
24. Bolinder, E. F., Fourier Transforms and Tapered Transmission Lines, Proc. I.R.E., **44,** April 1956, p. 557.
25. Klopfenstein, R. W., A Transmission Line Taper of Improved Design, Proc. I.R.E., **44,** Jan. 1956, pp. 31–35.
26. Collin, R. F., The Optimum Tapered Transmission Line Matching Section, Proc. I.R.E., **44,** April 1956, pp. 539–548.
27. Kaufman, H., Bibliography of Nonuniform Transmission Lines, I.R.E. Trans. on Antennas and Propagation, Vol. **AP-3,** Oct. 1955, pp. 218–220.
28. Louisell, W. H., Analysis of the Single Tapered Mode Coupler, B.S.T.J., **34,** July 1955, pp. 853–870.
29. Mertz, P., and Pfleger, K. W., Irregularities in Broadband Wire Transmission Circuits, B.S.T.J., **16,** Oct. 1937, pp. 541–559.
30. Kaden, H., Advances Made in the Statistics of Impedance Irregularities of Television Cables, Archiv. der Electr. Uber., **8,** 1954, pp. 523–529.
31. Ince, E. L., *Ordinary Differential Equations*, Dover, New York, N. Y.; 1956.
32. Bellman, R., *Stability Theory of Differential Equations*, McGraw-Hill Book Co., Inc., New York, N. Y.; 1953.

33. Shannon, C. E., and Weaver, W., *The Mathematical Theory of Communication*, The University of Illinois Press, Urbana, Ill.; 1949; see p. 53.
34. Shannon, C. E., Communication in the Presence of Noise, Proc. I.R.E., **37**, Jan. 1949, pp. 10–21.
35. Unger, H. G., Circular Electric Wave Transmission Through Serpentine Bends, B.S.T.J., **36**, Sept. 1957, pp. 1279–1291.
36. Franklin, P., *Methods of Advanced Calculus*, McGraw-Hill Book Co., Inc., New York, N. Y.; 1944; see Chapter III.
37. Davenport, W. B., and Root, W. L., *Random Signals and Noise*, McGraw-Hill Book Co., Inc., New York, N. Y.; 1958.
38. Bellman, R., *Introduction to Matrix Analysis*, McGraw-Hill Book Co., Inc., New York, N. Y.; 1960.
39. King, A. P., and Mandeville, G. D., The Observed 33–90 Kmc. Attenuation of Two Inch Improved Waveguide, B.S.T.J., **40**, Sept. 1961, pp. 1323–1330.
40. Rice, S. O., Mathematical Analysis of Random Noise; *Noise and Stochastic Processes*, Nelson Wax, Editor, Dover, New York, N. Y., 1954.
41. Rowe, H. E., unpublished work.
42. Beck, A. C., and Rose, C. F. P., Waveguide for Circular Electric Mode Transmission, Proc. I. E. E., **106**, Part B, Supplement No. 13, Sept. 1959, pp. 159–162.

APPENDIX A

Coupling Coefficients for Tilts, Offsets, and Diameter Changes[15, 16]

General formulas for the coupling coefficients from TE_{01} to the first-order spurious modes at offsets, tilts, and diameter changes, as determined by S. P. Morgan, are given in Table XIII. Numerical values are tabulated at 55 kmc for 2-inch diameter guide in Tables XIV, XV and XVI; the computations here and in Appendix D were performed by Mrs. C. L. Beattie.

Notation

$C_{o[m]}^{\pm}$ — coupling coefficient between TE_{01} and forward (+) or backward (−) TE_{1m} for an offset in copper guide.

$C_{t[m]}^{\pm}$ — coupling coefficient between TE_{01} and forward (+) or backward (−) TE_{1m} for a tilt in copper guide.

$C_{t(11)}^{+}$ — coupling coefficient between TE_{01} and forward TM_{11} for a tilt in copper guide.

$C_{d[m]}^{\pm}$ — coupling coefficient between TE_{01} and forward (+) or backward (−) TE_{0m} for a diameter change in copper or helix guide.

a — guide radius.

λ — free-space wavelength.

k_{nm} — Bessel root given by $J_n'(k_{nm}) = 0$.

$\nu_{nm} = \dfrac{k_{nm}\lambda}{2\pi a}$, cutoff factor for the TE_{nm} mode.

$\beta_{nm} = \dfrac{2\pi}{\lambda}\sqrt{1 - \nu_{nm}^2}$, propagation constant for the TE_{nm} mode.

TABLE XIII

Coupling Coefficient	Spurious Mode	Equation
$C_{o[m]}^{\pm} = \frac{1}{\sqrt{2}\,a}\,\frac{k_{01}k_{1m}^2}{(k_{1m}^2 - k_{01}^2)\sqrt{k_{1m}^2-1}}\,\frac{\beta_{01} \pm \beta_{1m}}{\sqrt{\beta_{01}\beta_{1m}}}$	TE_{1m}	(A-1)
$C_{t[m]}^{\pm} = \frac{a}{\sqrt{2}}\,\frac{k_{01}k_{1m}^2}{(k_{01}^2 - k_{1m}^2)^2\sqrt{k_{1m}^2-1}}\,\frac{(\beta_{01} \pm \beta_{1m})^2}{\sqrt{\beta_{01}\beta_{1m}}}$	TE_{1m}	(A-2)
$C_{t(11)}^{+} = \frac{\sqrt{2}\pi a}{k_{01}\lambda}$	TM_{11}	(A-3)
$C_{d[m]}^{\pm} = \frac{1}{a}\,\frac{k_{01}k_{0m}}{k_{0m}^2 - k_{01}^2}\,\frac{\beta_{0m} \pm \beta_{01}}{\sqrt{\beta_{01}\beta_{0m}}}, \quad m \neq 1.$	TE_{0m}	(A-4)

TABLE XIV — COUPLING COEFFICIENTS FOR OFFSET (f = 55 kmc; a = 1 inch):

Spurious Mode	$C_{o[m]}^{+}$	$C_{o[m]}^{-}$
	inch^{-1}	inch^{-1}
TE_{11}	−1.052295	0.0035023
TE_{12}	2.140300	0.0087996
TE_{13}	0.800615	0.0143221
TE_{14}	0.520766	0.0204174
TE_{15}	0.392376	0.0274958
TE_{16}	0.317601	0.0362493
TE_{17}	0.269338	0.0480943
TE_{18}	0.238323	0.0668142
TE_{19}	0.230068	0.1105813

TABLE XV — COUPLING COEFFICIENTS FOR TILT (f = 55 kmc; a = 1 inch)

Spurious Mode	$C_{t[m]}^{+}$	$C_{t[m]}^{-}$
	radian^{-1}	radian^{-1}
TE_{11}	5.428116	0.000060129
TE_{12}	9.004674	0.000152211
TE_{13}	0.784756	0.000251132
TE_{14}	0.237781	0.000365504
TE_{15}	0.103215	0.000506837
TE_{16}	0.0534059	0.000695704
TE_{17}	0.0306226	0.000976413
TE_{18}	0.0187490	0.00147362
TE_{19}	0.0121822	0.00282165
	$C_{t(11)}^{+}$	$C_{t(11)}^{-}$
	radian^{-1}	radian^{-1}
TM_{11}	5.403	0.

TABLE XVI — COUPLING COEFFICENTS FOR DIAMETER CHANGE
(f = 55 kmc; a = 1 inch)

Spurious Mode	$C_{d[m]^+}$	$C_{d[m]^-}$
	inch^{-1}	inch^{-1}
TE_{02}	1.556796	−0.0162900
TE_{03}	0.878135	−0.0244495
TE_{04}	0.627935	−0.0336831
TE_{05}	0.493929	−0.0447267
TE_{06}	0.410428	−0.0589493
TE_{07}	0.355528	−0.0795021
TE_{08}	0.324255	−0.1168700
TE_{09}	0.425098	−0.329569

APPENDIX B

Geometry of Discrete Tilts

Let unit vectors directed along the guide axes in the two guide sections adjacent to a discrete tilt be $\mathbf{t}_1$ and $\mathbf{t}_2$. Then

$$\mathbf{t}_1 = \mathbf{i}x_1 + \mathbf{j}y_1 + \mathbf{k}z_1 ; \qquad |\mathbf{t}_1| = 1. \tag{B-1}$$

$$\mathbf{t}_2 = \mathbf{i}x_2 + \mathbf{j}y_2 + \mathbf{k}z_2 ; \qquad |\mathbf{t}_2| = 1. \tag{B-2}$$

$\mathbf{i}$, $\mathbf{j}$, and $\mathbf{k}$ are unit vectors along the x, y, and z axes respectively. Since $\mathbf{t}_1$ and $\mathbf{t}_2$ are unit vectors,

$$x_1^2 + y_1^2 + z_1^2 = 1, \tag{B-3}$$

$$x_2^2 + y_2^2 + z_2^2 = 1. \tag{B-4}$$

Let the tilt have angle α, orientation θ as defined in Section 2.1.2; further let the corresponding angles of the projections of the guide axes on the x-z and y-z planes be α_x and α_y, as in (38). Then by taking appropriate dot products we have:

$$\cos \alpha = x_1x_2 + y_1y_2 + z_1z_2, \tag{B-5}$$

$$\cos \alpha_x = \frac{x_1x_2 + z_1z_2}{\sqrt{x_1^2 + z_1^2}\sqrt{x_2^2 + z_2^2}}, \tag{B-6}$$

$$\cos \alpha_y = \frac{y_1y_2 + z_1z_2}{\sqrt{y_1^2 + z_1^2}\sqrt{y_2^2 + z_2^2}}, \tag{B-7}$$

where (B-3) and (B-4) of course hold true. If the angular deviation of the guide axis from the z-axis is small, we have

$$x_1 \ll 1, \qquad y_1 \ll 1, \qquad x_2 \ll 1, \qquad y_2 \ll 1. \tag{B-8}$$

Under these conditions (B-5) to (B-7) yield to first order

$$\alpha \approx \sqrt{(x_2 - x_1)^2 + (y_2 - y_1)^2}, \tag{B-9}$$

$$\alpha_x \approx x_2 - x_1 , \tag{B-10}$$

$$\alpha_y \approx y_2 - y_1 , \tag{B-11}$$

where we have made use of (B-3) and (B-4).

Now define the unit vector $\mathbf{p}$ as follows:

$$\mathbf{p} = \frac{\mathbf{t}_2 - \mathbf{t}_1}{|\mathbf{t}_2 - \mathbf{t}_1|} = \frac{\mathbf{t}_2 - \mathbf{t}_1}{2 \sin (\alpha/2)} \tag{B-12}$$

$\mathbf{p}$ lies in the plane of the tilt, i.e., in the $\varphi = \theta$ plane, and bisects the angle made by the guide axes on the two sides of the tilt. The vectors $\mathbf{t} = (\mathbf{t}_1 + \mathbf{t}_2)/2$ and $\mathbf{p}$ are the analogs for the discrete case of the tangent and principal normal vectors of differential geometry, introduced in Section 2.4, in the treatment of the continuous case. Denote the transverse component of $\mathbf{p}$ by $\mathbf{p}_{x,y}$; then by (B-12), (B-1) and (B-2)

$$\mathbf{p}_{x,y} = \frac{1}{2 \sin (\alpha/2)} [\mathbf{i}(x_2 - x_1) + \mathbf{j}(y_2 - y_1)]. \tag{B-13}$$

Now if the angular deviation of the guide axis from the z-axis is small (on both sides of the tilt), as assumed in (B-8), and if a unit vector perpendicular to the guide axis and lying in the $\varphi = 0$ plane is almost parallel to the x-axis, then the angle of $\mathbf{p}_{x,y}$ with respect to the x-axis will be approximately equal to the orientation θ of the tilt; under these conditions we have from (B-13)

$$\cos \theta \approx \frac{x_2 - x_1}{\sqrt{(x_2 - x_1)^2 + (y_2 - y_1)^2}}, \tag{B-14}$$

$$\sin \theta \approx \frac{y_2 - y_1}{\sqrt{(x_2 - x_1)^2 + (y_2 - y_1)^2}}. \tag{B-15}$$

From (B-9) to (B-11), (B-14) and (B-15) we then have

$$\alpha \cos \theta \approx \alpha_x , \tag{B-16}$$

$$\alpha \sin \theta \approx \alpha_y , \tag{B-17}$$

as stated in (38).

APPENDIX C

Energy Relations for Guides with Real Coupling Coefficients

Consider the coupled line equations given in (85)

$$\begin{aligned} I_0'(z) &= -\Gamma_0 I_0(z) + jc(z)I_1(z) \\ I_1'(z) &= jc(z)I_0(z) - \Gamma_1 I_1(z) \end{aligned} \tag{C-1}$$

$$\Gamma_0 = \alpha_0 + j\beta_0 ; \qquad \Gamma_1 = \alpha_1 + j\beta_1 . \tag{C-2}$$

We assume in this appendix that $c(z)$ is pure real;

$$\text{Im } c(z) = 0. \tag{C-3}$$

Consider first the case of ideal metallic guide, for which $\alpha_0 = \alpha_1 = 0$. The total power $P(z)$ flowing in the guide at the point z is simply

$$P(z) = | I_0(z) |^2 + | I_1(z) |^2 = I_0(z)I_0^*(z) + I_1(z)I_1^*(z). \tag{C-4}$$

Now in general, for guide whose walls are not perfect conductors, the α's will not be identically zero, and neither (C-3) nor (C-4) hold true. Helix waveguide furnishes an interesting example. Here the coupling coefficients are complex, so that (C-3) is not valid; further the powers in the various modes are not orthogonal, so that (C-4) is untrue. In this appendix we consider cases where $\alpha \neq 0$ but where (C-3) holds true, so that $c(z)$ is pure real. We define a quantity $P(z)$ by (C-4); however only for ideal metallic guide, where the α's are equal to zero, are we assured that $P(z)$ really represents the total power. If the α's are not zero we have no reason to think that $P(z)$ should be the total power; however the results given below render this plausible when $c(z)$ is real.

From (C-4) we write

$$\begin{aligned} P'(z) = \frac{dP(z)}{dz} &= I_0(z)I_0^{*\prime}(z) + I_0'(z)I_0^*(z) \\ &\quad + I_1(z)I_1^{*\prime}(z) + I_1'(z)I_1^*(z). \end{aligned} \tag{C-5}$$

Substituting (C-1) into (C-5), making use of (C-2) and (C-3), we find

$$P'(z) = -2\alpha_0 | I_0(z) |^2 - 2\alpha_1 | I_1(z) |^2. \tag{C-6}$$

If $P(z)$ is the total power flowing along the guide, (C-6) has a simple physical interpretation. It says that each mode contributes to the de-

crease in power along the guide in proportion to the product of its attenuation constant and the power it carries. Equation (C-6) may be extended to any number of modes via straightforward matrix techniques.

Finally, consider the case where

$$\alpha_0 = \alpha_1 \equiv \alpha, \qquad \Delta\alpha \equiv \alpha_0 - \alpha_1 = 0. \tag{C-7}$$

From the transformation of (88)–(89), (C-4) becomes

$$P(z) = e^{-2\alpha z}[\,|\,G_0(z)\,|^2 + |\,G_1(z)\,|^2]. \tag{C-8}$$

Similarly from (C-6), (C-7), and (C-4), we find

$$P'(z) = -2\alpha P(z), \tag{C-9}$$

which has the solution

$$P(z) = e^{-2\alpha z}P(0) = e^{-2\alpha z}[\,|\,I_0(0)\,|^2 + |\,I_1(0)\,|^2]. \tag{C-10}$$

Assuming as usual that the guide is excited by a unit TE_{01} wave so that the initial conditions of (87) apply, i.e.,

$$I_0(0) = 1, \qquad I_1(0) = 0, \tag{C-11}$$

(C-10) becomes

$$P(z) = e^{-2\alpha z}. \tag{C-12}$$

From (C-8) and (C-12) we have finally

$$|\,G_0(z)\,|^2 + |\,G_1(z)\,|^2 = 1, \tag{C-13}$$

subject of course to the following conditions:

$$G_0(0) = 1, \qquad G_1(0) = 0. \tag{C-14}$$

$$\alpha_0 = \alpha_1\,, \qquad \Delta\alpha = \alpha_0 - \alpha_1 = 0. \tag{C-15}$$

A similar treatment may of course be given for the coupled line equations of (93).

APPENDIX D (See Section 2.3.8)

Coupling Coefficients $\Xi_{[nm]}$ for General Continuous Deformations, and Beat Wavelengths $B_{[nm]}{}^{+}$, for Metallic Guide (Guide Diameter = 2 Inches)

n	m	Frequency = 50 Kmc		Frequency = 55 Kmc		Frequency = 60 Kmc	
		$B_{[nm]}{}^{+}$ feet	$\Xi_{[nm]}$ inch^{-2}	$B_{[nm]}{}^{+}$ feet	$\Xi_{[nm]}$ inch^{-2}	$B_{[nm]}{}^{+}$ feet	$\Xi_{[nm]}$ inch^{-2}
0							
	2	0.78861	1.033665	0.87104	0.935818	0.95318	0.855165
	3	0.30028	1.531489	0.33298	1.380849	0.36543	1.258058
	4	0.15879	2.072235	0.17717	1.855771	0.19531	1.682663
	5	0.09641	2.689180	0.10863	2.380811	0.12055	2.142344
	6	0.06272	3.452634	0.07182	2.992239	0.08053	2.658456
	7	0.04176	4.574033	0.04936	3.771644	0.05630	3.271486
	8	0.02590	7.815578	0.03405	4.986672	0.04021	4.077331
	9	CUT OFF		0.02066	10.765911	0.02842	5.422487
1							
	1	-2.45264	0.224648	-2.70093	0.203996	-2.94898	0.186837
	2	1.99720	0.561114	2.20291	0.508716	2.40812	0.465363
	3	0.46389	0.903729	0.51323	0.816787	0.56232	0.745451
	4	0.21503	1.268585	0.23908	1.140518	0.26289	1.036959
	5	0.12293	1.673662	0.13773	1.491619	0.15228	1.348056
	6	0.07762	2.151892	0.08805	1.888713	0.09815	1.690415
	7	0.05134	2.784072	0.05953	2.368870	0.06723	2.084309
	8	0.03377	3.901930	0.04119	3.029237	0.04763	2.572121
	9	CUT OFF		0.02776	4.333118	0.03402	3.272356
	10	CUT OFF		CUT OFF		0.02321	4.869801
2							
	1	-5.16225	0.414888	-5.68694	0.376608	-6.21100	0.344833
	2	0.90059	0.730808	0.99444	0.661825	1.08797	0.604918
	3	0.31537	1.081401	0.34959	0.975358	0.38358	0.888839
	4	0.16314	1.462636	0.18196	1.310395	0.20053	1.188501
	5	0.09816	1.897242	0.11054	1.680662	0.12263	1.512888
	6	0.06357	2.433890	0.07274	2.111386	0.08153	1.876880
	7	0.04225	3.217515	0.04987	2.659138	0.05685	2.308706
	8	0.02631	5.387660	0.03437	3.507377	0.04054	2.874896
	9	CUT OFF		0.02108	7.134864	0.02865	3.812804
3							
	1	9.28358	0.617958	10.23270	0.560645	11.18001	0.513138
	2	0.54642	0.905720	0.60417	0.819106	0.66165	0.747918
	3	0.23147	1.265707	0.25719	1.138773	0.28266	1.035917
	4	0.12849	1.667518	0.14385	1.487579	0.15895	1.345276
	5	0.08006	2.141126	0.09072	1.881991	0.10105	1.685882
	6	0.05262	2.763190	0.06091	2.357577	0.06872	2.077242
	7	0.03459	3.837927	0.04200	3.006912	0.04848	2.560340
	8	CUT OFF		0.02835	4.252809	0.03457	3.248210
	9	CUT OFF		CUT OFF		0.02366	4.759583
4							
	1	2.01904	0.834246	2.22697	0.756350	2.43441	0.691899
	2	0.37568	1.087248	0.41603	0.981657	0.45615	0.895260
	3	0.17821	1.458404	0.19854	1.308247	0.21863	1.187591
	4	0.10386	1.886313	0.11679	1.673870	0.12945	1.508455
	5	0.06627	2.412943	0.07568	2.099151	0.08471	1.868999
	6	0.04377	3.169891	0.05147	2.636799	0.05856	2.295676
	7	0.02754	5.053602	0.03538	3.454117	0.04157	2.851181
	8	CUT OFF		0.02221	6.258648	0.02936	3.751777
	9	CUT OFF		CUT OFF		0.01672	24.592342

n	m	Frequency = 50 Kmc		Frequency = 55 Kmc		Frequency = 60 Kmc	
		$B_{[nm]^+}$ feet	$\Xi_{[nm]}$ inch^{-2}	$B_{[nm]^+}$ feet	$\Xi_{[nm]}$ inch^{-2}	$B_{[nm]^+}$ feet	$\Xi_{[nm]}$ inch^{-2}
5							
	1	1.03171	1.063496	1.13893	0.963362	1.24582	0.880700
	2	0.27706	1.276544	0.30740	1.150302	0.33750	1.047565
	3	0.14174	1.661453	0.15842	1.485036	0.17484	1.344734
	4	0.08552	2.123151	0.09669	1.871474	0.10755	1.679382
	5	0.05538	2.725027	0.06388	2.337156	0.07193	2.064780
	6	0.03629	3.724150	0.04371	2.965282	0.05029	2.538314
	7	CUT OFF		0.02954	4.111601	0.03571	3.202782
	8	CUT OFF		CUT OFF		0.02456	4.570756
6							
	1	0.65318	1.305633	0.72180	1.181454	0.79015	1.079233
	2	0.21378	1.474795	0.23771	1.325829	0.26139	1.205391
	3	0.11540	1.877243	0.12947	1.670557	0.14326	1.508273
	4	0.07137	2.383934	0.08123	2.083255	0.09074	1.859682
	5	0.04651	3.099496	0.05437	2.603525	0.06168	2.276663
	6	0.02954	4.663254	0.03715	3.374330	0.04340	2.814772
	7	CUT OFF		0.02386	5.492384	0.03060	3.660164
	8	CUT OFF		CUT OFF		0.01927	7.278403
7							
	1	0.45817	1.560845	0.50693	1.410610	0.55543	1.287362
	2	0.17024	1.683378	0.18977	1.509104	0.20906	1.369320
	3	0.09560	2.108882	0.10773	1.866529	0.11957	1.679271
	4	0.06011	2.677695	0.06899	2.313116	0.07746	2.051409
	5	0.03903	3.582532	0.04652	2.910415	0.05327	2.509531
	6	0.02148	10.369537	0.03140	3.937248	0.03755	3.141452
	7	CUT OFF		CUT OFF		0.02593	4.344516
8							
	1	0.34163	1.829591	0.37853	1.651012	0.41518	1.505110
	2	0.13874	1.903988	0.15512	1.701141	0.17125	1.540005
	3	0.08022	2.360640	0.09090	2.075128	0.10125	1.858998
	4	0.05092	3.019453	0.05908	2.566671	0.06674	2.257265
	5	0.03243	4.298900	0.03988	3.279521	0.04625	2.770706
	6	CUT OFF		0.02603	4.903585	0.03244	3.549922
	7	CUT OFF		CUT OFF		0.02122	5.845324
9							
	1	0.26536	2.112618	0.29451	1.903044	0.32342	1.732653
	2	0.11507	2.138800	0.12910	1.903182	0.14287	1.718219
	3	0.06797	2.638691	0.07752	2.299234	0.08671	2.049035
	4	0.04320	3.437147	0.05087	2.852480	0.05792	2.480954
	5	0.02597	5.866004	0.03410	3.755552	0.04026	3.071952
	6	CUT OFF		0.01929	11.251662	0.02784	4.113642
10							
	1	0.21225	2.410992	0.23602	2.167296	0.25955	1.970313
	2	0.09673	2.390696	0.10898	2.116784	0.12093	1.904895
	3	0.05796	2.952529	0.06666	2.542807	0.07494	2.251409
	4	0.03650	3.992360	0.04393	3.184628	0.05052	2.727785
	5	CUT OFF		0.02886	4.456392	0.03506	3.434148
	6	CUT OFF		CUT OFF		0.02344	5.078573

n	m	Frequency = 50 Kmc		Frequency = 55 Kmc		Frequency = 60 Kmc	
		$B_{[nm]}{}^{+}$ feet	$\Xi_{[nm]}$ inch^{-2}	$B_{[nm]}{}^{+}$ feet	$\Xi_{[nm]}$ inch^{-2}	$B_{[nm]}{}^{+}$ feet	$\Xi_{[nm]}$ inch^{-2}
11							
	1	0.17355	2.726150	0.19341	2.444582	0.21303	2.218565
	2	0.08217	2.663620	0.09302	2.343950	0.10356	2.101187
	3	0.04961	3.317918	0.05768	2.811536	0.06524	2.468802
	4	0.03040	4.869555	0.03794	3.588797	0.04422	3.005794
	5	CUT OFF		0.02364	5.918920	0.03042	3.899372
	6	CUT OFF		CUT OFF		0.01796	10.206978
12							
	1	0.14434	3.059998	0.16128	2.735980	0.17796	2.478048
	2	0.07035	2.963187	0.08012	2.587323	0.08953	2.308543
	3	0.04248	3.763972	0.05011	3.114056	0.05711	2.704883
	4	0.02390	7.400976	0.03262	4.119666	0.03877	3.328012
	5	CUT OFF		CUT OFF		0.02614	4.574673
13							
	1	0.12168	3.415043	0.13636	3.042884	0.15078	2.749591
	2	0.06057	3.297766	0.06949	2.850485	0.07800	2.528816
	3	0.03621	4.353961	0.04363	3.464397	0.05020	2.964872
	4	CUT OFF		0.02769	4.929759	0.03396	3.717676
	5	CUT OFF		CUT OFF		0.02185	5.901255
14							
	1	0.10368	3.794611	0.11660	3.367083	0.12924	3.034244
	2	0.05233	3.680631	0.06060	3.138458	0.06838	2.764429
	3	0.03043	5.271752	0.03797	3.887661	0.04425	3.256582
	4	CUT OFF		0.02257	6.850328	0.02962	4.222458
15							
	1	0.08911	4.203178	0.10063	3.710887	0.11183	3.333332
	2	0.04526	4.134654	0.05305	3.458593	0.06025	3.018632
	3	0.02433	7.682039	0.03290	4.435549	0.03905	3.592421
	4	CUT OFF		CUT OFF		0.02555	4.966220
16							
	1	0.07711	4.646904	0.08750	4.077300	0.09755	3.648526
	2	0.03905	4.704352	0.04654	3.822244	0.05330	3.295920
	3	CUT OFF		0.02820	5.243552	0.03443	3.993906
	4	CUT OFF		CUT OFF		0.02139	6.491317
17							
	1	0.06707	5.134532	0.07655	4.470288	0.08566	3.981936
	2	0.03343	5.495075	0.04085	4.248284	0.04727	3.602748
	3	CUT OFF		0.02341	6.919841	0.03025	4.503227
18							
	1	0.05856	5.679004	0.06731	4.895211	0.07564	4.336278
	2	0.02801	6.872935	0.03579	4.771480	0.04199	3.948853
	3	CUT OFF		CUT OFF		0.02634	5.221466
19							
	1	0.05122	6.300569	0.05941	5.359516	0.06710	4.715079
	2	0.02050	22.459224	0.03116	5.466895	0.03730	4.349893
	3	CUT OFF		CUT OFF		0.02244	6.509164

n	m	Frequency = 50 Kmc		Frequency = 55 Kmc		Frequency = 60 Kmc	
		$B_{[nm]}{}^{+}$ feet	$\Xi_{[nm]}$ inch^{-2}	$B_{[nm]}{}^{+}$ feet	$\Xi_{[nm]}$ inch^{-2}	$B_{[nm]}{}^{+}$ feet	$\Xi_{[nm]}$ inch^{-2}
20	1	0.04481	7.033398	0.05257	5.873928	0.05974	5.123026
	2	CUT OFF		0.02675	6.549116	0.03308	4.833374
21	1	0.03910	7.941831	0.04659	6.454660	0.05335	5.566509
	2	CUT OFF		0.02197	9.289222	0.02920	5.454350
22	1	0.03388	9.169691	0.04130	7.127805	0.04774	6.054504
	2	CUT OFF		CUT OFF		0.02552	6.349417
23	1	0.02886	11.158150	0.03654	7.939276	0.04277	6.600202
	2	CUT OFF.		CUT OFF		0.02175	8.047971
24	1	0.02315	17.444425	0.03217	8.981077	0.03832	7.224001
25	1	CUT OFF		0.02804	10.482049	0.03428	7.959870
26	1	CUT OFF		0.02382	13.335010	0.03057	8.870500
27	1	CUT OFF		CUT OFF		0.02707	10.091403
28	1	CUT OFF		CUT OFF		0.02364	12.010406
29	1	CUT OFF		CUT OFF		0.01979	16.923252

APPENDIX E

Geometry of Continuous Bends

Let $x(z)$ and $y(z)$ be the transverse displacements of the guide axis from the z-axis, in a rectangular co-ordinate system. Then we write

$$\mathbf{r}(z) = \mathbf{i}x(z) + \mathbf{j}y(z) + \mathbf{k}z, \tag{E-1}$$

where **i**, **j**, and **k** are unit vectors along the x, y, and z axes respectively. Assuming that (215) holds true, from (216a) we have

$$s \approx z. \tag{E-2}$$

Thus, arc length along the bent guide axis is approximately equal to distance measured along the z-axis. From (211a) and (E-2),

$$\mathbf{t} = \frac{d\mathbf{r}}{ds} \approx \frac{d\mathbf{r}}{dz} = \mathbf{i}x'(z) + \mathbf{j}y'(z) + \mathbf{k}, \tag{E-3}$$

where primes indicate differentiation with respect to z. From (211b)

$$\frac{1}{\rho}\mathbf{p} = \frac{d\mathbf{t}}{ds} \approx \frac{d\mathbf{t}}{dz} \approx \mathbf{i}x''(z) + \mathbf{j}y''(z). \tag{E-4}$$

Therefore the curvature is approximately

$$\frac{1}{\rho} \approx \sqrt{x''^2(z) + y''^2(z)} \tag{E-5}$$

so that

$$\mathbf{p} \approx \frac{\mathbf{i}x''(z) + \mathbf{j}y''(z)}{\sqrt{x''^2(z) + y''^2(z)}}. \tag{E-6}$$

Then from (211c)

$$\mathbf{b} = \mathbf{t} \times \mathbf{p} \approx \mathbf{k} \times \mathbf{p} \approx \frac{\mathbf{j}x''(z) - \mathbf{i}y''(z)}{1/\rho}. \tag{E-7}$$

Since $\mathbf{p}$ and $\mathbf{b}$ are approximately transverse, i.e., their z-components are small, from (211) and (212)

$$\theta \approx \angle\mathbf{b} - \frac{\pi}{2} \approx \angle\mathbf{p}, \tag{E-8}$$

since by (211c) $\mathbf{b} \perp \mathbf{p}$. From (E-4)

$$\tan\theta \approx \frac{y''(z)}{x''(z)}. \tag{E-9}$$

Thus,

$$\cos\theta \approx \frac{x''(z)}{\sqrt{x''^2(z) + y''^2(z)}} \approx \rho \cdot x''(z), \tag{E-10}$$

$$\sin\theta \approx \frac{y''(z)}{\sqrt{x''^2(z) + y''^2(z)}} \approx \rho \cdot y''(z). \tag{E-11}$$

From (E-10) and (E-11) we finally obtain the approximation of (216);

$$\frac{\cos\theta}{\rho} \approx x''(z), \tag{E-12}$$

$$\frac{\sin\theta}{\rho} \approx y''(z). \tag{E-13}$$

The above analysis has been a little crude; it is helpful to get a precise estimate on the error in the approximate result of (E-4) for the vector $\frac{1}{\rho}\cdot\mathbf{p}$, which in the above approximation is assumed to be purely transverse. We write

$$\mathbf{r}(z) = \mathbf{i}x(z) + \mathbf{j}y(z) + \mathbf{k}z \tag{E-14}$$

as before. Next,

$$ds = \sqrt{dx^2 + dy^2 + dz^2}, \tag{E-15}$$

$$\frac{ds}{dz} = \sqrt{1 + x'^2(z) + y'^2(z)}\,, \tag{E-16}$$

where as before we reserve the prime to denote differentiation with respect to z. Then

$$\begin{aligned}\mathbf{t} = \frac{d\mathbf{r}}{ds} &= \frac{d\mathbf{r}}{dz}\frac{dz}{ds} \\ &= \frac{1}{\sqrt{1 + x'^2(z) + y'^2(z)}}\,[\mathbf{i}x'(z) + \mathbf{j}y'(z) + \mathbf{k}].\end{aligned} \tag{E-17}$$

Further

$$\begin{aligned}\frac{1}{\rho}\cdot\mathbf{p} = \frac{d\mathbf{t}}{ds} = \frac{d\mathbf{t}}{dz}\frac{dz}{ds} &= \frac{1}{1 + x'^2(z) + y'^2(z)}\cdot\Big\{\mathbf{i}x''(z) + \mathbf{j}y''(z) \\ &\quad - \frac{x'(z)x''(z) + y'(z)y''(z)}{1 + x'^2(z) + y'^2(z)}\,[\mathbf{i}x'(z) + \mathbf{j}y'(z) + \mathbf{k}]\Big\}.\end{aligned} \tag{E-18}$$

Now we may write (E-18) as follows:

$$\frac{1}{\rho}\cdot\mathbf{p} = \mathbf{i}x''(z) + \mathbf{j}y''(z) - \mathbf{A} - \mathbf{B}. \tag{E-19}$$

$$\mathbf{A} = \frac{x'^2(z) + y'^2(z)}{1 + x'^2(z) + y'^2(z)}\,[\mathbf{i}x''(z) + \mathbf{j}y''(z)]. \tag{E-20}$$

$$\mathbf{B} = \frac{x'(z)x''(z) + y'(z)y''(z)}{[1 + x'^2(z) + y'^2(z)]^2}\,[\mathbf{i}x'(z) + \mathbf{j}y'(z) + \mathbf{k}]. \tag{E-21}$$

The first two terms of (E-19) are identical to the approximation of (E-4); the vectors **A** and **B** represent correction terms that we shall show to be small compared to the first two terms.

From (E-20)

$$\frac{|\mathbf{A}|}{\sqrt{x''^2(z) + y''^2(z)}} = \frac{x'^2(z) + y'^2(z)}{1 + x'^2(z) + y'^2(z)} \leqq x'^2(z) + y'^2(z). \quad \text{(E-22)}$$

From (E-21)

$$\begin{aligned} |\mathbf{B}| &= \frac{|x'(z)x''(z) + y'(z)y''(z)|}{[1 + x'^2(z) + y'^2(z)]^2} [1 + x'^2(z) + y'^2(z)]^{\frac{1}{2}} \\ &\leqq |x'(z)x''(z) + y'(z)y''(z)| \\ &\leqq \sqrt{x'^2(z) + y'^2(z)}\ \sqrt{x''^2(z) + y''^2(z)}, \end{aligned} \quad \text{(E-23)}$$

where the last step follows from the Schwarz inequality. Then

$$\frac{|\mathbf{B}|}{\sqrt{x''^2(z) + y''^2(z)}} \leqq \sqrt{x'^2(z) + y'^2(z)}. \quad \text{(E-24)}$$

If (215) is satisfied, (E-22) and (E-24) show that the correction terms **A** and **B** of (E-19) are small compared to the first two terms, so that the approximation of (E-4) will be valid.

APPENDIX F

Rigorous Treatment of TE_{01} Loss Statistics for the Discrete Case

In treating the TE_{01} loss as a Fourier series with random coefficients, the frequency dependence of the $\Delta\alpha$'s and the C's in (218) was neglected, since the principal frequency dependence occurs through the $\Delta\beta$'s. While this provides a simple and accurate analysis, a rigorous treatment of the TE_{01} loss statistics as a function of frequency is of interest.

We consider only the case of independent offsets or tilts, treated in Sections 3.3.1 and 3.3.2 respectively. From (218), (235), and (236)

$$A = \tilde{A} + \delta A \quad \text{(F-1)}$$

$$\tilde{A} = \tfrac{1}{2}A_0 \quad \text{(F-2)}$$

$$\delta A = \sum_{k=1}^{N-1} A_k \cos k\Delta\beta l_0 \quad \text{(F-3)}$$

$$A_k = e^{k\Delta\alpha l_0} \sum_{i=1}^{N-k} (x_i^{\parallel} x_{i+k}^{\parallel} + x_i^{\perp} x_{i+k}^{\perp}) \quad \text{(F-4)}$$

$$\langle A_0 \rangle = \hat{x}^2 N, \qquad \langle A_0^2 \rangle = \hat{x}^4 N(N+1) \quad \text{(F-5a)}$$

$$\langle A_k \rangle = 0, \qquad \langle A_k^2 \rangle = \frac{\hat{x}^4}{2}(N-k)\, e^{k2\Delta\alpha l_0}; \quad 1 \leqq k \leqq N-1. \quad \text{(F-5b)}$$

$$\langle A_k A_l \rangle = 0, \quad k \neq l. \tag{F-5c}$$

The new quantity $\tilde{A}$ is defined by (F-2); δA remains the same as before.

We have for the expected values of the various losses:

$$\langle \tilde{A} \rangle = \tfrac{1}{2}\langle A_0 \rangle, \qquad \langle \delta A \rangle = 0. \tag{F-6}$$

Therefore

$$\langle A \rangle = \langle \tilde{A} \rangle = \tfrac{1}{2}\langle A_0 \rangle = \frac{\hat{x}^2}{2} N. \tag{F-7}$$

Equation (F-7) gives the expected value of the TE_{01} loss as a function of frequency, since the rms conversion coefficient $\hat{x}$ will in general vary with frequency (this variation will be small for offsets and diameter changes, approximately inversely with the free-space wavelength λ for tilts). We may now average over wavelength (indicated by a bar) and obtain instead of the result given in (237):

$$\langle \bar{A} \rangle = \overline{\langle A \rangle} = \frac{\overline{\hat{x}^2}}{2} N. \tag{F-8}$$

Thus, the average of $\hat{x}^2$ over the band should be used instead of the value of $\hat{x}^2$ at the middle of the band. Over reasonable bandwidths the error will be small.

Next from (F-5c), $\tilde{A}$ and δA are easily shown to be uncorrelated.

$$\langle \tilde{A}(\delta A) \rangle = 0. \tag{F-9}$$

We next find the mean square value of δA. From (F-3), (F-5b), and (F-5c):

$$\begin{aligned} \langle (\delta A)^2 \rangle &= \sum_{k=1}^{N-1} \sum_{l=1}^{N-1} \langle A_k A_l \rangle \cos k\Delta\beta l_0 \cos l\Delta\beta l_0 \\ &= \sum_{k=1}^{N-1} \langle A_k{}^2 \rangle \cos^2 k\Delta\beta l_0 \\ \langle (\delta A)^2 \rangle &= \frac{\hat{x}^4}{2} \sum_{k=1}^{N-1} (N - k)\, e^{k2\Delta\alpha l_0} \cos^2 k\Delta\beta l_0 . \end{aligned} \tag{F-10}$$

The summation of (F-10) is easily written in closed form, but its general behavior is much more easily seen by examining the usual two special cases, small and large differential loss.

1. *Small differential loss over total length* $L_N = Nl_0$.

$$\langle (\delta A)^2 \rangle = \frac{\hat{x}^4}{8} \left[N(N - 2) + \left(\frac{\sin N\Delta\beta l_0}{\sin \Delta\beta l_0} \right)^2 \right]; \quad -N2\Delta\alpha l_0 \ll 1. \tag{F-11}$$

2. *Large differential loss over total length L_N, small differential loss over pipe length l_0.*

$$\langle(\delta A)^2\rangle = \frac{\hat{x}^4}{4}\frac{N}{-\Delta\alpha l_0}\frac{1+\frac{1}{2}\left(\frac{\sin\Delta\beta l_0}{-\Delta\alpha l_0}\right)^2}{1+\left(\frac{\sin\Delta\beta l_0}{-\Delta\alpha l_0}\right)^2}; \quad -N2\Delta\alpha l_0 \gg 1, \quad -2\Delta\alpha l_0 \ll 1. \tag{F-12}$$

Sketches of the general behavior of $\langle(\delta A)^2\rangle$ vs $\Delta\beta l_0$ (proportional to the free-space wavelength λ) are given in Fig. 11 for a single period, these functions being periodic of period π. In both cases $\langle(\delta A)^2\rangle$ is almost constant except in narrow bands centered at $\Delta\beta l_0 = m\pi$, where it becomes twice as large; these peaks occur because we have assumed equally spaced mode converters. The half-width of these peaks initially decreases as $1.39/N$ as long as the differential loss remains small, approaching a limiting value of $(-\Delta\alpha l_0)$ when the differential loss becomes large. Since these peaks are narrow, they may be neglected in averaging over λ (or $\Delta\beta l_0$), yielding for small and large differential loss respectively:

$$\langle\overline{(\delta A)^2}\rangle = \overline{\langle(\delta A)^2\rangle} = \frac{\overline{\hat{x}^4}}{8}N(N-2); \quad -N2\Delta\alpha l_0 \ll 1 \tag{F-13}$$

$$\langle\overline{(\delta A)^2}\rangle = \overline{\langle(\delta A)^2\rangle} = \overline{\left(\frac{\hat{x}^4}{-\Delta\alpha}\right)}\frac{N}{8l_0}; \quad -N2\Delta\alpha l_0 \gg 1, \quad -2\Delta\alpha l_0 \ll 1. \tag{F-14}$$

Comparing with (241) and (242), we see that the average of $\hat{x}^4$ or of $\frac{\hat{x}^4}{-\Delta\alpha}$ over the band should be used rather than their values at the middle of the band. Again, over reasonable bandwidths the error will be small.

The minor difference between (F-13) and (241) for $\hat{x}^4$ independent of frequency — i.e., the factor $(N-2)$ instead of $(N-1)$ — arises because of our approximate integration of the function of Fig. 11(a), in which the narrow peaks and small ripples were ignored and the function set equal to $N(N-2)$. It is clear that this yields a result that is too small. An exact integration of (F-11) yields a result identical to (241).

The above calculations have considered only a single mode, the mode subscript being omitted as usual. For the total δA, including all first order spurious modes, we have

$$\delta A = \sum_{[m]}\delta A_{[m]}, \tag{F-15}$$

$$\langle(\delta A)^2\rangle = \sum_{[m]}\sum_{[n]}\langle\delta A_{[m]}\delta A_{[n]}\rangle. \tag{F-16}$$

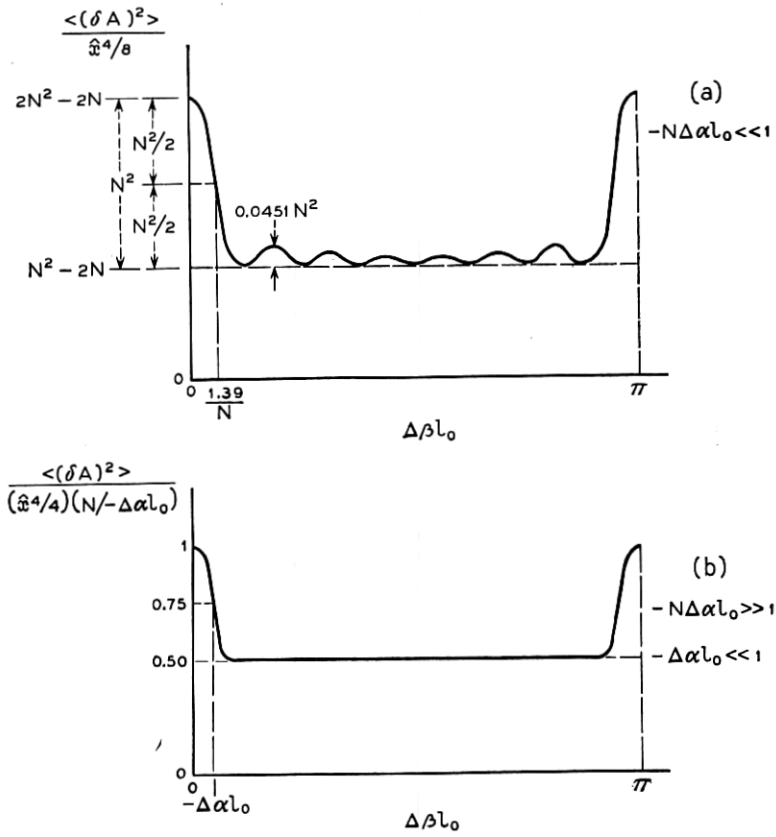

Fig. 11 — General behavior of $\langle(\delta A)^2\rangle$ vs $\Delta\beta l_0$.

In violation of our usual convention that [ ] indicate only TE spurious modes, in the present appendix this notation includes in addition the TM_{11}^{+} spurious mode in the case of tilts.

The $\langle(\delta A_{[m]})^2\rangle$ have been discussed above; we need in addition the cross terms $\langle\delta A_{[m]}\delta A_{[n]}\rangle$. These cross terms did not appear in the approximate analysis, so we expect to find them negligible here. The different $\delta A_{[m]}$ are of course not independent. From (218), (221) and (173) we see that $\delta A_{[m]}(\lambda_1) \propto \delta A_{[n]}(\lambda_2)$ where $\lambda_1 \propto \lambda_2$; i.e., the TE_{01} loss component due to the m^{th} spurious mode at one frequency is proportional to the TE_{01} loss component due to the n^{th} spurious mode at a widely separated frequency. However, at the *same* frequency $\delta A_{[m]}$ and $\delta A_{[n]}$ are almost uncorrelated, so that the cross terms in (F-16) may be neglected.

We have

$$\langle \delta A_{[m]} \delta A_{[n]} \rangle = \sum_{k=1}^{N-1} \sum_{l=1}^{N-1} \langle A_{k[m]} A_{l[n]} \rangle \cos k\Delta\beta_{[m]} l_0 \cos l\Delta\beta_{[n]} l_0 \quad \text{(F-17)}$$

where

$$\langle A_{k[m]} A_{k[n]} \rangle = \frac{\hat{x}_{[m]}^2 \hat{x}_{[n]}^2}{2} (N - k)\, e^{k(\Delta\alpha_{[m]} + \Delta\alpha_{[n]}) l_0}; \quad \text{(F-18)}$$

$$\langle A_{k[m]} A_{l[n]} \rangle = 0, \quad k \neq l.$$

Setting

$$\cos k\Delta\beta_{[m]} l_0 \cos k\Delta\beta_{[n]} l_0 = \tfrac{1}{2} \cos k(\Delta\beta_{[m]} - \Delta\beta_{[n]}) l_0 + \tfrac{1}{2} \cos k(\Delta\beta_{[m]} + \Delta\beta_{[n]}) l_0$$

(F-17) now becomes

$$\langle \delta A_{[m]} \delta A_{[n]} \rangle = \frac{\hat{x}_{[m]}^2 \hat{x}_{[n]}^2}{4} \sum_{k=1}^{N-1} (N - k)\, e^{k(\Delta\alpha_{[m]} + \Delta\alpha_{[n]}) l_0} \cdot [\cos k(\Delta\beta_{[m]} - \Delta\beta_{[n]}) l_0 + \cos k(\Delta\beta_{[m]} + \Delta\beta_{[n]}) l_0] \quad \text{(F-19)}$$

This summation is of the same general type as (F-10). In the special cases of small and large differential loss:

$$\langle \delta A_{[m]} \delta A_{[n]} \rangle = \frac{\hat{x}_{[m]}^2 \hat{x}_{[n]}^2}{8} \left[-2N + \left(\frac{\sin \tfrac{1}{2} N (\Delta\beta_{[m]} - \Delta\beta_{[n]}) l_0}{\sin \tfrac{1}{2} (\Delta\beta_{[m]} - \Delta\beta_{[n]}) l_0} \right)^2 + \left(\frac{\sin \tfrac{1}{2} N (\Delta\beta_{[m]} + \Delta\beta_{[n]}) l_0}{\sin \tfrac{1}{2} (\Delta\beta_{[m]} + \Delta\beta_{[n]}) l_0} \right)^2 \right]; \quad -N(\Delta\alpha_{[m]} + \Delta\alpha_{[n]}) l_0 \ll 1. \quad \text{(F-20)}$$

$$\langle \delta A_{[m]} \delta A_{[n]} \rangle = \frac{\hat{x}_{[m]}^2 \hat{x}_{[n]}^2}{4} \frac{N}{-(\Delta\alpha_{[m]} + \Delta\alpha_{[n]}) l_0} \cdot \left[\frac{1 - \dfrac{2}{-(\Delta\alpha_{[m]} + \Delta\alpha_{[n]}) l_0} [\sin \tfrac{1}{2} (\Delta\beta_{[m]} - \Delta\beta_{[n]}) l_0]^2}{1 + \left(\dfrac{2}{-(\Delta\alpha_{[m]} + \Delta\alpha_{[n]}) l_0} \right)^2 [\sin \tfrac{1}{2} (\Delta\beta_{[m]} - \Delta\beta_{[n]}) l_0]^2} + \frac{1 - \dfrac{2}{-(\Delta\alpha_{[m]} + \Delta\alpha_{[n]}) l_0} [\sin \tfrac{1}{2} (\Delta\beta_{[m]} + \Delta\beta_{[n]}) l_0]^2}{1 + \left(\dfrac{2}{-(\Delta\alpha_{[m]} + \Delta\alpha_{[n]}) l_0} \right)^2 [\sin \tfrac{1}{2} (\Delta\beta_{[m]} + \Delta\beta_{[n]}) l_0]^2} \right]; \quad \text{(F-21)}$$

$$-N(\Delta\alpha_{[m]} + \Delta\alpha_{[n]}) l_0 \gg 1, \quad -(\Delta\alpha_{[m]} + \Delta\alpha_{[n]}) l_0 \ll 1.$$

Equations (F-20) and (F-21) again exhibit narrow peaks of the same general type as illustrated in Fig. 11; away from these peaks the functions will be quite small. Thus if $(\Delta\beta_{[m]} \mp \Delta\beta_{[n]})l_0 \not\approx m\pi$, from (F-20) and (F-21) for either small or large differential loss:

$$\langle \delta A_{[m]} \delta A_{[n]} \rangle = -\frac{\hat{x}_{[m]}^2 \hat{x}_{[n]}^2}{4} N; \qquad -(\Delta\alpha_{[m]} + \Delta\alpha_{[n]})l_0 \ll 1, \quad (\Delta\beta_{[m]} \mp \Delta\beta_{[n]})l_0 \not\approx m\pi. \tag{F-22}$$

From (F-22) the correlation coefficient of $\delta A_{[m]}$ and $\delta A_{[n]}$ will be small for moderately large values of N. Therefore, for those modes that make a significant contribution to the total $\langle(\delta A)^2\rangle$, the cross terms in (F-16) will be negligible.

APPENDIX G

Correlation Coefficient of TE_{01} Loss Components due to Different Spurious Modes for the Continuous Case

Consider the ac components $\delta A_{[m]}$ and $\delta A_{[n]}$ of the total TE_{01} loss, due to two different spurious modes, each with two polarizations, generated by the same type of geometric imperfection. The geometric imperfection and thus the coupling coefficients are assumed to have white power spectra.

As a specific example, consider random deviations of the guide axis from perfect straightness, which generate principally the forward TE_{12} and TE_{11} spurious modes. The coupling coefficients to the two polarizations of the TE_{1m} mode are given in (308) in terms of the second derivatives of the rectangular co-ordinates of the guide axis, $x''(z)$ and $y''(z)$. We assume that $x''(z)$ and $y''(z)$ have white power spectra.

We expand the geometric imperfection to which the coupling coefficients are proportional in a Fourier series. For random straightness deviations:

$$x''(z) = \sum_{n=-\infty}^{\infty} \gamma_n^{\parallel} e^{j2\pi nz/L}; \qquad y''(z) = \sum_{n=-\infty}^{\infty} \gamma_n^{\perp} e^{j2\pi nz/L}; \qquad \gamma_n^{\parallel} = \alpha_n^{\parallel} + j\beta_n^{\parallel}, \quad \gamma_n^{\perp} = \alpha_n^{\perp} + j\beta_n^{\perp}. \tag{G-1}$$

The complex Fourier coefficients c_n in Section 4.1 are simply proportional to the corresponding γ_n. For straightness deviations, for the TE_{1m} mode

we have:

$$\begin{aligned} c_{n[m]}{}^{\parallel} &= C_{t[m]}\gamma_n{}^{\parallel}, \quad \mathrm{TE}_{1m}{}^{\parallel}; \\ c_{n[m]}{}^{\perp} &= C_{t[m]}\gamma_n{}^{\perp}, \quad \mathrm{TE}_{1m}{}^{\perp}. \end{aligned} \tag{G-2}$$

Consequently, the γ_n's have the same statistical properties as the c_n's, given in Section 4.2. Since $x''(z)$ and $y''(z)$ have white power spectra,

$$\langle |\gamma_n{}^{\parallel}|^2 \rangle = \langle |\gamma_n{}^{\perp}|^2 \rangle = \hat{\gamma}^2. \tag{G-3}$$

Further, the different γ's are strictly independent.

We next define for convenience the following quantities:

$$\begin{bmatrix} g_\alpha{}^{\parallel}(t) \\ g_\beta{}^{\parallel}(t) \\ g_\alpha{}^{\perp}(t) \\ g_\beta{}^{\perp}(t) \end{bmatrix} = \sum_{n=-\infty}^{\infty} \begin{bmatrix} \alpha_n{}^{\parallel} \\ \beta_n{}^{\parallel} \\ \alpha_n{}^{\perp} \\ \beta_n{}^{\perp} \end{bmatrix} (-1)^n \frac{\sin \pi(t-n)}{\pi(t-n)}, \quad t \equiv \frac{\Delta\beta L}{2\pi} = \frac{L}{B}. \tag{G-4}$$

These quantities are proportional to the real or imaginary parts of I in (285b). These four quantities are approximately independent stationary band-limited Gaussian random processes in the practical case where the length L is large compared to the beat wavelength B, so that $|t| \gg 1$. The autocorrelation function of each of these quantities, found directly from (G-4), is therefore

$$r(\tau) \equiv \langle g_{\alpha,\beta}{}^{\parallel,\perp}(t) g_{\alpha,\beta}{}^{\parallel,\perp}(t+\tau) \rangle = \tfrac{1}{2}\hat{\gamma}^2 \frac{\sin \pi\tau}{\pi\tau}. \tag{G-5}$$

Next we define for convenience the quantity $g^2(t)$ as

$$g^2(t) = g_\alpha{}^{\parallel 2}(t) + g_\beta{}^{\parallel 2}(t) + g_\alpha{}^{\perp 2}(t) + g_\beta{}^{\perp 2}(t). \tag{G-6}$$

The autocorrelation function of $g^2(t)$ is easily found in terms of the autocorrelation function of the individual g's, given in (G-5). If x is a stationary Gaussian random process with autocorrelation $R_x(\tau)$ and $y = x^2$, then the autocorrelation of y, $R_y(\tau)$, is given by [37, 40]

$$R_y(\tau) = R_x{}^2(0) + 2R_x{}^2(\tau), \tag{G-7}$$

where the first term corresponds to the dc component, the second to the ac component of y. Since the individual quantities whose squares appear on the right-hand side of (G-6) are independent random variables, we have from (G-7) and (G-5) for the autocorrelation function $R(\tau)$ of $g^2(t)$

$$R(\tau) \equiv \langle g^2(t)g^2(t+\tau)\rangle = 4\hat{\gamma}^4 + 2\hat{\gamma}^4\left(\frac{\sin \pi\tau}{\pi\tau}\right)^2, \qquad \text{(G-8)}$$

where again the first term corresponds to the dc component, the second to the ac component of $g^2(t)$.

From the results of Section 4.1 we may now write the TE_{01} loss due to the two polarizations of the m^{th} spurious mode (TE_{1m} for straightness deviations) in terms of the function $g^2(t)$ defined in (G-6):

$$A_{[m]} = \frac{C_{t[m]}{}^2 \cdot L^2}{2} g^2(t_{[m]}), \qquad t_{[m]} = \frac{|\Delta\beta_{[m]}|L}{2\pi}. \qquad \text{(G-9)}$$

Equation (G-9) is appropriate for our present purposes because it places in evidence the relation between the different TE_{01} loss components $A_{[m]}$. From (G-9), (G-8), and the results of Section 4.1, the normalized correlation coefficient ρ_{mn} of $\delta A_{[m]}$ and $\delta A_{[n]}$, the ac components of TE_{01} loss due to the m^{th} and n^{th} spurious modes, may be written in the following form:

$$\rho_{mn} \equiv \frac{\langle \delta A_{[m]}\delta A_{[n]}\rangle}{\sqrt{\langle(\delta A_{[m]})^2\rangle}\sqrt{\langle(\delta A_{[n]})^2\rangle}} = \left(\frac{\sin \pi\tau_{mn}}{\pi\tau_{nm}}\right)^2,$$
$$\tau_{mn} = \frac{(|\Delta\beta_{[m]}| - |\Delta\beta_{[n]}|)L}{2\pi}. \qquad \text{(G-10)}$$

Thus,

$$\rho_{mn} < \left(\frac{1}{\pi\tau_{mn}}\right)^2. \qquad \text{(G-11)}$$

Since the different spurious modes have substantially different beat wavelengths (Appendix D), $\rho_{mn} \ll 1$ for moderate values of length L. As a numerical example consider $TE_{12}{}^+$ and $TE_{11}{}^+$, for a total length between mode filters $L = 200$ feet. From (C-11), $\rho < 0.00036$. In practical cases the TE_{01} loss contributions of the different spurious modes will be almost uncorrelated, so that $\langle(\delta A)^2\rangle$ will be given by (322).